Pulmonary gammaherpesvirus infection and pneumonitis development following murine bone marrow transplant

by

Stephanie Michael Coomes

A dissertation submitted in partial fulfillment
of the requirements for the degree of
Doctor of Philosophy
(Immunology)
in the University of Michigan
2011

Doctoral Committee:

Associate Professor Bethany B. Moore, Chair
Professor Nicholas W. Lukacs
Assistant Professor Yasmina Laouar
Assistant Professor Jason B. Weinberg
Research Assistant Professor Steven K. Lundy

Acknowledgments

This dissertation work would not have been possible without the help, guidance, and support of many individuals. First and foremost, I would like to thank my mentor, Beth Moore, for her scientific guidance, support, and unwavering confidence in my abilities. My graduate experience has been greatly enhanced because she has been extremely generous with her time and resources, teaching me how to read, write, and speak scientifically. I am indebted to our lab manager, Carol Wilke, for her patience in teaching me many of the techniques I needed to perform experiments for this work, as well as her technical assistance. I would also like to thank former and current members of the Moore Lab, including Megan Ballinger, Brian Bauman, Paul Bozyk, Chris Fry, Leah Hubbard, Tracy Luckhardt, Payal Naik, Josh Stoolman, and Kevin Vannella for help and discussions. Additionally, I would like to thank my undergraduate students, Stefanie Gibson and Laura Leach, for their contributions to this work.

I am grateful to the members of my thesis committee, Yasmina Laouar, Nick Lukacs, Steve Lundy, and Jason Weinberg, who have been exceptionally helpful in providing a clear direction for my research project, as well as research reagents, protocols, and experimental guidance.

I am also thankful to the Graduate Program in Immunology, especially Zarinah Aquil, members of Bruce Richardson's lab for accommodating my access to the irradiation facility, John Erb-Downward for providing advice on flow cytometry, Susan

Foust and Keith Bishop for providing T cell DN mice, Weiping Zou and Cailin Wilke for helpful discussions and providing IL-10KO mice, and Ashley Sandy and Ivan Maillard for collaborations. I am grateful for the collaboration with Sara Farmen which has made the histology analysis possible. I would like to thank Tom Moore for providing flow cytometry guidance and for allowing me the opportunity to teach with him for two semesters. I also appreciate the generosity of Herman and Dorothy Miller for supporting my research.

I am especially thankful for the personal support provided from my family, parents, and friends, especially my fiancé Ian and my friends Cheryl, Heather, Ilea, Kaanan, Kadee, and Val, who have supported me throughout my time at the University of Michigan.

Table of Contents

List of Figures

List of Tables

Abstract

Pulmonary complications are frequent following hematopoietic stem cell transplantation, including infections and pneumonitis. We have used a murine bone marrow transplant (BMT) model and murine gammaherpesvirus, γHV-68, to study alterations in anti-viral immunity post-transplant. When challenged with γHV-68, BMT mice have reduced ability to control lytic viral replication in the lung, despite immune reconstitution. By day 21 post-infection the virus is latent, and BMT mice, but not control, develop pneumonitis with reduced oxygenation, fibrosis, inflammation, hyaline membranes, and foamy alveolar macrophages, a phenotype which persists 7 weeks post-infection. BMT mice have an increase in cells harvested by bronchoalveolar lavage (BAL), and this population is enriched in neutrophils, CD4, and CD8 cells. BAL fluid from BMT mice at day 21 has increased pro-fibrotic factors, including hydrogen peroxide, nitrite, and transforming growth factor-beta (TGFβ). Defective control of lytic virus infection in BMT mice is not related to impaired leukocyte recruitment or defective antigen presenting cell function. Rather, BMT lungs have decreased numbers of protective Th1 cells and increased numbers of Th17 cells in response to γHV-68. BMT mice are also characterized by an immunosuppressive lung environment at the time of infection that includes overexpression of TGFβ1, prostaglandin-E_2, and increased Tregs. Neither pharmacological blockade of prostaglandin synthesis nor depletion of Tregs improved host defense. To understand the role of TGFβ, BMT mice were transplanted with transgenic bone marrow expressing dominant negative TGFβ receptor II in T cells

(Tcell-DN-TGFβRII) or under the CD11c promoter (CD11c-DN-TGFβRII), blocking TGFβ signaling in CD4 and CD8 cells or CD11c-expressing cells, respectively. Tcell-DN-TGFβRII BMT mice have restored lytic viral load and improved Th1 response; these mice are largely protected from the pneumonitis phenotype. However, CD11cDN-TGFβRII BMT mice show increased susceptibility to lytic infection, similar to wild type BMT, and are only moderately protected from pneumonitis. Thus, our results indicate that overexpression of TGFβ1 following myeloablative BMT results in impaired T cell responses to viral infection, resulting in increased lytic viral load and pneumonitis. Our data provide new insight into the potential causes of impaired anti-viral immune responses and development of pneumonitis in hematopoietic stem cell transplant patients.

Chapter 1

Introduction

Overview and Hypothesis

Hematopoietic stem cell transplant (HSCT) is an important therapy used to treat several life-threatening diseases. Despite success in disease treatment, transplant recipients are at-risk for a number of post-transplant complications, both non-infectious and infectious. Pulmonary complications are particularly prominent. Because opportunistic infections have been reported to occur late post-transplant in autologous HSCT recipients (6, 7), and because functional deficits of immune cell function post-transplant have been reported *in vitro* (8-12), we hypothesized that post-transplant alterations in immune cell function could contribute to increased susceptibility to virus infection post-HSCT. Additionally, based on the recent prospective study showing that early post-HSCT virus infection was associated with development of late non-infectious pulmonary complications (13), we hypothesized that uncontrolled pulmonary virus infection post-HSCT, due to functional deficits in immune cells, could contribute to later development of pneumonitis. In these studies, we have used a murine bone marrow transplant (BMT) model and murine gammaherpesvirus, γHV-68, to study alterations in anti-viral immunity and development of pneumonitis and pulmonary fibrosis post-transplant.

Hematopoietic Stem Cell Transplantation: Definition

HSCT involves ablation of hematopoietic cells by chemotherapy and/or total body irradiation (TBI) followed by subsequent infusion of self or donor-derived hematopoietic stem cells (HSCs), which will repopulate the immune system. Since the first transplants were performed in cancer patients in the late 1950s (14, 15), HSCT has become an important therapy for the treatment of a number of diseases, including several types of malignancies such as multiple myeloma, leukemias, and lymphomas. HSCT may be used as a rescue therapy following high-intensity chemotherapy or TBI used to eradicate cancer cells. HSCT allows for replacement of non-malignant cells which are also destroyed during treatment. Often times in the allogeneic setting, HSCT is used so that alloreactive T cells in the graft mediate graft-versus-tumor effects, with the end goal of eradicating the cancer (16).

HSCT is also an important treatment option for inherited hematological disorders, including aplastic anemia, sickle cell anemia, and severe combined immunodeficiency (16). Recently, HSCT has been increasingly considered as a therapeutic option for severe autoimmune disorders, including systemic sclerosis, rheumatoid arthritis, and multiple sclerosis. Randomized clinical trials evaluating the effectiveness of autologous HSCT in treating these disorders are ongoing. The immune system is thought to "reset" post-transplant, replacing the autoimmune repertoire (17).

Following conditioning, patients are intravenously infused with HSCs derived from bone marrow, umbilical cord blood (18), or mobilized peripheral blood cells from donors treated with growth factors such as granulocyte colony stimulating factor (G-CSF)

(19). In allogeneic transplants, patients receive donor-derived cells, and in autologous transplants, which are performed more frequently (20), patients are infused with their own cells (harvested and cryopreserved prior to conditioning). These transplanted cells will expand and differentiate to fill the niche of the conditioned host. It is estimated that 30,000 autologous and 15,000 allogeneic transplants are performed annually worldwide (16).

Despite the increasing use of HSCT as a therapeutic option, its effectiveness is severely limited by post-transplant complications that lead to significant morbidity and mortality in transplant patients. Post-transplant complications, particularly in the lung, both infections and non-infectious, are significant barriers to HSCT success.

Hematopoiesis and Stem Cell Homing

Cells of the immune system are derived from HSC precursors in the bone marrow, a self-renewing population which has the potential to differentiate into nearly all hematopoietic cell lineages. HSCs are identified by their expression of the marker CD34. HSCs give rise to multipotent progenitor cells, which in turn give rise to the common myeloid progenitor (CMP) and common lymphoid progenitor (CLP). Erythrocytes, platelets, neutrophils, monocytes, eosinophils, basophils and myeloid dendritic cells are ultimately derived from CMP cells. Lymphocytes, including T and B cells, arise following multiple differentiation steps from the CLP, as do natural killer (NK) cells and plasmacytoid dendritic cells (1, 2) (Figure 1.1).

Development of both B and T cells involves the genomic rearrangement of antigen receptor genes, creating a diverse repertoire of antigen specificity. These cells are

the main cell types involved in the adaptive immune response, which is able to generate immunological memory following activation. T cells develop from CLPs which emigrate from the bone marrow to the thymus, where these cells undergo a series of developmental steps, resulting in positive and negative selection. B cells undergo development in the bone marrow. The diverse antigen specificity of B and T lymphocyte populations is in contrast with the more limited, germline-encoded receptors expressed on innate immune cells. Innate immune cells recognize antigens via binding to pattern-recognition receptors (PRRs), including toll-like receptors (TLR). PRRs recognize general repeated pathogen and endogenous danger-associated motifs. Activation of the innate immune system does not directly result in generation of immunological memory (21).

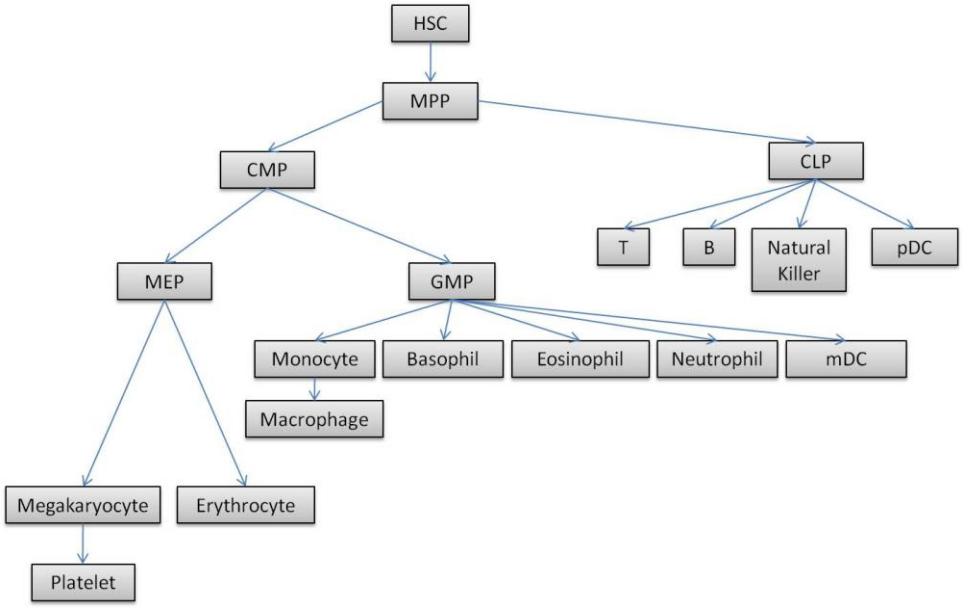

Figure 1.1. Hematopoiesis (Adapted from (1, 2)). HSCs differentiate into the multipotent progenitors (MPP), which further differentiate into the common myeloid progenitor (CMP) and the common lymphoid progenitor (CLP). CMP cells give rise to the megakaryocyte-erythrocyte progenitor (MEP) and the granulocyte-monocyte progenitor (GMP). These progenitor cells then differentiate into the effector cell populations shown.

The self-renewal and pluripotent capacity of HSCs is demonstrated by a study reporting that a single HSC transferred into a lethally irradiated recipient could lead to repopulation of the hematopoietic compartment (22). HSCT takes advantage of the ability of HSCs to traffic and home from the blood (where they are infused during transplant) to the bone marrow niche. The signals involved in the homing of HSCs to the bone marrow post-transplant are the same as those involved in initial homing during development. Studies have shown that HSC homing is very rapid, occurring within 1-2 hours post-infusion (23). Homing of HSCs occurs via the expression of the chemokine receptor CXCR4 on HSCs, which interacts with SDF-1 expressed on bone marrow endothelium and bone marrow stromal cells (23).

HSCT Conditioning

Specific conditioning regimens for HSCT vary widely between transplant centers and depend on clinical disease course, as well as the health and age of the patient. The standard preparative regimen since the 1980s has been a combination of treatment with fractioned TBI and cyclophosphamide (16). TBI is given in fractionated doses to reduce overall toxicity, and organ shielding may be used to prevent further toxicity. Other preparative regimens do not include TBI and involve the use of different chemotherapeutic agents including busulfan, sometimes in combination with cyclophosphamide (24). Clinical trials indicate that different conditioning regimens may be more effective in treatment of different diseases. For instance, a study has shown that treatment of myeloid leukemia is similar between groups with or without TBI, but TBI was reported to be advantageous to patients receiving HSCT for acute lymphoblastic leukemia (24).

Treating patients with these regimens has several consequences, including eradication of malignant or self-reactive cells. Conditioning ablates recipient immune cells, providing an immunosuppressed environment for the transplantation of allogeneic cells and reducing the risk of graft rejection (24, 25). It has also been suggested that conditioning provides a niche for transplanted cells. In the case of malignancy, conditioning regimens can break down tumors, releasing tumor antigen to be taken up and presented by antigen presenting cells (16).

Conditioning regimens have historically been myeloablative. More recently, reduced-intensity conditioning has been used. Reduced-intensity regimens allow HSCT to be performed in older patients and patients with organ dysfunction who could not withstand the more intense myeloablative regimens. In the case of malignancy, a balance exists between preventing conditioning-associated morbidity and prevention of disease relapse by thorough eradication of malignant cells (16). Many of the short and long-term complications of HSCT relate to damage caused by conditioning; thus, efforts have been focused on adjusting regimens to reduce damage while maintaining all the benefits of conditioning.

Sources of Hematopoietic Stem Cells

Bone marrow has been the historical source of HSCs for transplantation. To harvest bone marrow, donors are given anesthesia, and bone marrow cells are collected by repeated aspiration of the posterior iliac crests of the hip (16). Because of the need for anesthesia and the pain associated with this procedure, other sources of HSCs have been used for transplant.

Recently, peripheral blood has become an important source of HSCs, replacing bone marrow for most transplants. Blood is a convenient source for HSCs, as cells can be harvested by leukapheresis. The normally low numbers of CD34-expressing HSCs in the peripheral blood can be substantially increased by treating donors with G-CSF, which mobilizes these cells out of the bone marrow and into the circulation (19). The inclusion of a small molecule CXCR4 inhibitor can further increase mobilization. CXCR4 is the chemokine receptor involved in HSC homing to bone marrow; CXCR4 is expressed on HSCs and binds SDF-1 expressed by bone marrow stromal cells and endothelium (26).

Finally, umbilical cord blood has become an important HSC source. Placental and umbilical cord blood can be harvested after birth and frozen prior to transplantation. In these transplants, greater HLA mismatches between donor and recipient can be tolerated. However, the use of cord blood for HSCT is associated with slower engraftment and thus greater risk of infectious complications. Additionally, the use of cord blood can be limited by low numbers of cells harvested, though recent studies have investigated the ex-vivo expansion of cord blood-derived HSCs (16, 18).

Cell infusions used for transplantation are generally complex mixtures of HSCs and mature hematopoietic cells which are present in the donor bone marrow, peripheral blood, or cord blood. Therefore, grafts may include mature T cells. Inclusion of mature T cells in grafts promotes immune reconstitution and, in the allogeneic setting, promotes an immune response of grafted cells against malignant cells (27). Greater numbers of T cells are found in peripheral blood-derived grafts, thus increasing the graft-versus-tumor effect. This is in contrast with cord blood grafts, which contain relatively few T cells. Grafts may also be depleted of T cells to prevent development of graft-versus-host

disease (GVHD), where engrafted allogeneic T cells are activated against recipient antigens, causing severe tissue and organ damage. In allogeneic transplants for the treatment of malignant diseases, there is a balance between promoting alloreactive T cell responses against host malignant tissue and preventing alloreactive T cell-mediated destruction of normal host tissue.

Complications of HSCT

Despite promising success in the treatment of many diseases, the efficacy of HSCT is limited due to significant transplant-related morbidity and mortality. There are a wide variety of complications that can occur following HSCT, both non-infectious and infectious. Many complications persist long-term post-transplant, and this is most clearly demonstrated in pediatric HSCT survivors who are at-risk for a myriad of long-term side effects (28). Complications can be related to consequences of the conditioning regimen, the development of acute and chronic GVHD mediated by alloreactive T cells, or the manifestation of infectious complications.

Pulmonary Complications of HSCT

Pulmonary complications comprise a large group of post-transplant complications and are reported to occur in up to 60% of HSCT recipients (29); one study of 82 deceased HSCT recipients found pulmonary complications in 89% of the cohort (30). Additionally, HSCT patients have been reported to have abnormal pulmonary function tests long-term post-transplant (31, 32). The frequent occurrence of pulmonary complications in HSCT recipients may be associated with toxic effects of both TBI (33, 34) and chemotherapeutic agents (35) on lung tissue. Infectious and non-infectious pulmonary complications post-HSCT are outlined in Figure 1.2.

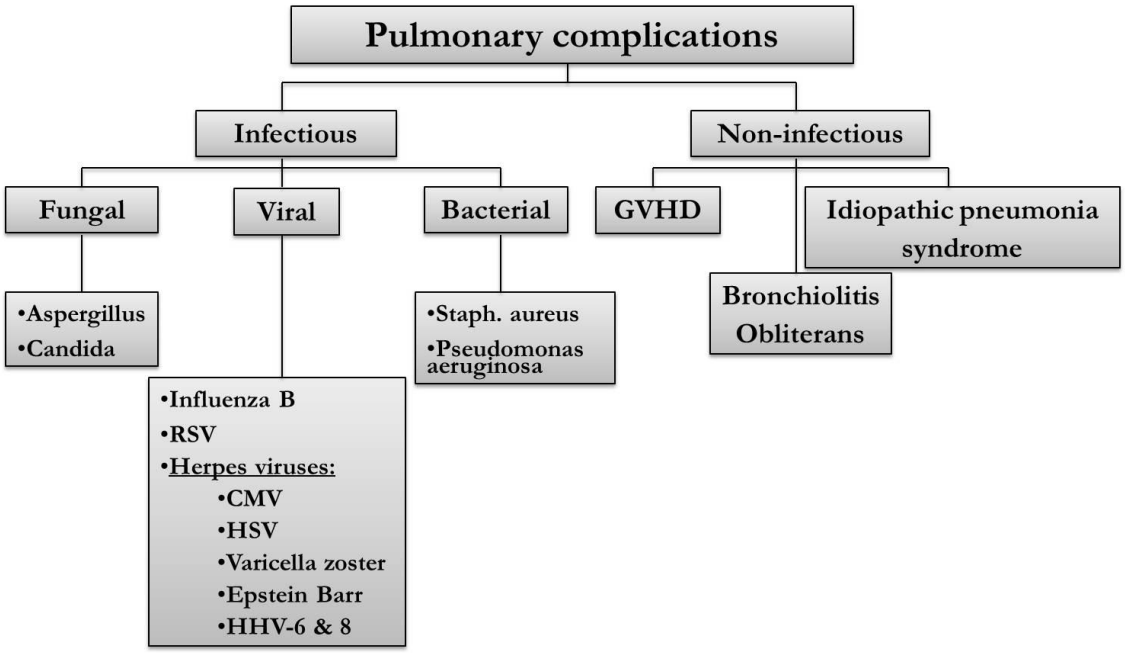

Figure 1.2 Pulmonary complications post-HSCT (adapted from (2, 3)). This diagram outlines a subset of infectious and non-infectious pulmonary complications which have been reported to occur in HSCT recipients.

Two major non-infectious pulmonary complications of HSCT are bronchiolitis obliterans and idiopathic pneumonia syndrome (IPS). Bronchiolitis obliterans involves airflow obstruction and occurs almost exclusively in the allogeneic setting (36). Bronchiolitis obliterans is thought to be a pulmonary manifestation of GVHD, where alloreactive donor T cells are activated against host antigens (37). Symptoms of IPS mimic infectious pneumonia (36), with mortality occurring in 60-80% of cases. There are currently no effective therapies for the treatment of IPS, but some recent studies have shown success using etanercept, blocking TNF in IPS treatment (38). The pathogenesis of IPS is not well understood, and it is likely that the disease is multi-factorial, including the effects of conditioning, GVHD, inflammatory cell recruitment, cytokine production and possibly undiagnosed infection (36, 38, 39). IPS is notably more frequent in the allogeneic setting; however, several studies have reported its occurrence in a significant percentage of autologous transplant recipients (36, 40, 41), suggesting that the mechanism for this complication is likely multi-factorial.

A recent prospective study of pediatric allogeneic HSCT recipients closely monitored respiratory viral infections post-transplant and found that early respiratory virus infection post-transplant was correlated significantly with development of IPS and bronchiolitis obliterans in their cohort. Importantly, patients had recovered from their initial respiratory symptoms prior to development of later respiratory complications associated with IPS or bronchiolitis obliterans (13). It is interesting to speculate that an inflammatory stimulus, such as a virus, can lead to pneumonitis and lung injury at later time points, even after resolution of the initial lytic insult. Work presented in this dissertation will support such speculation.

Infectious complications can occur in both allogeneic (42) and autologous recipients (43, 44), though they are more common in allogeneic transplants (29), presumably due to GVHD and immunosuppressive drug therapy to prevent or treat GVHD. Pulmonary infections post-HSCT can be caused by fungi, bacteria, and viruses (45). Invasive fungal infections in the lungs in HSCT patients are principally caused by *Aspergillus* and *Candida* species (46, 47), and bacterial pneumonia is reported to be caused by *Pseuodomonas aeruginosa*, *Klebsiella pneumonia*, and *Legionella* (48). Viral pneumonia in HSCT patients can be caused by herpesviruses, including cytomegalovirus (CMV) varicella zoster (VZV), human herpesvirus-6 (HHV-6), Epstein-Barr Virus (EBV) and herpes simplex virus (HSV), as well as other viruses, including influenza, adenovirus, and respiratory syncytial virus (4, 45, 49). Historically, CMV infection was the most significant viral complication of HSCT; mortality rates of CMV pneumonia in HSCT recipients were near 85% prior to the development of anti-viral drug therapy (50). Despite advances in prophylaxis and antiviral therapy, however, CMV disease remains a significant complication of HSCT (51).

Infectious complications in HSCT recipients are characterized by when they occur post-HSCT, including pre-engraftment (during neutropenia, 1 month post-HSCT), early post-engraftment, and late post-engraftment (approximately 3 months post-transplant) (3, 48, 52). Figure 1.3 summarizes infections reported to occur during these post-transplant time periods (4).

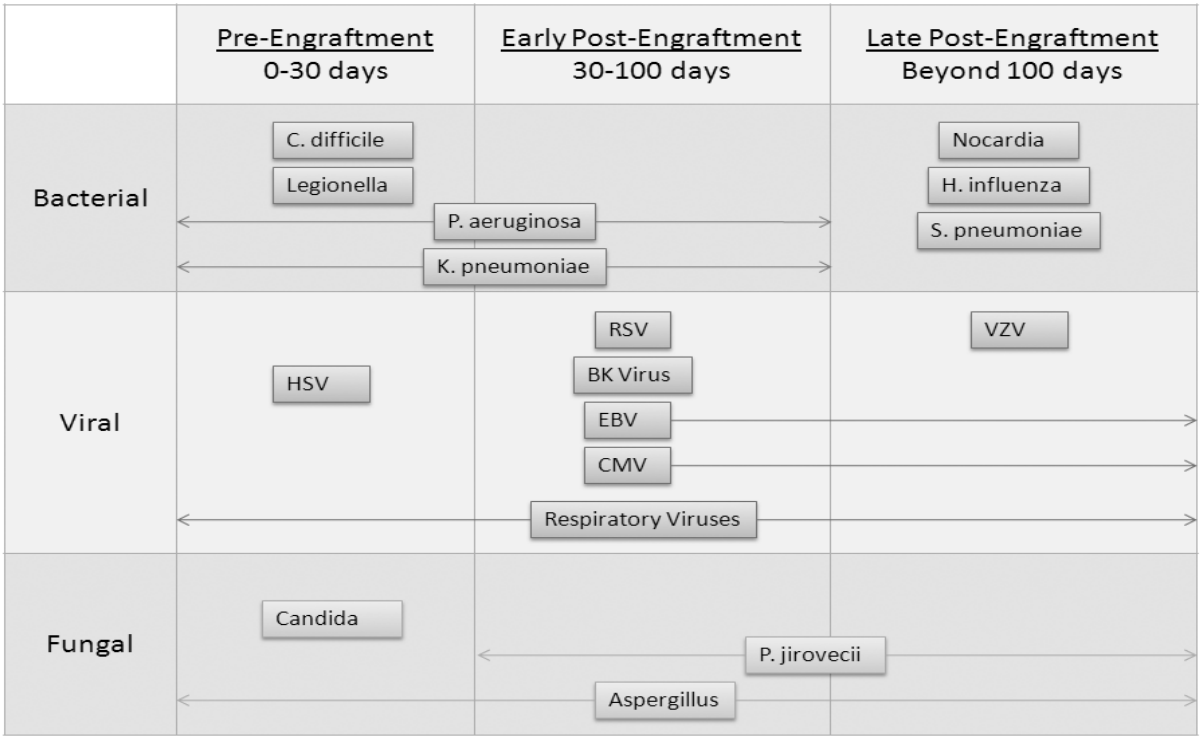

Figure 1.3 Timeline of infectious complications post-HSCT (4). Specific bacterial, viral, and fungal infectious complications have a tendency to occur during differential time periods post-HSCT.

Impaired Immune Responses Post-Transplant

The occurrence of severe infectious complications in HSCT recipients is indicative of immunosuppression post-HSCT. While infectious complications are common prior to engraftment of immune cells, patients continue to be susceptible even late post-engraftment (Figure 1.3). This is partially explained by the administration of

immunosuppressive drug therapy in allogeneic transplant recipients as an effort to control development of GVHD. However, opportunistic infections have been reported to occur late post-transplant in autologous patients as well (6, 7). This fact suggests that conditioning and subsequent transplantation, even in the absence of immunosuppressive therapy and GVHD, can lead to immune dysfunction post-transplant.

Indeed, several studies have shown impaired cellular immune responses in HSCT recipients. Reconstitution of immune cell subset numbers occurs within the first few months post-transplant, with innate populations such as NK cells, macrophages, and neutrophils reconstituting prior to adaptive immune cells (8, 53). Although NK cells have been reported to be largely functional post-HSCT, both neutrophils and macrophages have been reported to have diminished function post-HSCT (8). B cell numbers reconstitute in peripheral blood within the first 4 months post-transplant. Despite normal proliferative responses to mitogen stimulation, these cells produce little to no isotype-switched antibody within the first year post-HSCT (9). In transplant patients, the total number of CD3+ T cells reconstitutes in peripheral blood by several months post-transplant; however, the ratio of CD4 to CD8 cells in peripheral blood is inverted, with increased CD8 and decreased CD4 numbers (8, 54-56). In the months following transplant, peripheral T cells are thought to be expanded by homeostatic proliferation, leading to a limited T cell repertoire in HSCT patients, which has been reported to persist even 3 years post-transplant (56). In addition to limited T cell repertoire, several studies have reported deficiencies in peripheral T cell function post-HSCT using *in vitro* assays of T cell function. T cells from autologous HSCT recipients were shown in one study to have diminished proliferation in response to both PHA stimulation and in a mixed

leukocyte reaction (MLR); T cell proliferation to these stimuli did not reach pre-transplant levels even 1 year post-transplant (10). Other studies have found similar decreases in proliferation in response to anti-CD3, anti-CD2 and PHA stimulation (11, 12). One group found a greater reduction in frequencies of mitogen-responsive T cells from peripheral blood of autologous recipients compared to allogeneic (57), suggesting that immunodeficiency post-HSCT is not solely related to graft-versus-host effects.

Taken together, studies of immune reconstitution in HSCT patients suggest that significant alterations in immune cell phenotype and function occur following transplant. Mechanisms for these alterations have not been completely elucidated for each cell type and may depend on the type of transplant, clinical disease course, or the specific time post-HSCT.

Murine Models of Bone Marrow Transplant

The wide variety of indications, conditioning regimens, and variations in protocols among transplant centers and patients complicate the understanding of mechanisms of immune dysfunction in HSCT patients. The development of a small animal model of HSCT has been critical for controlled study of the mechanisms of impaired immunity post-transplant. Murine models of HSCT typically involve TBI followed by bone marrow transplantation (BMT) between inbred mouse strains (58). One major advantage of murine BMT models is the ability to use transgenic mice as BMT donors or recipients in order to understand roles of specific genes in transplantation. The large number of inbred mouse strains also allows for the development of several allogeneic transplant models. Additionally, the use of syngeneic BMT (transfer between

genetically identical donors and recipients) models autologous transplant and, furthermore, allows for study of conditioning and transplantation in the absence of the confounding effects of GVHD or immunosuppressive drug therapy. Another important advantage of murine BMT models is the ability to study function of tissue-resident hematopoietic cells; human studies are largely limited to studying functions of cells derived from peripheral blood.

Innate Immune Defects in Murine BMT

Our laboratory has previously used murine BMT to understand alterations in innate immune responses to pulmonary bacterial infections post-transplant. These studies have established a syngeneic BMT model wherein transplanted mice are more susceptible to lung infection by *Pseudomonas aeruginosa*, despite having completely restored their hematopoietic compartment in both the periphery and the lung. Transplanted mice have increased bacterial burden in the lung and bacterial dissemination to the blood at 24 hours following intratracheal infection when compared with non-transplanted control mice (59). This inability to control *P. aeruginosa* infection is related to dysfunctional innate immune responses, including defective phagocytosis and killing of bacteria by alveolar macrophages and defective bacterial killing by lung neutrophils. Alveolar macrophages also produce reduced levels of the proinflammatory cytokine TNFα (60).

In this model, lungs from BMT mice overproduce the immunosuppressive lipid mediator prostaglandin E_2 (PGE_2), which impairs innate immunity to *P. aeruginosa* (60). When BMT mice are treated with indomethacin, a cyclooxygenase inhibitor which blocks PGE_2 synthesis, bacterial burdens in the lung and blood are significantly reduced to levels

observed in non-transplant control mice. Additionally, indomethacin treatment can restore function of BMT alveolar macrophages and neutrophils *in vitro* (60). Recent data suggest that PGE_2 suppresses alveolar macrophage function by inducing the upregulation of IL-1R-associated kinase (IRAK)-M in these cells, thus inhibiting MyD88-dependent signaling responses. Bacterial clearance, phagocytosis, and TNFα production can be restored in the BMT setting by using IRAK-M knock-out mice as BMT donors (61).

Murine Gammaherpesvirus-68

For studies in this dissertation, we chose to use a murine gammaherpesvirus as a model pathogen to understand how anti-viral may be altered following murine BMT. Murine gammaherpesvirus-68 (γHV-68; also known as MuHV4 or MHV-68) is a double-stranded DNA virus with genetic similarity to the human gammaherpesviruses, Epstein-Barr Virus and Kaposi's Sarcoma Associated Herpesvirus (also known as human herpesvirus-8). Its genome consists of 118, 237 base pairs, encoding approximately 100 viral genes (62). Although γHV-68 was first isolated from bank voles in Slovakia (63), it is able to establish infection in laboratory mouse strains, thus making γHV-68 infection in mice an important model for understanding of gammaherpesvirus pathogenesis *in vivo* (64, 65). The natural route of γHV-68 infection has not been definitively established, though it is thought to be via the respiratory route.

When delivered intranasally to mice, γHV-68 establishes an acute, lytic infection primarily in respiratory epithelial cells, which lasts approximately 10 days. Viral replication peaks approximately 6-9 days post-infection, and lytic replication is largely absent from the lung after 14 days (66). Following the acute infection, γHV-68

establishes a chronic infection by establishing latency primarily in splenic B cells, but data from our laboratory show that the virus also persists in lung fibroblasts, epithelial cells, macrophages, and B cells (64, 67). γHV-68 infection can persist for the life of the host, with presumed periodic reactivation from latency. Only under conditions of immunosuppression does γHV-68 cause disease in the infected host.

Similar to EBV infection, γHV-68 induces the development of infectious mononucleosis and splenomegaly. This involves the expansion of polyclonal B cell populations, as well as expansion of CD8 T cells which express the Vβ4 T cell receptor (66). Splenomegaly peaks approximately 2 to 3 weeks after initial acute infection. Thereafter, the number of latently infected splenocytes normalizes to steady-state; it has been estimated that 1 in 10^5 to 1 to 10^6 splenocytes maintain latent infection (68). During persistent infection, γHV-68 reactivation is largely prevented by adaptive immune responses; however, some viral reactivation is thought to occur. The mechanisms of reactivation are not clearly described; however, TLR ligation has been suggested (69). Interestingly, several studies have indicated that the latent viral load does *not* correlate with the degree of viral replication during acute infection (70, 71). One study found equivalent levels of latency in the spleen in mice challenged with an initial intranasal viral dose ranging from 40 to $4x10^5$ pfu (72).

γHV-68 expresses several genes which are important for its pathogenesis, and these genes are differentially expressed during lytic replication and viral latency. During lytic replication, γHV-68 expresses several genes, including its viral DNA polymerase gene and the viral capsid glycoprotein gene gB (73), as well as ORF50, which encodes the viral lytic switch gene product, essential for lytic replication and reactivation. Several

genes have been identified as important in the establishment of viral latency, including mLANA, which functions to maintain the viral episome. ORF72 is a Cyclin D homolog which is required for viral reactivation from latency. Other viral gene products have been found to promote viral immune evasion, including K3, which targets MHC Class I proteins for ubiquitination and M3, a CC chemokine-binding protein (69).

Immune control of γHV-68 involves interplay between many cell types. The immune response to γHV-68 involves activation of CD4, CD8, and B cells, and each of these cell types is important in controlling γHV-68 replication *in vivo*. Studies have revealed that C57BL/6 mice deficient in CD4 cells have increased viral titers and develop a chronic wasting disease (74). While C57BL/6 mice lacking CD8 cells or B cells also have increased viral titers, these mice do not develop disease from infection (65, 75, 76). The relative contribution of each cell type seems to depend on the specific inbred mouse strain. Several studies have established that IFNγ production by CD4 cells specifically is critical for control of lytic replication (77-79) and that CD4 cells have direct effector function (as opposed to controlling infection via providing help to CD8 cells) (75, 76). Natural killer cells do not seem to play a critical role in controlling γHV-68 infection, though these cells are activated during γHV-68 infection (80, 81). The cytokine environment during acute γHV-68 infection is dominated by proinflammatory, Th1 type cytokines, including IFNγ, IL-6, IL-1β, IL-10, and TNFα (66).

Data from our laboratory have shown that in the lung, γHV-68 latency alters production of proinflammatory and profibrotic mediators in several cell types. Lung fibroblasts, alveolar macrophages, and B cells isolated from latently infected mice all produce increased levels of the profibrotic and immunomodulatory cytokine transforming

growth factor (TGF)β relative to saline-treated control mice. Additionally, increased chemokine and TNFα expression were reported in latently-infected cells (67). These data indicate that virus latency alters the immune and inflammatory environment of the persistently infected host.

Transforming Growth Factor-Beta

TGFβ is an important pleiotropic cytokine produced by leukocytes, including lymphocytes, antigen presenting cells and NK cells (82), as well as structural cells (83). It has multiple roles in embryonic development, cellular migration, differentiation, and the immune system. While TGFβ1 is the prototypical TGFβ family member, there are three isoforms of TGFβ expressed in mammals (TGFβ1, -β2, and -β3) (84). Each of these is secreted in the latent form, non-covalently associated with a homodimer of the latency-associated peptide (23, 85), which is capable of inhibiting TGFβ activity (86). LAP, in turn, can be linked by disulfide bonds to the latent-TGFβ-associated protein which allows the whole latent TGFβ complex to be associated with the extracellular matrix (85). TGFβ must be released from its latent form, disassociating from LAP, in order to function. There are several ways in which TGFβ can become activated including proteases (87), integrins (88), or change in pH (89). TGFβ1 is the main isoform with effects on the immune system.

Activated TGFβ dimers mediate their functions via serine/threonine kinase receptors. TGFβ receptors are expressed on a wide variety of cells, including hematopoietic cells. TGFβ binds the transmembrane TGFβ type II receptor (TGFβRII), which then phosphorylates the TGFβ type I receptor (TGFβRI, also known as ALK5).

ALK5 is not required for initial TGFβ binding, but it is required for signal transduction to occur. After ALK5 becomes phosphorylated, it will then phosphorylate and activate SMAD proteins. Receptor-associated SMAD 2 and 3 and Co-SMAD-4 translocate to the nucleus to arbitrate changes in gene expression via recruitment of transcription factors and binding the SMAD-binding element (82, 90) (Figure 1.4). TGFβ has also been reported to signal in a SMAD-independent process (82).

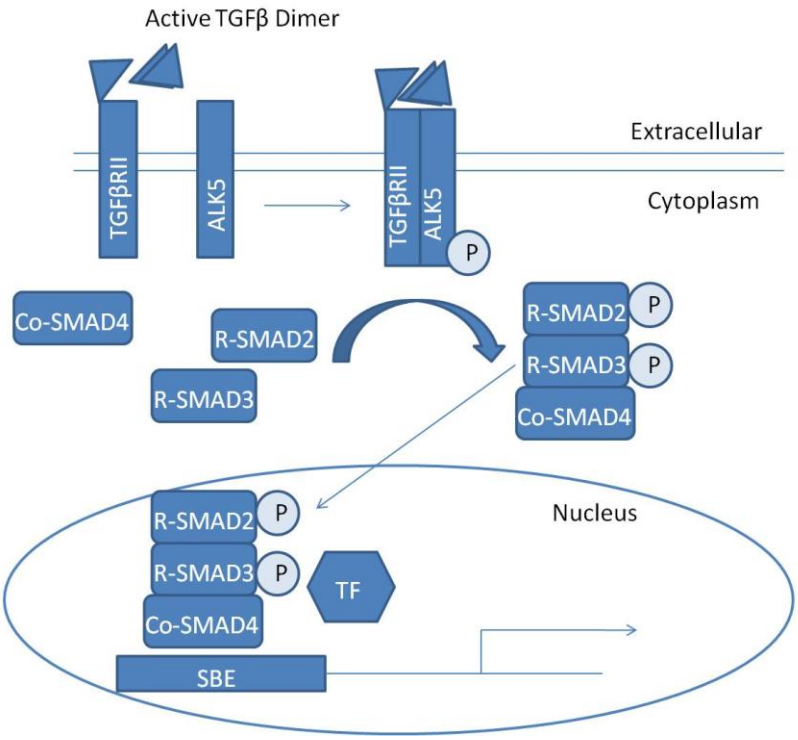

Figure 1.4. SMAD-dependent TGFβ signaling (adapted from (82, 91)). Active TGFβ dimers bind TGFβRII. Upon ligand binding, TGFβRII phosphorylates ALK5. Phosphorylated ALK5 then phosphorylates the receptor-associated SMADS, R-SMAD2 and R-SMAD3. These phosphorylated R-SMADs then associate with Co-SMAD4, which allows the complex to translocate to the nucleus. Here, the complex binds the SMAD-binding element (92) and associates with transcription factors (93) to mediate changes in gene transcription.

Effects of TGFβ on Hematopoietic Cells

TGFβ has been reported to have both immunosuppressive and immunostimulatory functions, even on the same cell types, and these functions appear to be context-dependent (82, 94). Most strikingly, TGFβ is known to be critical for maintenance of peripheral tolerance, as TGFβ knock-out (KO) mice develop severe inflammation and autoimmunity (95, 96). In addition to being a known T cell chemoattractant (97), TGFβ can also act on T cells to limit their proliferation (98) and their differentiation into Th1 and Th2 phenotypes, subsets of helper T cells characterized by production of the cytokines IFN-γ and IL-4, respectively (99, 100). TGFβ-mediated inhibition of naïve T cell proliferation can be attributed in large part to its ability of inhibit transcription of IL-2 (101); addition of exogenous IL-2 to T cell cultures treated with TGFβ can restore T cell proliferation (albeit not completely) (98). Inhibition of Th1 differentiation has been shown to be due to the ability of TGFβ to inhibit transcription of *Tbet*, the transcription factor required for Th1 development (102). TGFβ treatment blocks Th2 differentiation by blocking expression of GATA-3, the Th2-associated transcription factor (82). Studies using transgenic mice expressing a DN-TGFβRII in T cells and mice with a T-cell specific deletion in the *tgfbr1* gene indicate that both the ability of T cells to signal in response to TGFβ and produce TGFβ are critical in prevention of T cell-mediated autoimmunity (103, 104). These studies described a decisive role for TGFβ in dampening T cell activation and differentiation.

In contrast, TGFβ1 in conjunction with IL-6 can induce the differentiation of naïve CD4 T cells into the IL-17a- producing Th17 phenotype (105). TGFβ1 can also induce the differentiation and *in vivo* expansion of regulatory T cells (Tregs), a subset of

immunoregulatory T cells which can be identified by expression of the transcription factor Foxp3 and are critical for maintenance of peripheral tolerance (106, 107). The importance of TGFβ in Treg differentiation was first shown by its ability to convert naïve, CD25- CD4 T cells to Foxp3-expressing Tregs *in vitro* (106). The ability of TGFβ to induce Treg expansion *in vivo* was shown in a murine model of autoimmune diabetes; in this study, intraislet injection of TGFβ was sufficient to induce expansion of Tregs and prevent disease (107).

Although TGFβ signaling has been shown to inhibit B cell proliferation and inhibit IgG serum immunoglobulin levels (108), it also promotes IgA production which is essential for protection of mucosal sites (108). Indeed, conditional inactivation of the TGFβ receptor in B cells leads to a reduction in antigen-specific antibody responses following immunization at mucosal sites (109).

With respect to innate immune cells, TGFβ acts as a chemoattractant for neutrophils (110) and monocytes (111). Additionally, TGFβ can induce these cells to produce the proinflammatory cytokine IL-1β (111). In contrast, macrophage activation can be limited by the presence of TGFβ1 and -β2, and NK cell function is also limited by TGFβ (112, 113). TGFβ can limit both NK cell homeostasis and NK cell production of IFNγ, as evidenced by studies performed in mice expressing a DN-TGFβRII construct under the CD11c promoter(114). Table 1.1 summarizes some of the known effects of TGFβ on hematopoietic cells.

As a result of its pleiotropic functions and potent effects of hematopoietic cells, TGFβ has important effects on immunity to infections. Indeed, its suppressive effects on

the Th1 response would limit immunity to pathogens such as viruses and intracellular parasites, while TGFβ has been shown to be beneficial in the immune response to fungal infections (82).

Table 1.1 Effects of TGFβ on Immune Cells (adapted from (5))

Stimulatory	***Inhibitory***
With IL-6 induces Th17 (105)	Decreases T cell proliferation, activation (98, 104)
Promotes Treg differentiation (106)	Decreases Th1 and Th2 (99, 100)
Increases IgA production (109)	Decreases B cell proliferation and IgG production (108)
Increases monocyte, neutrophil, lymphocyte and mast cell chemotaxis (97, 110, 111, 115)	Decreases macrophage activation and NK function (112, 113)

Regulation of TGFβ post-HSCT

The production of TGFβ post-HSCT has been shown to be affected by the conditioning regimens used to prepare HSCT recipients for transplant. During the conditioning period, an initial drastic reduction in serum TGFβ1 levels was shown to occur in both autologous and allogeneic HSCT recipients (116), and TGFβ1 levels in the plasma of allogeneic HSCT recipients underwent a 4-fold decrease (117). This pattern was also noted in a mouse model of allogeneic transplant, where total serum TGFβ was greatly reduced 7 days post-transplant (118). Serum TGFβ levels in both allogeneic and autologous patients were shown to return to normal levels between 20 and 50 days post-transplant, and this recovery correlated with the return of white blood cell and platelet counts, major sources of TGFβ1 in the serum (116).

Production of TGFβ in other sites post-HSCT has been reported to be increased. TGFβ mRNA transcripts were found to be elevated in skin biopsies of patients experiencing cutaneous GVHD (119). Additionally, high dose irradiation can stimulate overproduction of TGFβ1 in the human lung (34). In a murine model of allogeneic HSCT, TGFβ transcript levels in the lung were shown by in situ hybridization to be increased relative to that of non-transplanted control mice at day 7 post-transplant; including cyclophosphamide in the pre-HSCT conditioning regimen potentiated this increase (118). Taken together, these studies suggest that production of TGFβ is dysregulated following conditioning and HSCT, though TGFβ production by individual cell types post-transplant has not been analyzed in a systematic study.

Because of the pleiotropic nature of TGFβ, the potential effects of its dysregulation post-HSCT are likely to be complex and contradictory. Studies have shown that although TGFβ may limit acute GVHD (117, 120), it may also contribute to the development of chronic GVHD and fibrosis (120, 121). Early post-allogeneic HSCT, the presence of TGFβ may prevent graft rejection and thus promote graft acceptance (122). The role of TGFβ in host defense post-HSCT is also complex. While there are potentially beneficial effects in terms of leukocyte recruitment (97, 110, 111, 115) and IgA production (109), there is also evidence from a murine BMT model indicating that TGFβ can directly promote virus-induced pneumonitis (123, 124). Potential effects of TGFβ post-HSCT are shown in Figure 1.5.

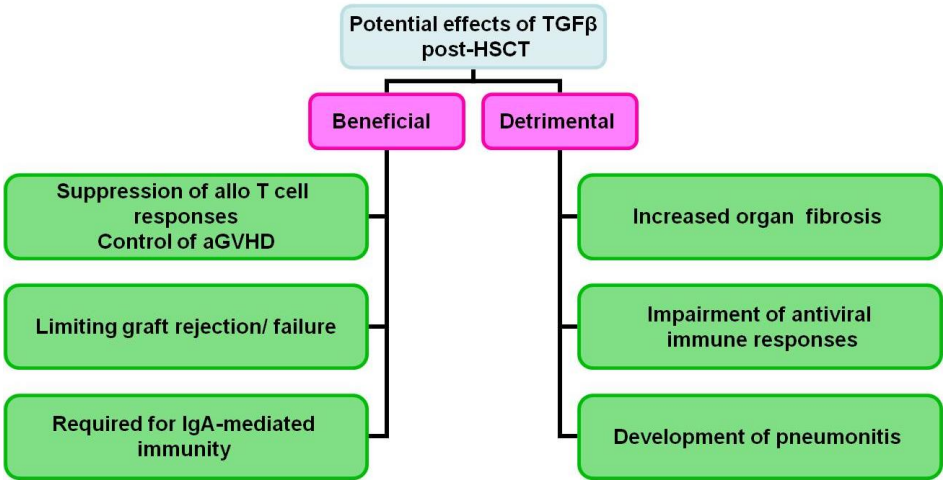

Figure 1.5 Potential effects of TGFβ post-HSCT (5). TGFβ is a pleiotropic cytokine with a complex role in the immune system. Dysregulation of TGFβ post-HSCT has several potential effects, both beneficial and detrimental.

Pulmonary Fibrosis and TGFβ

Organ injury and fibrosis are detrimental complications of HSCT. Fibrosis is characterized by dysregulated deposition of extracellular matrix (ECM) proteins such as collagen, ultimately leading to organ scarring and failure. The fibrotic process in the lung can be initiated following epithelial cell injury, where mesenchymal cells including fibroblasts and myofibroblasts produce collagen and other ECM proteins. Pulmonary fibrosis can occur as a complication of HSCT (3). TGFβ, as a central molecule in the pathogenesis of fibrotic disease (121), is a potential biomarker for development of fibrotic complications. TGFβ1 can stimulate collagen deposition by fibroblasts and myofibroblasts leading to fibrosis (83). Furthermore, the ability of TGFβ1 to induce alpha smooth muscle actin expression in lung myofibroblasts also leads to alveolar contraction, which further limits gas exchange (125).

Patients who developed pulmonary fibrosis as a result of autologous transplant for treatment of breast cancer had increased levels of plasma TGFβ prior to transplant conditioning when compared to patients who did not develop disease and healthy controls (126). The role of transplant-induced TGFβ in the induction of fibrotic disease following HSCT in humans has not been evaluated; however, irradiation injury has been shown to induce TGFβ1 in both human and animal lungs (34, 124, 127). Taken together, these data strongly support a role for TGFβ in mediating the fibrotic complications which occur late post-HSCT.

Pulmonary fibrosis is thought to be mediated by several pro-fibrotic factors in addition to TGFβ. Oxidative stress, including production of reactive oxygen and nitrogen species, has been implicated in contributing to pulmonary fibrosis in both human (128) and murine (129) studies. Indeed, reactive nitrogen intermediates have been shown in animal studies to stimulate production of TGFβ (130). The mechanisms by which reactive oxygen intermediates may promote fibrosis include their ability to activate the transcription factors NFκB and AP-1, promoting inflammation, and their ability to directly degrade ECM components (131). In addition, one study has shown that low levels of hydrogen peroxide can promote proliferation of human fibroblast cell lines *in vitro* (132). Activation of the coagulation cascade has also been shown to promote pulmonary fibrosis (133).

Alternatively Activated Macrophages

Alveolar macrophages are the cell type which comprises the large majority of cells in the alveolar space of the lung under baseline conditions. In general, macrophages

can be activated to one of two general phenotypes: classical activation or alternative activation. Classically-activated macrophages are pro-inflammatory cells which express inducible nitric oxide synthase (iNOS), and their phenotype is induced by IFNγ. Alternatively activated macrophages are phenotypically and functionally distinct from classically activated macrophages. These cells play a role in the normal wound repair process and have been shown to promote fibrosis. Alternatively activated macrophages are identified by expression of arginase-1, an enzyme which promotes collagen production and fibroblast proliferation (134, 135). Alveolar macrophages from idiopathic pulmonary fibrosis patients and in a murine model of γHV-68-induced pulmonary fibrosis have been shown to express arginase-1 (136). In this chronic γHV-68-induced pulmonary fibrosis model in IFNγ receptor knock-out mice, the alveolar macrophages were reported to be histologically large and foamy (136). Development of alternatively activated macrophages is thought to be largely dependent on the production of Th2-type cytokines, including IL-4 and IL-13 which can both directly induce alternative activation (135).

γHV-68 and Fibrosis

Infection with γHV-68 has been reported to potentiate the development of fibrosis in several murine model systems. γHV-68-infected IFNγ receptor KO mice develop multi-organ fibrosis (137), and splenic fibrosis in these mice has been related to the development of alternatively activated macrophages expressing the pro-fibrotic gene arginase-1 (138). Additionally, the development of γHV-68-induced pulmonary fibrosis in IFNγ receptor deficient mice also suggests a role for alternatively activated

macrophages in disease pathogenesis (136). In both of these cases, the Th2-skewed nature of the mouse likely contributed to the alternative activation of the macrophages.

Studies from our laboratory have shown the ability of γHV-68 infection to augment pulmonary fibrosis in wild type mice. γHV-68 can cause increased collagen deposition, fibrocyte recruitment, and diminished lung function when given to mice with established pulmonary fibrosis due to intratracheal instillation of fluorescein isothiocyanate (139). Additionally, mice develop more severe disease if given fibrotic challenge following γHV-68 infection and latency compared to uninfected mice (140). Potential mechanisms include virus-induced upregulation of pro-fibrotic factors, including TGFβ, which persist during viral latency (67).

Antigen Presenting Cells

Antigen presenting cells (APCs) are critical for development of an effective adaptive immune response to pathogens. Dendritic cells are considered to be professional APCs and the key cell type which bridges innate and adaptive immune responses. The current paradigm holds that immature dendritic cells in the tissues sample their environment by macropinocytosis and present antigens on surface MHC molecules. Dendritic cells can become activated upon recognition of a pathogen via PRRs, including TLR stimulation. Mature dendritic cells then migrate from the periphery to secondary lymphoid tissues, where they express high levels of MHC Class II and upregulate the costimulatory molecules CD80, CD86, and CD40, among others, which are important for initiation of T cell responses (141). Cytokine production by dendritic cells during T cell

priming in the lymph node is thought to, in turn, promote specific programs of cytokine production by T cells.

Dendritic cell numbers may remain reduced even at 1 year post-HSCT (142). The functionality of these cells post-HSCT may depend on the stem cell source, as cord blood-derived dendritic cells may have decreased MHC and adhesion molecule expression. While some studies have indicated that monocyte-derived dendritic cells from HSCT patients have reduced costimulatory and MHC expression (143), other studies have shown no reduced functionality. One study of autologous HSCT patients found that at six months post-transplant, these cells had even more potent antigen-presenting capacity than dendritic cells generated from the patients prior to transplant (10). Dendritic cell-based immunotherapies are being considered in the HSCT context, in terms of inducing tolerogenic responses to alloantigens and, conversely, promoting anti-tumor responses, as well as in promoting anti-pathogenic responses (142).

Helper T Cell Differentiation

Naïve CD4 cells (Th0) can differentiate into cytokine-producing Th1, Th2, and Th17 helper T cell subsets, generally characterized by the hallmark cytokines they produce, though recent studies have shown a degree of plasticity which exists between T cell subsets (144, 145). Cytokine signals from APCs, such as dendritic cells, at the time of T cell activation are thought to be important in skewing CD4 cells toward specific lineages.

Th1 cells are characterized by production of their hallmark cytokine, IFNγ, as well as IL-2. Th1 cells differentiate in the presence of IL-12p70 (a heterodimer consisting

of IL-12p35 and IL-12p40) and are affirmed through subsequent IFN-γ production. Th2 cells are thought to be induced by IL-4, and these cells produce IL-4, IL-13, and IL-5, among others. Th1 cells express the transcription factor Tbet, while Th2 cells express GATA-3; these two transcription factors are known to be mutually antagonistic. Th17 cells, identified by IL-17a, IL-17f, and IL-22 production, can be induced by TGFβ in conjunction with pro-inflammatory cytokines such as IL-6 or IL-1β (146). Th17 cells are also defined by expression of the transcription factors RORγt and RORα. Figure 1.6 diagrams the general paradigm regarding differentiation of naïve T cells. Naïve CD4 T cells can also differentiate into regulatory T cells, which are discussed in the next section.

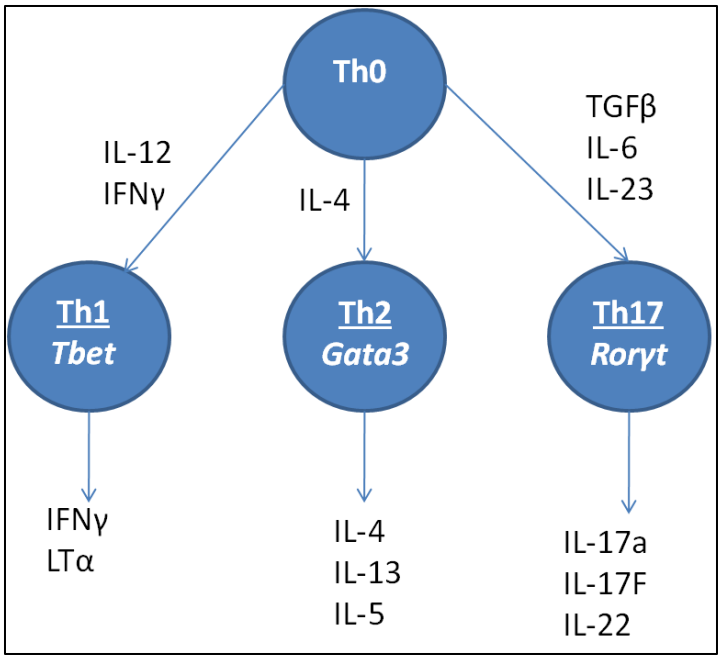

Figure 1.6. Helper T cell differentiation (Adapted from (147)). Undifferentiated CD4 T cells (Th0) can be skewed by the cytokine environment to adopt specific transcription factor and cytokine profiles.

Studies have indicated that alterations in T cell differentiation occur post-autologous HSCT. In addition to reduction in IL-2 production by peripheral T cells post-HSCT, it has been reported that upon *in vitro* stimulation with PHA and PMA, PBMCs from autologous transplant recipients produce significantly reduced IFNγ and IL-4 within 6 months post-engraftment (148). Whether these alterations have functional impact on immune responses to pathogens has not been evaluated.

Regulatory T Cells

Tregs are a specific subset of CD4 cells which function to suppress immune responses of effector T cells. Tregs can develop through the thymus (natural or nTregs) and are broadly defined by constitutive expression of the high-affinity IL-2 receptor, CD25, as well as the transcription factor Foxp3, CTLA-4 and GITR (149). Tregs can also develop in the periphery, as naïve CD4 cells can be induced to gain suppressive function (inducible or iTregs). TGFβ has been shown to convert naïve CD4 cells to Tregs and induce the expansion of these cells (106). Tregs play an important role in maintaining peripheral tolerance and immune homeostasis, preventing T cell mediated autoimmunity, as mice and humans deficient in Foxp3 develop multi-organ autoimmunity (149). The mechanisms by which Tregs mediate their immunosuppressive functions have not been definitively described, but studies indicate that production of TGFβ and IL-10 are important for Treg-mediated suppression (150).

In the setting of HSCT, Tregs have been best described in their ability to induce graft tolerance and suppress GVHD (151). It has also been suggested that Treg populations are altered following HSCT; indeed, several studies indicate that Treg

populations expand post-HSCT. One study showed a significant increase in the percent CD4+Foxp3+ cells in the bone marrow of multiple myeloma patients following allogeneic HSCT compared to newly diagnosed multiple myeloma patients and healthy donors (152). Accordingly, Foxp3 mRNA expression in peripheral CD4 cells was found to be increased post-transplant (compared to pre-transplant and donor levels) in a cohort of elderly patients despite receiving CD25-depleted allografts (153). Increased frequencies of CD4+CD25^{hi} Tregs were also reported in the peripheral blood of chronic myeloid leukemia patients that had undergone allogeneic HSCT compared to newly diagnosed patients and healthy controls; functionally, these cells were more effective at suppressing T cell proliferation in an in vitro assay as compared to healthy donors (154). In a mouse model of experimental BMT, it was shown that the host Treg population in the spleen could expand following transplant and that these host-derived cells could persist for months post-transplant (155).

The potent ability of Tregs to suppress effector T cell responses allows the possibility that upregulation of Tregs post-HSCT may impact T cell-mediated immunity and contribute to the infectious complications which occur post-transplant. However, one recent study demonstrated that adoptive transfer of Tregs into mice receiving an allogeneic BMT could limit GVHD, but did not impair the ability of the BMT mice to respond to lethal CMV infection (156).

Rationale for Virus Infection Studies in BMT Mice

Due to advances in prophylaxis, detection, and anti-viral therapy, infectious complications due to viral infections post-HSCT have been reduced in recent years (50,

51). Improved outcomes, however, are dependent on treatment with anti-viral drugs, and the emergence of viral strains that are resistant to drug therapy (157, 158) highlights the need to better understand the underlying immune responses that occur in transplant patients.

Because opportunistic infections have been reported to occur late post-transplant in autologous HSCT recipients (6, 7), and because functional deficits of immune cell function post-transplant have been reported *in vitro* (8-12), we hypothesized that post-transplant alterations in immune cell function could contribute to increased susceptibility to virus infection post-HSCT. Additionally, based on the recent prospective study showing that early post-HSCT virus infection was associated with development of late non-infectious pulmonary complications (13), we hypothesized that uncontrolled pulmonary virus infection post-HSCT, due to functional deficits in immune cells, could contribute to later development of pneumonitis.

To test these hypotheses, we chose to use a murine BMT model and pulmonary infection with γHV-68. Studies were performed using a syngeneic BMT model, which allows for controlled study of how conditioning and subsequent transfer of cells leads to alterations in immune responses following cellular reconstitution. This model provides insight into immune changes that occur as result of conditioning and transplantation alone, in the absence of GVHD and immunosuppressive drug therapy. Additional preliminary studies were performed to confirm results in a fully allogeneic BMT model. We chose to use well-studied murine herpesvirus, γHV-68, as a model pathogen for these studies, as herpesvirus infections are especially prominent in HSCT recipients (29, 159, 160).

Our studies establish a murine BMT model in which mice have increased susceptibility to pulmonary gammaherpesvirus infection in the absence of GVHD or immunosuppressive therapy, following reconstitution of immune cell numbers. Additionally, in our model, BMT mice develop severe gammaherpesvirus-induced pneumonitis, with pathological features similar to idiopathic pneumonia syndrome, which occurs during viral latency. Our model reveals alterations in immune cell responses and changes in cytokine production by hematopoietic and structural cells post-HSCT, which contribute to the impaired anti-viral response. Our data provide new insight into the potential causes of impaired anti-viral immune responses and development of pneumonitis in HSCT patients.

Chapter 2

Materials and Methods

Mice

C57BL/6 and CD4KO mice were purchased from The Jackson Laboratory (Bar Harbour, ME). Mice expressing dominant negative TGFβ receptor II under the permissive CD4 promoter backcrossed to the C57BL/6 background (104) were bred at the University of Michigan and obtained from Dr. Keith Bishop. Due to the nature of the promoter construct, these mice lack functional TGFβ receptor II in both CD4 and CD8 T cells (104). Mice expressing the same construct under the CD11c promoter (114), provided by Dr. Yasmina Laouar, were bred at the University of Michigan. IL-10KO and IL-17aKO mice were obtained from Dr. Weiping Zou at the University of Michigan. Mice were housed in specific pathogen-free conditions and were monitored daily by veterinary staff. Experiments were approved by the University of Michigan Committee on the Use and Care of Animals.

Bone Marrow Transplantation

We performed syngeneic BMT as described previously (59, 60, 161). Recipient mice were treated with 13 to 13.5 Gy of total body irradiation using a ^{137}Cs irradiator, delivered in two doses separated by 3 hours. $5x10^6$ donor whole bone marrow cells from a genetically identical donor in 0.2 mL Dulbecco's Modified Eagle Medium (DMEM; Invitrogen, Carlsbad, CA) without serum were delivered to irradiated mice via tail vein

injection. Mice were given acidified water (pH 3.3) for the first three weeks post-BMT. Total numbers of hematopoietic cells were fully reconstituted in the lungs and spleen at 5 weeks post-BMT, with lung lymphocytes being 93% donor-derived at this time point (161). In some experiments, B6Ly5.2 mice purchased from the Fredrick Cancer Research Facility (Fredrick, MD) were used as bone marrow donors for irradiated B6Ly5.1 (Jackson Laboratory) recipients so that donor vs. host leukocytes could be distinguished by staining for the CD45.1 (Ly5.2) and CD45.2 (Ly5.1) alleles using antibodies commercially available from BD PharMingen (San Diego, CA). All infections were performed at 5 to 6 weeks post-BMT. Allogeneic transplants (C57BL/6 → Balb/c or Balb/c → C57BL/6) were performed in the same manner as syngeneic transplants. At 5 weeks post-BMT, both total lung cell numbers and lung CD4 T cell numbers were reconstituted in these mice. In some experiments, mice were conditioned with reduced intensity radiation (6.5 or 9 Gy).

γHV-68 Infection

γHV-68, clone WUMS, ($5x10^4$ plaque-forming units (pfu); American Type Culture Collection, Manassas, VA) was diluted in 20 μl of phosphate-buffered saline (PBS) and delivered intranasally (i.n.) to mice which had been anesthetized with ketamine and xylazine. In some experiments, mice were infected with $1x10^3$, $3x10^5$ or $1x10^6$ pfu.

Plaque Assay

Quantification of lytic virus from right lungs of mice was determined by plaque assay, as described previously (139). Briefly, right lungs were dissected from mice 7 days after infection and homogenized in 1 mL DMEM with 10% fetal calf serum (FCS)

supplemented with Complete protease inhibitor (Sigma, St. Louis, MO). Supernatants from right lung homogenates were diluted and placed in triplicate on sub-confluent monolayers of 3T12 cells (American Type Cell Culture Collection); plaques were enumerated 7 days later.

Real Time Reverse-Transcriptase Polymerase Chain Reaction

Real-time reverse transcriptase–polymerase chain reaction (RT-PCR) was performed on an ABI Prism 7000 thermocycler (Applied Biosystems, Foster City, CA) using a previously described protocol (60). Gene-specific primers and probes (Table 2.1) were designed using Primer Express software (Applied Biosystems). Each reaction contained 12.5 µl Taqman 2x Universal PCR Mix (Applied Biosystems), 0.625 µl 40x MultiScribe and RNase Inhibitor Mix (Applied Biosystems), 0.25 µM Taqman FAM/TAMRA-labeled probe, 0.3 µM forward primer, 0.3 µM reverse primer, 300 ng RNA and DEPC-treated water to give a final volume of 25 µl. Relative expression was determined using the delta delta Ct method (162), using β-actin as a control gene.

Table 2.1 Primers and probes for real time RT-PCR

Gene	Oligo	Sequence
DNA polymerase (ORF9)	F. primer	ACAGCAGCTGGCCATAAAGG
	R. primer	TCCTGCCCTGGAAAGTGATG
	Probe	CCTCTGGAATGTTGCCTTGCCTCCA
Capsid gene gB (ORF8)	F. primer	CGCTCATTACGGCCCAAA

	R. primer	ACCACGCCCTGGACAACTC
	Probe	TTGCCTATGACAAGCTGACCACCA
β-actin	F. primer	CCGTGAAAAGATGACCCAGATC
	R. primer	CACAGCCTGGATGGCTACGT
	Probe	TTTGAGACCTTCAACACCCCCAGCCA
M3	F. primer	AGTGGGCTCACGCTGTACTTGT
	R. primer	TGTCTCTGCTCACTCCATTTGG
	Probe	CATGGGCAAGTGTTCATCTTAGCC
Collagen 1	F. primer	TGACTGGAAGAGCGGAGAGTACT
	R. primer	GGTCTGACCTGTCTCCATGTTG
	Probe	CTGCAACCTGGACGCCATCAAGG
Collagen 3	F. primer	GGATCTGTCCTTTGCGATGAC
	R. primer	GCTGTGGGCATATTGCACAA
	Probe	TGCCCCAACCCAGAGATCCCATTT
iNOS	F. primer	ACATCAGGTCGGCCATCACT
	R. primer	CGTACCGGATGAGCTGTGAAT
	Probe	CCCCAGCGGAGTGACGGCA

Arginase-1	F. primer	ACCACAGTCTGGCAGTTGGAA
	R. primer	GCATCCACCCAAATGACACA
	Probe	CTGGCCACGCCAGGGTCCAC

Histology

Lungs were harvested for histology as previously described (163). Lungs from euthanized animals were perfused with PBS, inflated with 1 mL of 10% neutral buffered formalin, removed, and fixed for 6-24 hours in formalin. Lungs were dehydrated in ethanol for at least 24h, embedded in paraffin and cut into 3-μm sections. Sections were placed on slides and stained with hematoxylin and eosin (H&E) or Masson's Trichrome Blue for collagen deposition.

Pathology Scoring

H&E and Trichrome-stained slides were analyzed by a pulmonary pathologist in a blinded fashion. Lungs were scored for the severity of fibrosis, perivascular inflammation, and peripheral inflammation on a scale of 0 (absent) to 3 (severe). The presence of foamy alveolar macrophages and hyaline membranes was graded as 0 (absent) or 1 (present). The scores for each parameter were totaled to give a pathology score, with 11 being the most severe phenotype. Scoresheet is shown in Figure 2.1.

	None/ Absent	Mild	Moderate	Severe
Fibrosis	0	1	2	3
Perivascular inflammation	0	1	2	3
Peripheral inflammation	0	1	2	3

	Absent	Present
Foamy AMs	0	1
Hyaline Membranes	0	1

Total_____/11

Figure 2.1. Pathology scoring system.

Oxygen Saturation Measurements

Oxygen saturation was measured using a MouseOx Pulse Oximeter according to the manufacturer's instructions (Starr Life Sciences Corp., Oakmont, PA). Mice were anesthetized and neck hair was removed using a depilatory cream. 24 hours later, collar clip sensors were placed on awake mice, and oxygen saturation was measured as an average over 15 seconds per mouse.

Bronchoalveolar Lavage (BAL)

BAL was performed as previously described, with modifications (60). Cells were isolated from the alveolar space by lavaging with 20 mL of PBS containing 5mM EDTA in successive 1 mL aliquots. BAL fluid (BALF) was harvested by instilling 1 mL of PBS containing 5mM EDTA into lung and removing fluid by suction; BALF was centrifuged to remove cells.

Measurement of Reactive Oxygen Species

Samples were assayed for hydrogen peroxide using the Amplex Red Hydrogen Peroxide/ Peroxidase Assay Kit (Invitrogen Molecular Probes, Inc., Eugene, OR) and for nitrite using the Griess Reagent System (Promega Corporation, Madison, WI) following the manufacturer's instructions.

Flow Cytometry

For some experiments, whole lungs or right lungs were prepared for flow cytometry by collagenase digestion, as described previously (164). $1x10^6 – 2.5 x10^6$ cells were stained for flow cytometry using fluorochrome-conjugated antibodies against the cell surface markers CD45, CD4, CD8, CD19, NK1.1, TCRβ, CD11c, I-A^b, and CD25 (BD Pharmingen, San Jose, CA) following incubation with anti-CD16/CD32 (FcBlock, BD Pharmingen). Forkhead box protein 3 (Foxp3) staining was performed using PE Anti-Mouse/ Rat Foxp3 Staining Set (eBioscience, San Diego, CA), following the manufacturer's instructions. For intracellular cytokine staining, cells were first stimulated with phorbol 12-myristate 13-acetate (PMA, Sigma, 0.05 μg/mL) and ionomycin (Sigma, 0.75 μg/mL) for 6 hours in the presence of Golgi Stop protein transport inhibitor (BD Pharmingen). Anti- IL-17a antibody was obtained from BD Pharmingen, and anti-IFNγ from eBioscience. For collagenase-digested lung cells, gates were first set on CD45-expressing cells followed by gating on the lymphocyte-sized subset when appropriate. Data was analyzed using FlowJo Flow Cytometry Analysis Software, version 7.5.

Mixed Leukocyte Reactions

Mixed leukocyte reactions (MLRs) were performed as described, with modifications (92). $2x10^5$ stimulator (irradiated, 1.6 Gy) and 1, 2, or $4x10^5$ responder cells were co-cultured in a 96-well plate for 4 days in RPMI-1640 (Hyclone Laboratories, Inc., Logan, UT) supplemented with 10% FCS. 1 μCi of ^{3}H- thymidine was added for the last 18 hours of culture. Proliferation was determined by subtracting counts per minute (cpm) of responders alone from cpm in wells containing both responders and stimulators. For some experiments, bone marrow derived dendritic cells (BMDCs) were used as stimulators. BMDCs were prepared as described (165), with modifications. Total bone marrow was seeded at $2x10^6$-$5x10^6$ cells in 100 mm Petri dishes containing 10 mL RPMI-1640 and 20 ng/mL GM-CSF (Peprotech, Rocky Hill, NJ). Cells were fed an additional 10 mL of media and GM-CSF at day 3, and non-adherent BMDCs were harvested from the plates at day 7. In other experiments, whole spleen cells were used as stimulators. Responder cells were either total spleen cells or CD4 cells magnetically purified from the spleen using MACS CD4 (L3T4) MicroBeads (Miltenyi Biotech, Auburn, CA). BMDCs were stained for expression of I-A^b, CD80 and CD86 using antibodies from Pharmingen.

Alveolar Epithelial Cell (AEC) Isolation

Type II AECs were isolated using dispase and DNase digestion of lungs as previously described (166, 167). Bone marrow-derived cells were removed via anti-CD32 and anti-CD45 magnetic depletion. Mesenchymal cells were removed by overnight adherence in a petri dish. Non-adherent cells were plated at $1x10^6$ cells per well in 24-well plates which

had been previously coated with fibronectin for 72 h. The media was changed to serum-free media and supernatants were collected 24 h later for determination of TGFβ1 levels by ELISA. Immunohistochemical staining of AEC preparations revealed cells were >94% positive for e-cadherin with less than 3% contamination by vimentin-positive mesenchymal cells.

Viral Genome Quantification

DNA was prepared from γHV-68-infected lungs using the Qiagen DNeasy Blood and Tissue Kit (Valencia, CA), and real time PCR was performed to detect viral gB DNA as previously described (67, 168). Values were compared to a standard curve consisting of gB plasmid DNA diluted at known copy numbers. Reported values were normalized to 100 ng of input DNA for each reaction. For gB DNA analysis, the forward primer was 5'GGCCCAAATTCAATTTGCCT, the reverse primer was 5'CCCTGGACAACTCCTCAAGC and the probe was 5'6-(FAM)-ACAAGCTGACCACCAGCGTCAACAAC-(TAMRA).

Viral Immunohistochemistry

Frozen lung sections were prepared from infected mice and γHV68 was detected using a rabbit polyclonal anti- γHV68 sera (169) provided by Dr. Skip Virgin (Washington University School of Medicine, St. Louis, MO). Staining was detected with a goat anti-rabbit secondary conjugated to alkaline phosphatase.

ELISA

Whole lungs were homogenized in 1 mL PBS supplemented with Complete protease inhibitor (Sigma); homogenates were spun down and resulting supernatant or cell culture supernatants were assayed for cytokines using the DuoSet ELISA Development System kits (R&D Systems, Minneapolis, MN) following the manufacturer's instructions. For TGFβ1 ELISAs, samples were acid-treated and then neutralized in order to activate TGFβ prior to assay. Prostaglandin E_2 (PGE_2) was measured using an EIA kit from Cayman Chemicals (Ann Arbor, MI) according to manufacturer's instructions.

Regulatory T cell (Treg) Depletion

Treg depletion was performed by giving mice a single intraperitoneal (i.p.) injection of 100 μl anti-CD25 ascites (PC61) at 4 weeks post-BMT. Control mice were given 100 μg isotype control antibody.

Reagents Used

Complete media is DMEM (Lonza, Walkersville, MD) with 10% fetal bovine serum (Fisher, Pittsburgh, PA), 1% penicillin-streptomycin (Gibco/Invitrogen, Carlsbad, CA), 1% L-glutamine (Fisher) and 0.1% amphotericin B (Lonza). Serum-free media is DMEM with 1% bovine serum albumin (Sigma, St. Louis, MO), 1% penicillin-streptomycin, 1%L-glutamine, 0.1% amphotericin B.

Statistical Analyses

Statistical significance between 2 groups was measured by Student's t-test using Graphpad Prism 5 software (La Jolla, CA). Data represent mean ± SEM; $p < 0.05$ was considered significant.

Chapter 3

Results

BMT mice have increased viral loads at d7 post-infection with γHV-68

In order to understand whether BMT mice were more susceptible to gammaherpesvirus infection following transplant and immune reconstitution, we first infected syngeneic BMT mice at 5 weeks post-transplant with $5x10^4$ pfu γHV-68 i.n. For comparison, we also infected naïve, non-transplanted control mice. We then harvested whole lungs from both groups at d7 post-infection, a time point near the peak of lytic virus replication. Left lungs were harvested for RNA, and expression of lytic viral genes was determined using real time RT-PCR. Expression of both the envelope glycoprotein gene *gB* (Figure 3.1A) and viral *DNA polymerase* (Figure 3.1B) was significantly increased in lungs from BMT mice compared to non-transplanted control mice. To confirm increased susceptibility to viral infection, right lungs were harvested for plaque assay to quantify lytic viral load. Again, BMT mice displayed significantly higher levels of lytic virus compared to non-transplanted control mice (Figure 3.1C). Immunohistochemistry on frozen lung sections using polyclonal anti-γHV-68 serum against lytic viral proteins further confirmed increased virus in the BMT mice (Figure 3.1D).

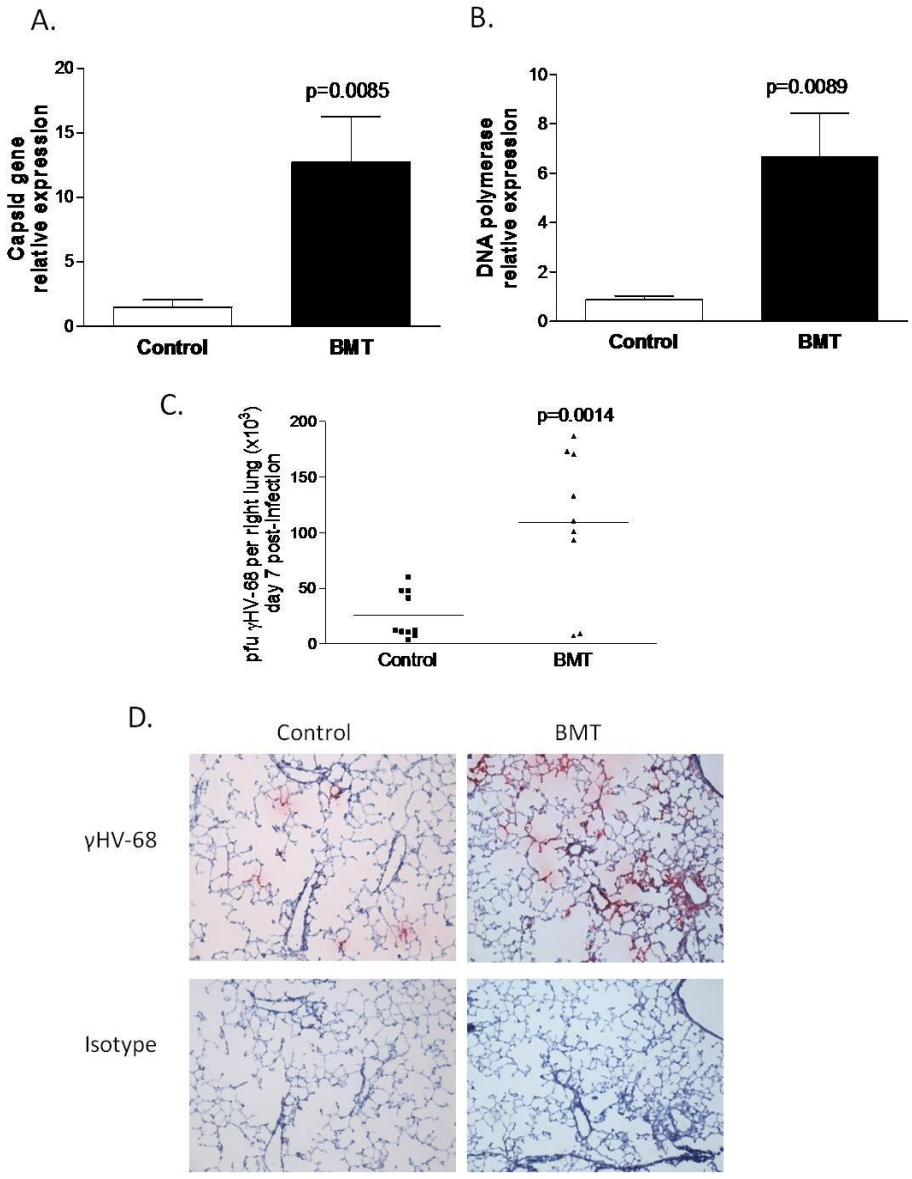

Figure 3.1. *BMT mice have higher viral burden in the lungs at d7 post-infection 5 weeks following BMT.* Control and syngeneic BMT mice were infected i.n. with $5x10^4$ pfu γHV-68 5 weeks following BMT. *A.* and *B.* At d7 post-infection, left lungs were processed for RNA and expression of lytic viral genes was measured using real time RT-PCR. Expression of the viral capsid gene *gB* and viral *DNA polymerase* was significantly increased (*p=0.0085* and *p=0.0089*, respectively*)* in the lungs of BMT mice when compared to non-transplanted controls (data combined from 2 experiments). *C.* At d7 post-infection, right lungs from BMT and control mice were harvested for plaque assay (*p*=0.0014, *n*=10 control, 9 BMT, data combined from 2 experiments). *D.* Frozen sections of lungs from control and BMT mice were prepared at day 7 post-infection and were stained with rabbit polyclonal antisera against γHV68 or with non-immune rabbit sera as control. The goat anti-rabbit secondary was linked to alkaline phosphatase. Original magnification is x100.

These studies were performed using a myeloablative conditioning regimen (1350 rads) which our laboratory previously described to result in maximum reconstitution of the lung by donor-derived leukocytes (170). To determine whether the increased susceptibility to γHV-68 post-BMT was related to myeloablative conditioning, we next transplanted mice using three conditioning regimens (650, 900, and 1350 rads). At 5 weeks post-transplant, mice were infected with $5x10^4$ pfu γHV-68. At d7 post-infection, lungs were harvested for RNA, and expression of the lytic viral genes, *gB* and DNA *polymerase*, was determined using real time RT-PCR. Expression of both the capsid gene and DNA polymerase increased with higher irradiation dose, reaching statistical significance in the mice conditioned with 1350 rads (Figure 3.2).

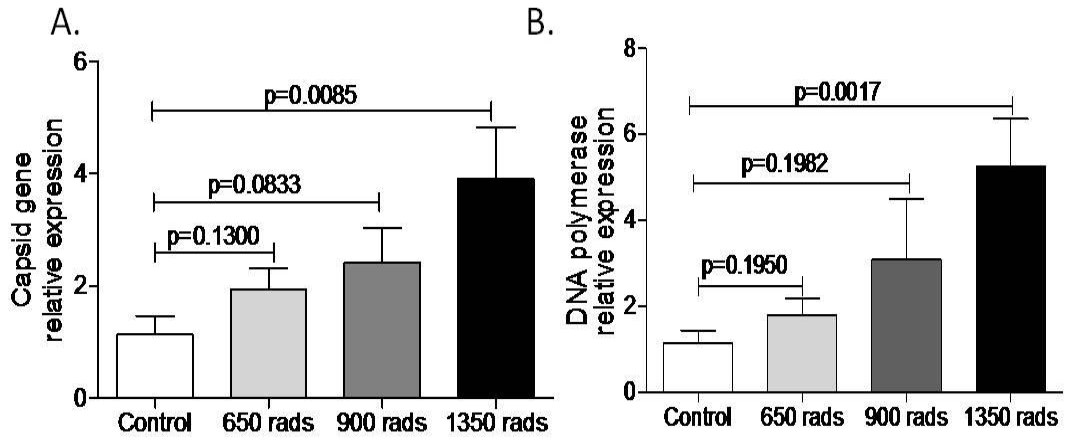

Figure 3.2 *Increased susceptibility to γHV-68 depends on myeloablative conditioning*. Control and BMT mice at 5 weeks post-BMT (conditioned with 650, 900, or 1350 rads) were infected i.n. with $5x10^4$ pfu γHV-68. At d7 post-infection, lungs were processed for RNA and expression of lytic viral genes was measured using real time RT-PCR. Expression of the viral capsid gene *gB* and viral *DNA polymerase* was significantly increased (*p=0.0085* and *p=0.0017*, respectively) in the lungs of BMT mice conditioned with 1350 rads when compared to non-transplanted controls (*n*=at least 9 mice per group; data combined from 2 experiments).

We next determined whether the increased susceptibility of BMT mice to γHV-68 infection was also dependent on the dose of virus. To test this, BMT and control mice were challenged with three doses of γHV-68. At d7 post-infection, lungs were harvested for RNA and relative expression of the viral capsid gene and viral DNA polymerase were determined using real time RT-PCR. Relative expression of both genes increased in the BMT lungs compared to non-transplant controls with increasing virus dose (Figure 3.3).

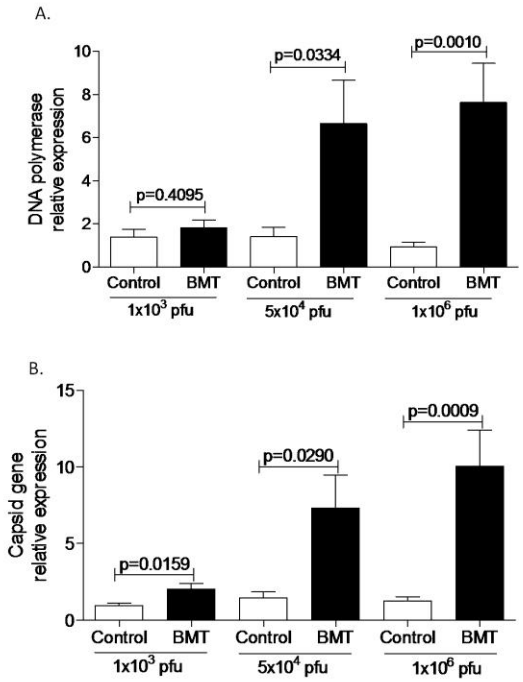

Figure 3.3. *BMT mice show increased susceptibility to γHV-68 when challenged with higher viral dose.* Control and BMT mice were infected i.n. with $1x10^3$, $5x10^4$ or $1x10^6$ pfu of γHV-68. At day 7 post-infection, left lungs were harvested, processed for RNA, and expression of viral genes was analyzed by real time RT-PCR. Expression in control lungs was normalized to 1 for each viral dose. *A.* Expression of viral *DNA polymerase* was significantly increased in the lungs of BMT mice challenged with $5x10^4$ and $1x10^6$ pfu γHV-68. *B.* Expression of the viral capsid gene *gB* was significantly increased in the lungs of BMT mice challenged with all three doses of virus (*n*= at least 5 mice per group; data combined from 2 experiments).

BMT and control mice have equivalent latent viral loads by d21 post-infection

Based on the conditioning and dose-titration experiments, subsequent studies were carried out using myeloablative conditioning and $5x10^4$ pfu γHV-68. Following i.n. infection in immunocompetent mice, lytic replication of γHV-68 in the lungs largely subsides by d14; by d21 post-infection, latency is established with very little viral replication occurring (140). To determine the course of virus infection in BMT mice beyond the peak lytic phase, lungs were harvested from BMT and control mice at days 14 and 21 post-infection with $5x10^4$ pfu γHV-68. Lungs were then analyzed for expression of viral transcripts and levels of viral genome were quantified. Using real time RT-PCR on lung RNA, we found that expression of the viral genes *K3* and *M3* (which can be expressed during both lytic infection and latency) were significantly increased in BMT lungs compared to control at d14 (Figure 3.4A, B). To confirm this increase, we harvested DNA from lungs at d14 post-infection and quantified copy numbers of the viral genome using real time PCR and a plasmid standard containing known copy numbers of gB DNA (Figure 3.4C). There was a trend towards increased viral genomes in BMT mouse lungs at d14.

At d21 post-infection, relative mRNA expression of the lytic/ latent viral gene *M3* was expressed at significantly higher levels compared to the lytic viral gene *gB*, suggesting that γHV-68 was predominantly latent at this time point in both BMT and control mice. Additionally, we found no significant difference between levels of either gene in lungs of BMT or control mice (Figure 3.5A). To confirm that there was no difference in latent viral load, we harvested DNA from lungs at d21 post-infection and quantified copy numbers of the viral genome using real time PCR. We found no

significant difference in quantities of viral genomes between BMT and control mice (Figure 3.5B). Thus, by three weeks post-infection, γHV-68 infection is latent and latent viral loads are not different between BMT and control mice.

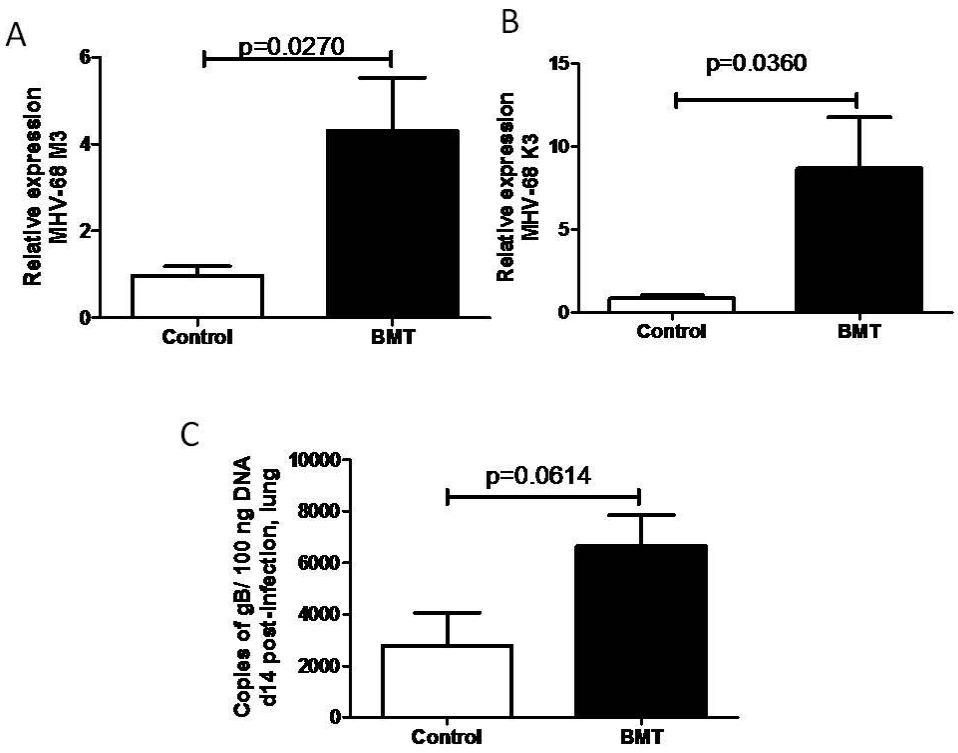

Figure 3.4 *BMT mice have increased viral load at d14 post-infection with γHV-68*. Control and BMT mice were infected with $5x10^4$ pfu γHV-68 i.n. *A.* and *B.* At d14 post-infection, lungs were harvested for RNA and expression of the viral genes *K3* and *M3* was measured using real time RT-PCR. Expression of both genes was significantly increased in BMT lungs. *C.* At d14 post-infection, lungs were harvested for DNA and copy number of viral *gB* gene was quantified using real time PCR using a standard with known quantities of *gB* DNA (*n=5* mice per group).

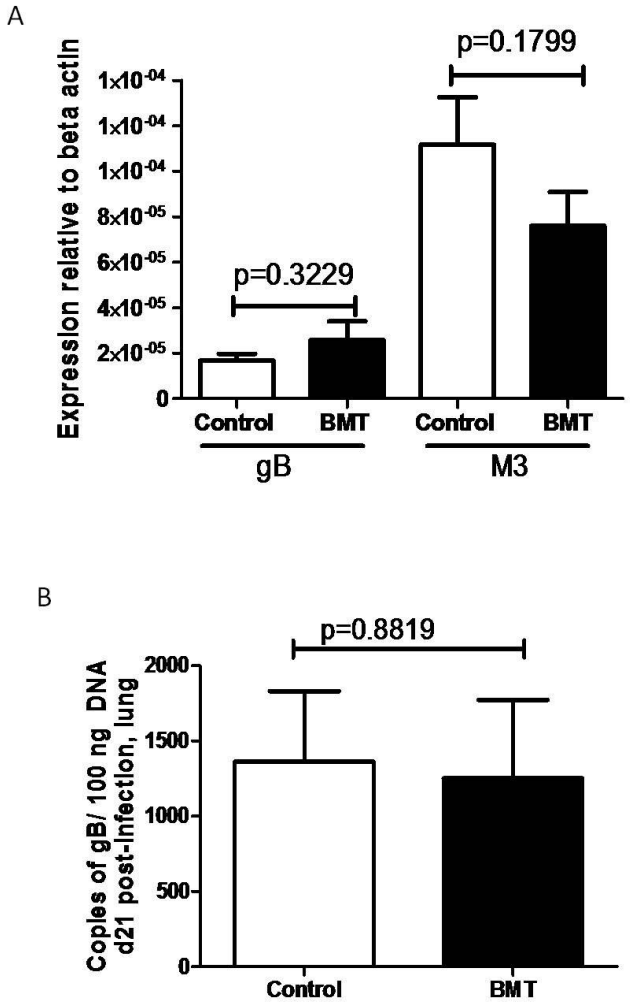

Figure 3.5 *BMT and control mice have similar latent viral load at d21 post-infection with γHV-68.* Control and BMT mice (5 weeks post-transplant) were infected with $5x10^4$ pfu γHV-68 intranasally. *A.* At d21 post-infection, lungs were harvested for RNA and expression of the lytic viral capsid gene *gB* and the predominantly latent viral gene *M3* were measured using real time RT-PCR. There was no significant difference in expression of either of these genes between BMT and control mice. Expression of *M3* was significantly increased over *gB* in both control and BMT lungs (*p=0.0002* and *p=0.0081*, respectively) (*n*=11 mice per group; data combined from 2 experiments). *B.* At d21 post-infection, lungs were harvested for DNA and copy number of viral *gB* gene was quantified using real time PCR using a standard with known quantities of *gB* DNA. There was no significant difference in latent viral genome load between BMT and control groups (*n*=3 mice per group; representative of 2 independent experiments).

BMT mice develop severe virus-induced pneumonitis and fibrosis during virus latency

Because of the differences in viral load noted in BMT mice at days 7 and 14 post-infection, we hypothesized that there might be differences in the inflammatory response to the lung between control and BMT mice. To test this hypothesis, lungs were harvested for histology and H&E staining at days 7, 14, and 21 post-infection with $5x10^4$ pfu γHV-68. We found similar infiltration of inflammatory cells between BMT and control mice at d7 post-infection (Figure 3.6A). However, at d14 and d21 post-infection, BMT mice develop a severe pneumonitis response not seen in the control setting (Figure 3.6B, C). Magnified lung sections at d21 post-infection show filling of the alveolar space with inflammatory cells, as well as evidence of diffuse alveolar damage and destruction of the alveolar architecture (Figure 3.7). Additionally, damaged airway epithelial cells are evident (Figure 3.7).

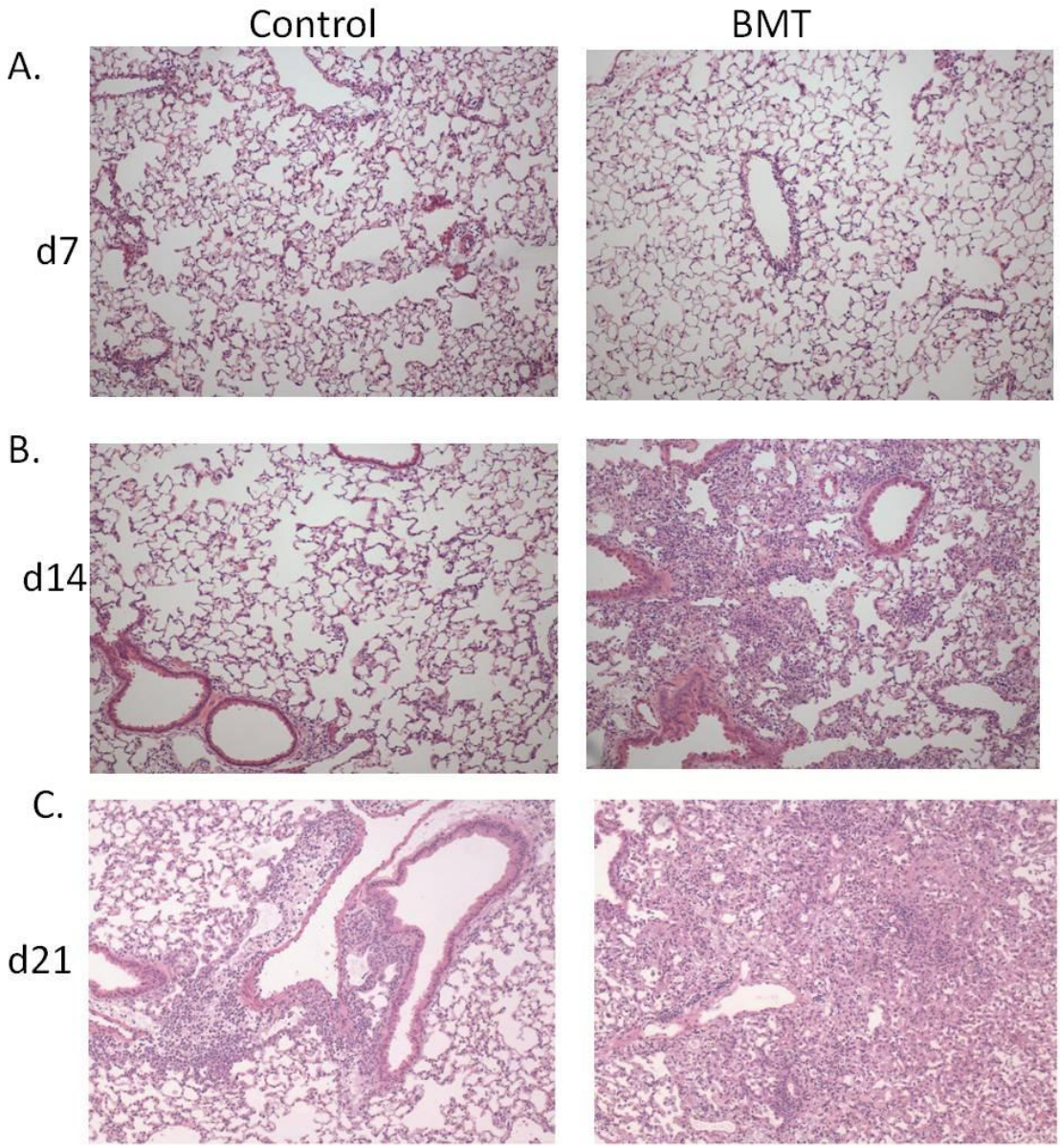

Figure 3.6 *BMT mice develop severe pneumonitis during virus latency*. BMT and control mice were infected i.n. with $5x10^4$ pfu γHV-68. At days 7, 14, and 21 post-infection, lungs were harvested for histology and sections were stained with H&E. Sections shown are representative of *n*=2 d7, 3 d14, and at least 10 d21 per group. Magnification is 100x.

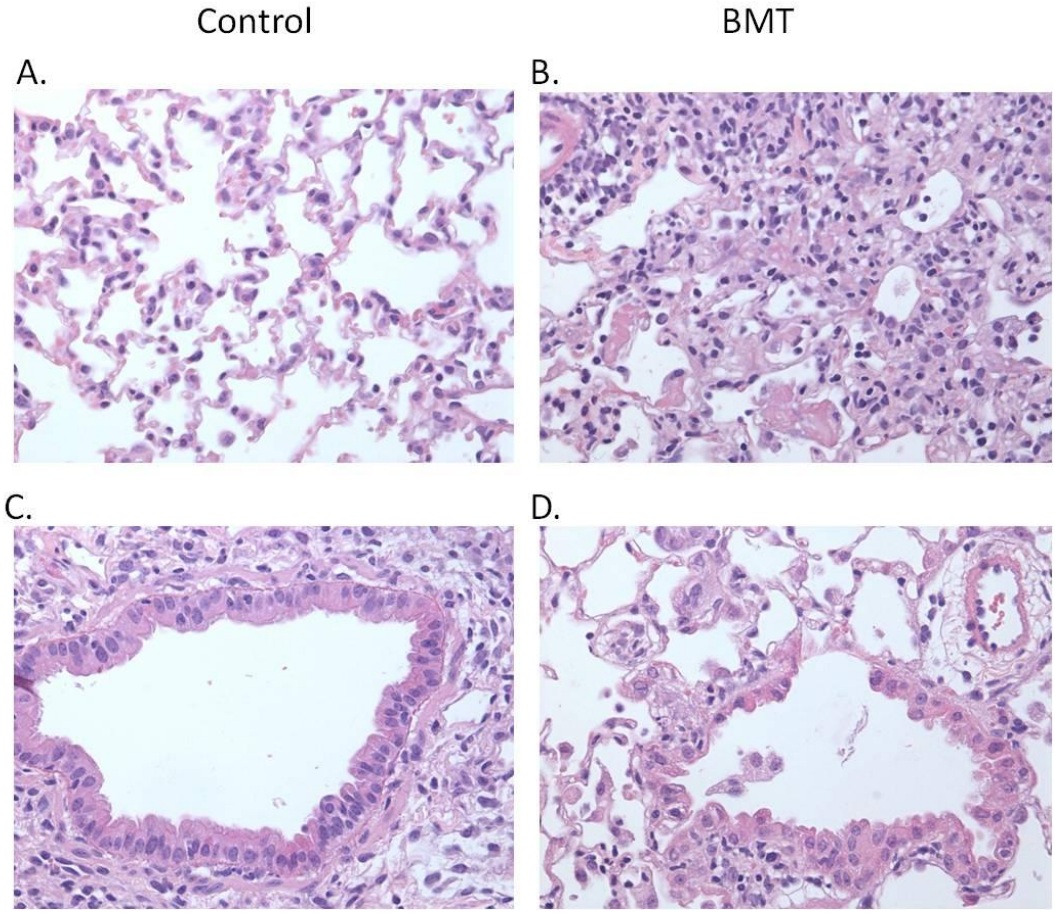

Figure 3.7 *Pneumonitis is increased following γHV-68 infection in BMT mice*. Non-transplant control mice (panels A, C) or mice at 5 weeks post-BMT (panels B, D) were infected with $5x10^4$ pfu γHV-68 and lungs were analyzed for histology 21 days post-infection. 400x magnification of H&E stained lung sections reveals alveolar filling, evidence of diffuse alveolar damage and destruction of alveolar architecture in BMT mice (B), as well as damaged airway epithelium (D).

Because of the severe inflammatory phenotype and lung damage observed in BMT mice at d21 post-infection, and due to data implicating γHV-68 as a factor for fibrosis development in murine models (136, 139, 140), we hypothesized that BMT lungs may be fibrotic during virus latency. Lung sections from control and BMT mice at days 7, 14, and 21 post-infection with $5x10^4$ pfu γHV-68 were stained with Trichrome to determine collagen deposition. Trichrome-stained lung sections indicated mild to moderate fibrosis in the BMT setting, but not control at d21 post-infection (Figure 3.8).

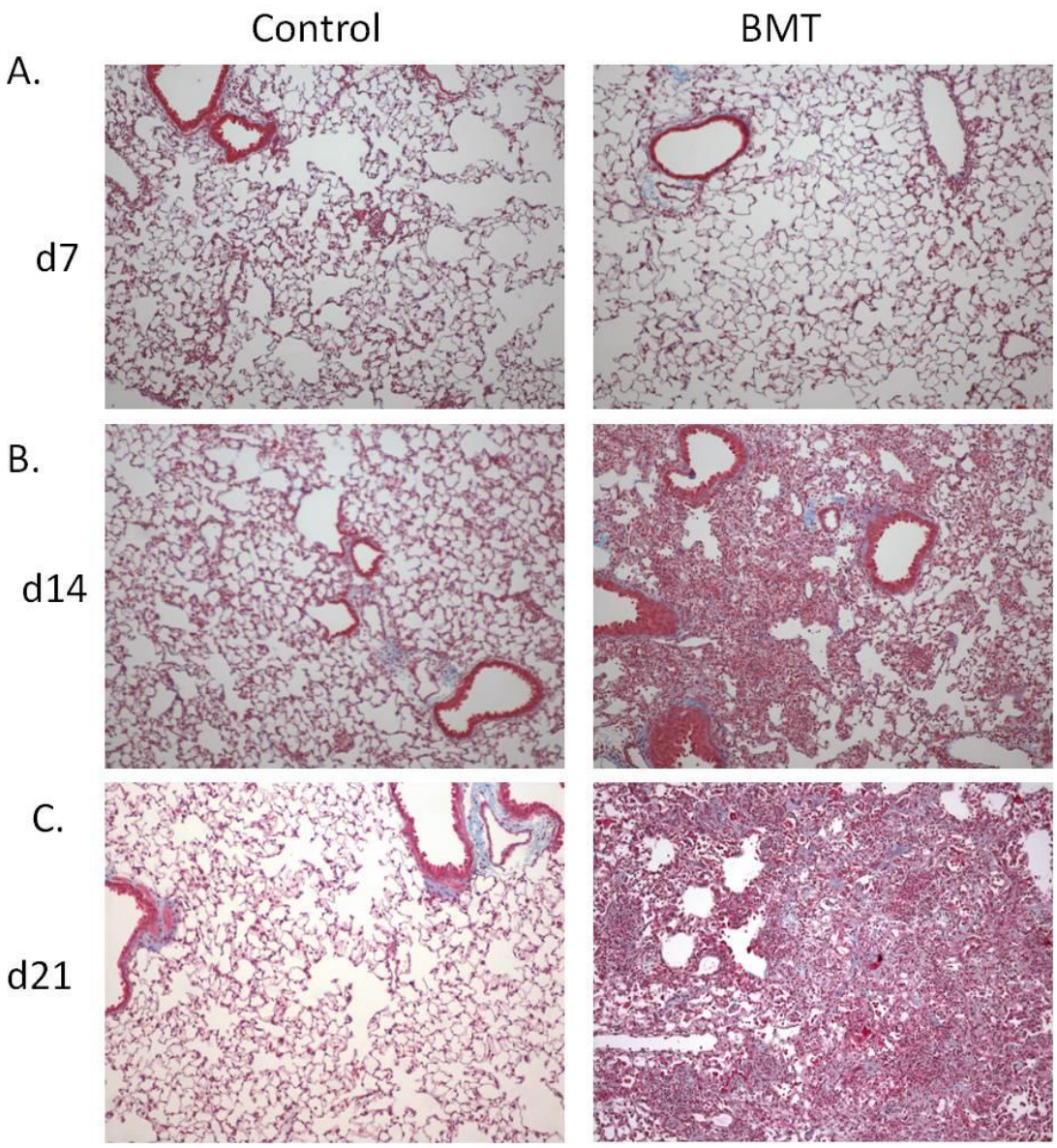

Figure 3.8 *BMT mice develop lung fibrosis during virus latency*. BMT and control mice were infected i.n. with $5x10^4$ pfu γHV-68. At days 7, 14, and 21 post-infection, lungs were harvested for histology and sections were stained with Trichrome for collagen deposition (in blue). Sections shown are representative of *n*=2 d7, 3 d14, and at least 10 d21 per group. Magnification is 100x.

Increased collagen in BMT lungs was confirmed at d21 post-infection by real time RT-PCR. *Collagen 1* and *collagen 3* transcripts were increased approximately 2 fold in BMT lungs compared to control lungs (Figure 3.9).

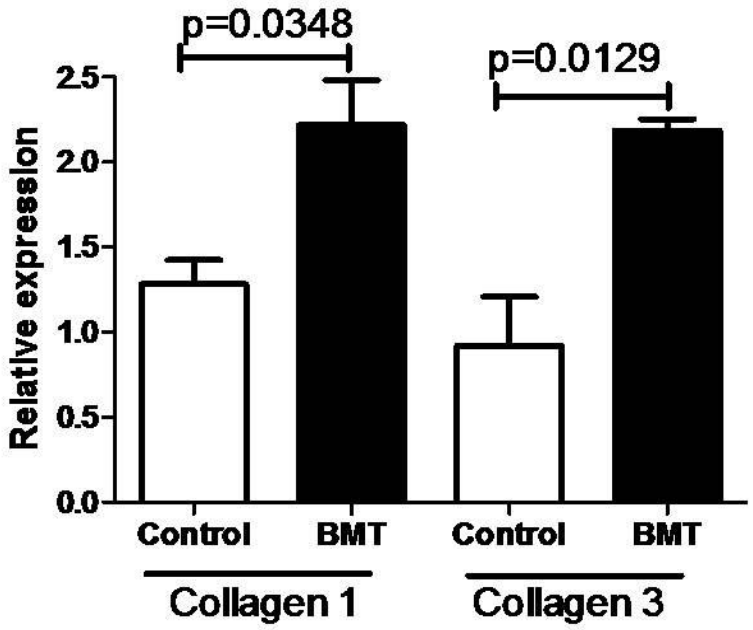

Figure 3.9. *BMT lungs have increased collagen expression during latent γHV-68 infection.* BMT and control mice were infected with $5x10^4$ pfu γHV-68 and lungs were harvested at d21 post-infection. Lungs were harvested for RNA, and expression of *collagen 1* and *collagen 3* was analyzed using real time RT-PCR. Expression was normalized to a control mouse for each gene. *Collagen 1* and *collagen 3* were significantly increased in BMT lungs (*p=0.0348* and *p=0.0129*, respectively. *n*=3 mice per group; representative of 2 independent experiments).

H&E and Trichrome-stained slides were analyzed in a blinded fashion by a pulmonary pathologist, and lungs from BMT mice were shown to have mild to moderate fibrosis, foamy alveolar macrophages, peripheral inflammation, and diffuse alveolar damage. Both control and BMT mice showed perivascular inflammation (Figure 3.10A).

In order to quantify the histologic changes, lungs were scored on a scale of 0 (normal lung) to 11 (most severe pathology) based on the presence and severity of these pathological features, as described in Materials and Methods (Figure 2.1). BMT mice had a significant increase in histology score at days 14 and 21 post-infection compared to control mice (Figure 3.10B).

A.

Pathological Features	Control	BMT
Mild to moderate fibrosis	0/5	4/4
Foamy alveolar macrophages	1/5	4/4
Perivascular inflammation	5/5	4/4
Moderate/ extensive peripheral inflammation	0/5	4/4
Hyaline membranes/ Diffuse alveolar damage	0/5	4/4

B.

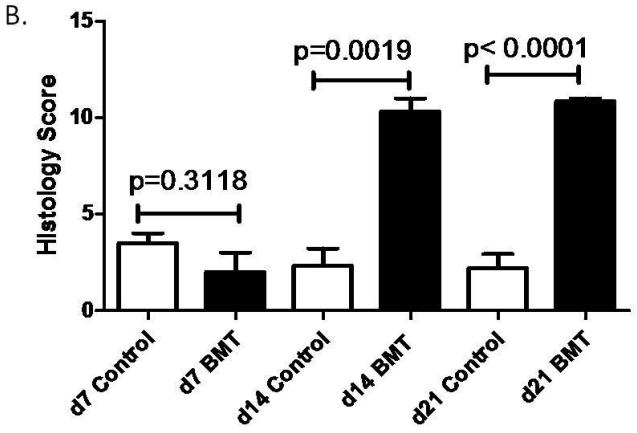

Figure 3.10. *BMT mice display distinct pathological features at d21 post-infection with γHV-68. A.* H&E and Trichrome-stained lung sections from BMT and control mice at d21 post-infection with γHV-68 were analyzed for presence of pathological features in a blinded fashion by a lung pathologist (*n*=5 control, 4 BMT; representative of at least 3 independent experiments). *B.* Lung sections were scored on the basis of presence and severity of pathological features, and a composite score was generated for each mouse. A mean histology score was generated for each group (*n*=2 d7 Control and BMT, 3 d14 Control and BMT, and 5 d21 Control and 7 d21 BMT).

To determine whether the pathology observed in BMT mice was virus-induced or due to the conditioning regimen alone, lung sections from uninfected BMT mice at 8 weeks post-transplant were analyzed. H&E staining shows that uninfected BMT lungs did not display the pathological features found in latently infected BMT lungs, and Trichrome staining revealed no abnormal collagen deposition (Figure 3.11), suggesting that the pathology was virus-induced and not the result of irradiation-induced lung damage.

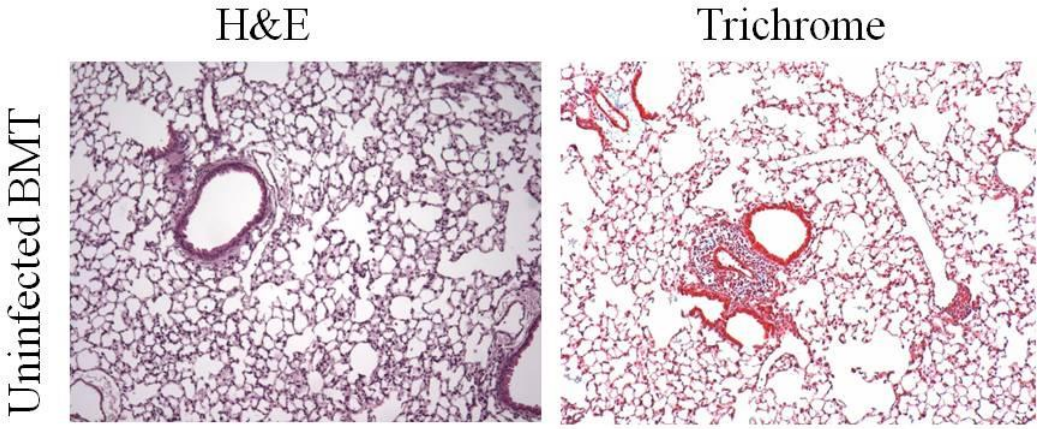

Figure 3.11 *Uninfected BMT lungs do not display pathological features observed in latently-infected BMT lungs.* Lungs from uninfected BMT mice were harvested at 8 weeks post-BMT, and sections were stained with H&E and Trichrome (100x magnification). Representative of n=3 mice.

To determine whether virus-induced pneumonitis observed in BMT lungs during virus latency was persistent or a transient response to virus latency, BMT and control mice were infected with $5x10^4$ pfu γHV-68. At 7 weeks post-infection, lungs were harvested for histology. Lung sections stained with H&E and Trichrome reveal a persistence of the pneumonitis phenotype and increased histology score, even 7 weeks-post infection (Figure 3.12).

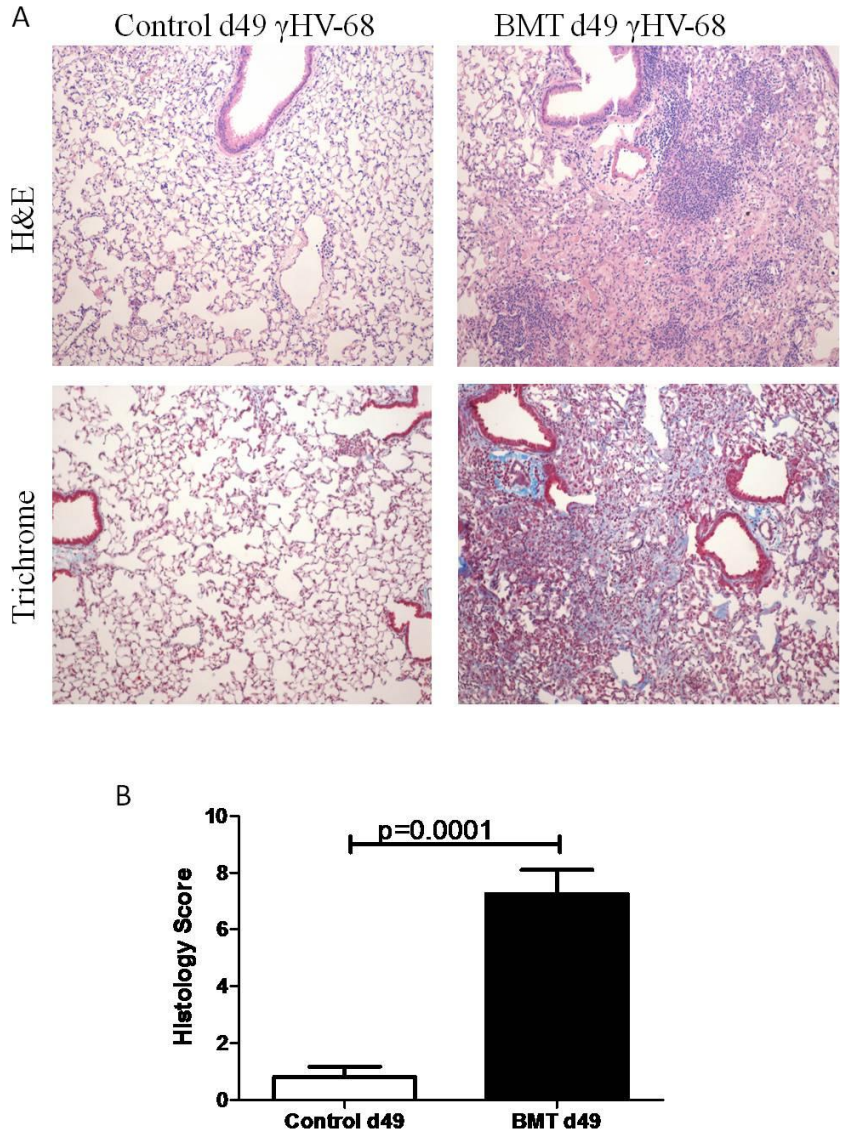

Figure 3.12 *Pneumonitis and fibrosis in BMT mice persist even 7 weeks post-infection.* Lungs from BMT and control mice, infected with $5x10^4$ pfu γHV-68, were harvested for histology at d49 post-infection. *A.* H&E and Trichrome-stained lung sections from BMT and control mice 49 days post-infection (100x magnification). *B.* Lung sections from BMT and control mice at d49 post-infection were analyzed in a blinded fashion by a pathologist and scored on the basis of the presence and severity of pathological features (*n*=4 BMT, 5 control).

BMT mice have increased infiltration of inflammatory cells in the alveolar space during latent γHV-68 infection

To characterize the cells present in the alveolar space at d21 post-infection, BAL was performed on BMT and control mice and total cells were counted. There was a significant increase in total cell numbers harvested from BMT lungs compared to control (Figure 3.13A). BAL cells from control mice were largely monocytes/ macrophages, as determined by differential counting. However, BMT BAL cells included an influx of lymphocytes and neutrophils (Figure 3.13B).

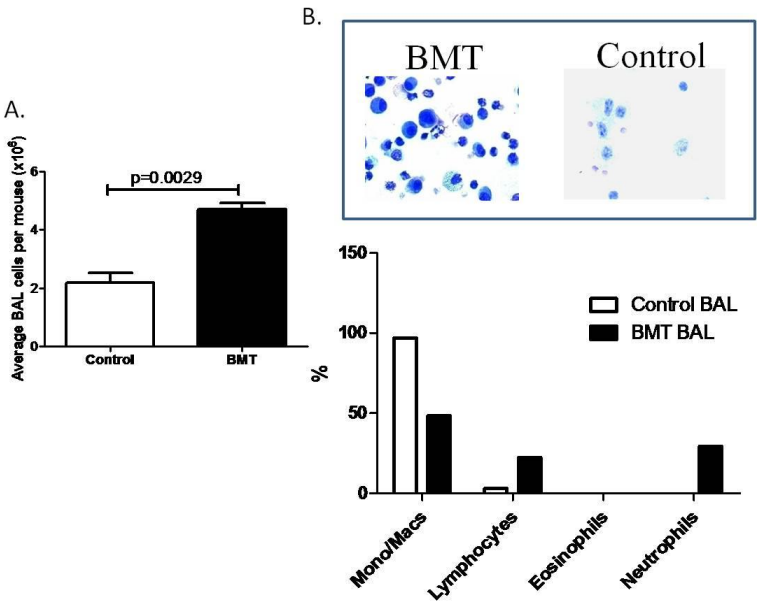

Figure 3.13 *BMT mice have increased infiltration of lymphocytes and neutrophils in the alveolar space during latent γHV-68 infection*. At d21 post-infection with $5x10^4$ pfu γHV-68, cells were harvested from the alveolar space of BMT and control mice using BAL. *A.* BMT mice have a significant increase in total numbers of cells harvested by BAL compared to control (*p=0.0029*, *n*=5 mice per group; representative of 3 independent experiments). *B.* BMT mice have increased percentages of lymphocytes and neutrophils in the alveolar space, as determined by differential counting (*n=5* mice per group; representative of 2 independent experiments).

To characterize lymphocyte populations in the alveolar space, BAL cells were analyzed by flow cytometry. BMT mice had significant increases in numbers of both CD4 and CD8 cells compared to control mice, while very few B cells were present in either group (Figure 3.14).

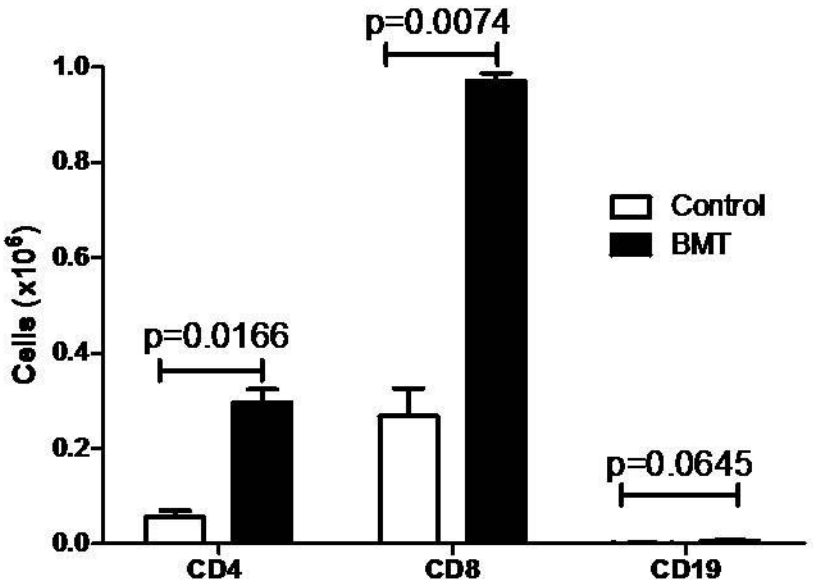

Figure 3.14 *BMT mice have increased T cells in the alveolar space at d21 post-infection*. BAL cells were harvested and stained by flow cytometry for CD4, CD8, and CD19. Numbers of CD4 and CD8 cells were significantly increased in BMT mice (*p=0.0166* and *p=0.0074*, respectively. *n*=5 mice per group; representative of 2 independent experiments).

Latently infected BMT mice have reduced oxygen saturation

To understand whether pneumonitis in BMT mice led to changes in lung physiology, we used the MouseOx Pulse Oximeter to measure oxygen saturation in mice at d21 post-infection. We hypothesized that the increased numbers of inflammatory cells and the presence of fibrotic lung tissue in the BMT setting would result in reduced pulmonary function. We found a significant decrease in oxygen saturation in BMT mice compared to control at d21 post-infection with γHV-68 (Figure 3.15A). However, there was no difference in oxygen saturation between these groups prior to infection (Figure 3.15B). These data indicate that latent gammaherpesvirus infection in BMT mice leads to reduced oxygen saturation.

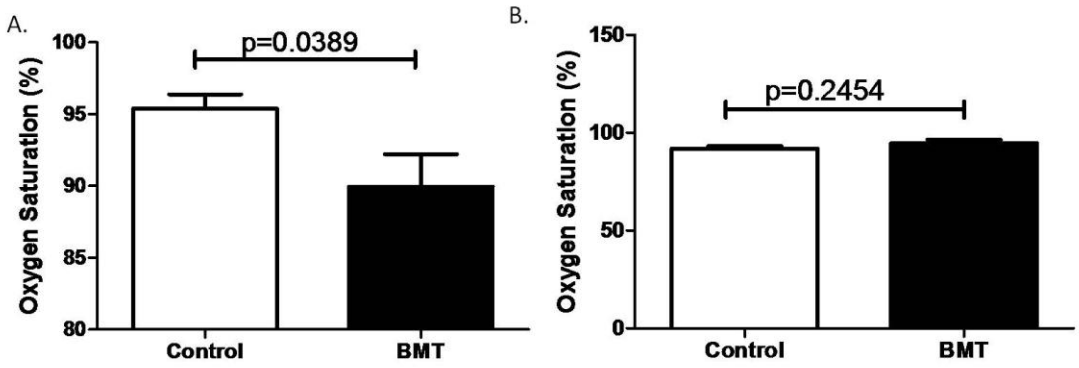

Figure 3.15 *Oxygen saturation is reduced in BMT mice during latent γHV-68 infection.* Oxygen saturation was measured in BMT and control mice using a MouseOx Pulse Oximeter at d21 post-infection with $5x10^4$ pfu γHV-68 (*A*) and at 5 weeks-post transplant (uninfected, *B*). *A.* BMT mice had significantly decreased oxygen saturation compared to control at d21 post-infection (*p=0.0389*, *n*=11 mice per group; data combined from 3 independent experiments). *B.* There was no difference in oxygen saturation in control and BMT mice prior to infection (*n*=5 per group).

Alveolar macrophages show a mixed classical and alternative activation phenotype

As indicated in Figure 3.10A, lungs from BMT mice latently infected with γHV-68 contained foamy alveolar macrophages. H&E staining at 400x magnification shows these macrophages in the BMT mouse lung (Figure 3.16A). Because alternative activation of macrophages has been implicated in contributing to pulmonary fibrosis in mice (136), we hypothesized that alveolar macrophages in our model might express markers of alternative activation. Alveolar macrophages from BMT and control mice at d21 post-infection with γHV-68 were harvested by BAL and enriched by plastic adherence. Expression of the classical marker *iNOS* and the alternative activation marker *Arginase 1* was determined using real time RT-PCR. We found a significant increase in expression of both genes in BMT cells compared to control (Figure 3.16B), although *Arginase 1* was upregulated to a greater extent than *iNOS.* Interestingly, alveolar macrophages from BMT mice did not express IL-4 or IL-13 RNA (Appendix Figure 1), cytokines thought to be critical for alternative activation (135). IL-4 and IL-13 protein could also not be detected by ELISA in collagenase-digested lungs, and very little IL-13 and no IL-4 RNA could be detected in cultured BAL cells, including lymphocytes in the BMT mice (Appendix Figure 1). Taken together, these data suggest that the alternative activation of macrophages in this model may be Th2-independent.

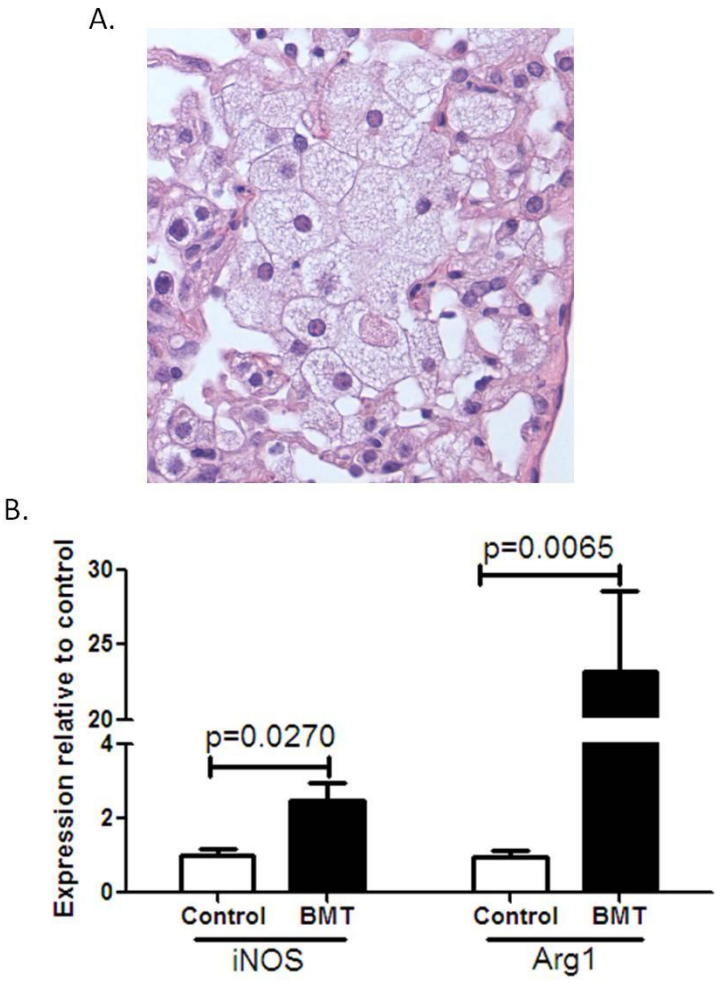

Figure 3.16 *BMT alveolar macrophages are foamy and express increased iNOS and arginase-1.* BMT and control mice were infected with $5x10^4$ pfu γHV-68 for 21 days. *A.* H&E stained BMT lung section showing foamy alveolar macrophages (400x magnification). *B.* BAL cells from BMT and control mice were plated for 1.5h in serum-free DMEM. Non-adherent cells were removed, and adherent cells were harvested for RNA. Expression of the classical activation marker, *iNOS*, and an alternative activation marker, *Arginase 1* (*Arg1*), was significantly increased in BMT cells (*p=0.0270* and *p=0.0065*, respectively) as determined by real time RT-PCR. Expression of each gene in a control mouse was set to 1 (*n*=4 mice per group; representative of 2 independent experiments).

BALF from BMT mice contains pro-fibrotic mediators

Because oxidative stress has been implicated in promoting pulmonary fibrosis in both human (128) and murine (129) studies, we tested levels of reactive oxygen species in the BALF of BMT and control mice at d21 post-infection. Levels of H_2O_2 and NO_2- were significantly increased in BALF from BMT mice compared to control (Figure 3.17A, B). We next determined whether levels of TGFβ, a potent pro-fibrotic mediator (33, 121), were increased in BALF from BMT mice. At d21 post-infection, BMT mice had a significant increase in total TGFβ1 protein in BALF compared to control (Figure 3.17C). Thus, these data show that BALF from BMT mice at d21 post-infection contains increased levels of TGFβ and reactive oxygen species that may be contributing to fibrotic outcomes.

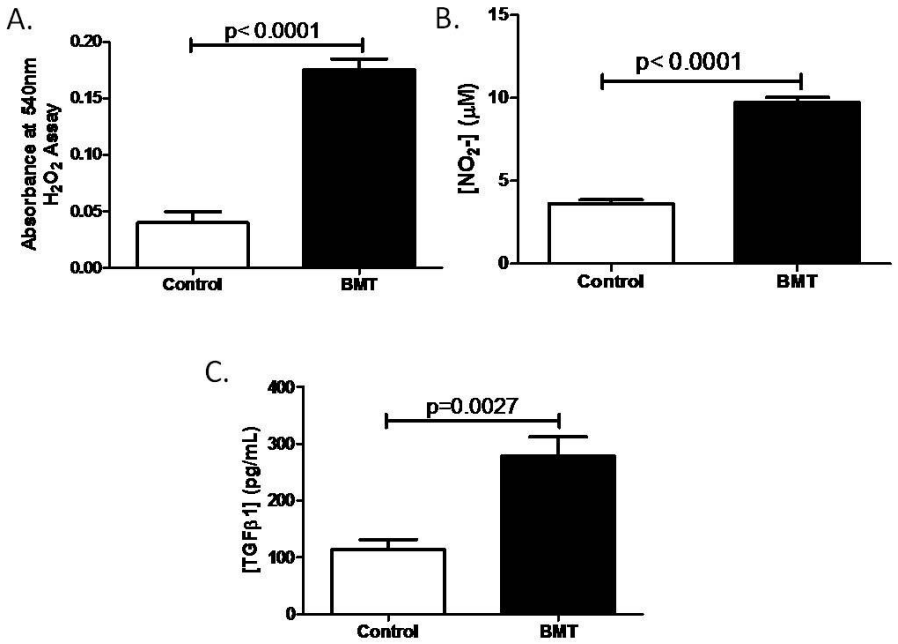

Figure 3.17 *BMT mice have increased H_20_2, NO_2-, and TGFβ1 in BALF*. BALF was harvested from BMT and control mice at d21 post-infection with $5x10^4$ pfu γHV-68. The relative level of H_20_2 (*A*), NO_2- (*B*), and total TGFβ1 (*C*) were significantly increased in BMT BAL fluid compared to infected controls (*p<0.0001*, *p<0.0001*, *and p=0.0027*, respectively). (*n*=5 per group; representative of 2 independent experiments).

Susceptibility to infection is not explained by an early defect in inflammatory cell recruitment

We were next interested in understanding the potential mechanisms contributing to increased lytic γHV-68 replication and pneumonitis development in our BMT model. We hypothesized that the increased lytic viral load observed in BMT lungs at d7 post-infection could be attributed to defects in initial inflammatory cell recruitment or defects in immune cell function. To distinguish these possibilities, lungs from BMT and non-transplanted control mice were enzymatically digested using collagenase and leukocytes were isolated. Total cell numbers were determined in uninfected mice and in mice at d7

post-infection with γHV-68. At 5 weeks post-transplant, BMT mice had equivalent total cell numbers both before and at d7 post-infection when compared to non-transplanted control mice (Figure 3.18A). Inflammatory cell subsets in the lung were also identified following infection using flow cytometry. At d7 post-infection, BMT mice had equivalent numbers of T cells, B cells, NK cells, NKT cells, and CD11c+I-A^B+ APCs as non-transplanted control mice (Figure 3.18B). Thus, there is no evidence for a defect in immune cell accumulation post-infection in BMT mice.

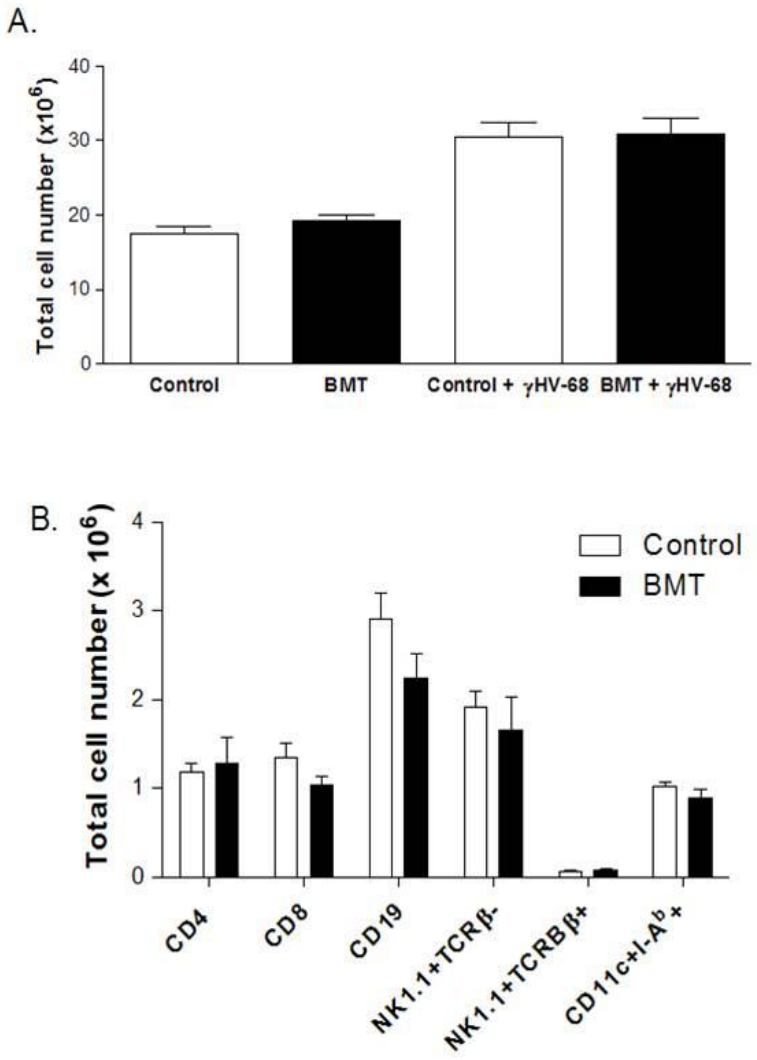

Figure 3.18 *BMT mice do not have a defect in inflammatory cell recruitment*. *A.* Whole lungs from uninfected or infected ($5x10^4$ pfu γHV-68 i.n., d7 post-infection) non-transplanted control and BMT mice were digested with collagenase and total cells were enumerated. Total cell numbers between control and BMT mice did not differ significantly in the uninfected or infected groups (*n*=4 mice per group, representative of at least 3 independent experiments). *B.* 7 days post-infection with γHV-68 ($5x10^4$ pfu, i.n.), whole lungs from control and BMT mice were digested in collagenase and analyzed by flow cytometry for expression of cell surface molecules. Numbers of each subset were not statistically different between control and BMT mice (Data in each group is representative of at least 2 independent experiments, *n*= at least 3 mice per group).

BMT APCs are effective stimulators in an MLR

Because inflammatory cell recruitment to the lung in response to γHV-68 infection in BMT mice was not deficient (Figure 3.18), we next explored the hypothesis that immune cells from BMT mice have intrinsic functional deficits. Because of the central importance of APCs in initiating the adaptive immune response to pathogens, we first determined whether APC function was altered in the BMT setting. We analyzed cell surface expression of MHC class II and costimulatory molecules on BMDCs from BMT and non-transplanted control mice. We found that BMDCs from both groups expressed equivalent levels of the costimulatory molecules CD80 and CD86 as well as the MHC class II molecule I-A^b on the cell surface (Figure 3.19A-C). Accordingly, expression of these molecules on lung-derived CD11c+ cells purified from BMT mice (either uninfected or d7 post-infection) were similar or greater than levels on cells derived from control mice, suggesting that BMT mice do not display defects in important T cell stimulatory molecules (Figure 3.20, Figure 3.21).

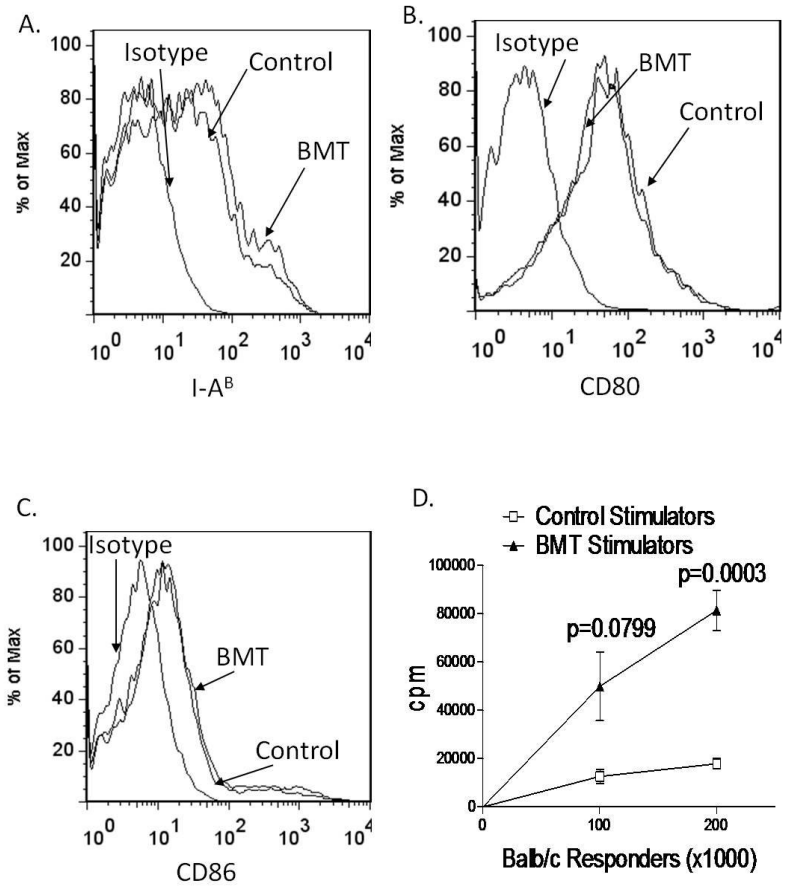

Figure 3.19 *BMT BMDCs are efficient stimulators in an MLR.* BMDCs from non-transplanted control or BMT mice 5 weeks post-transplant were grown for 7 days in GM-CSF and analyzed by flow cytometry for expression of I-A^b (A), CD80 (B), and CD86 (C). BMT BMDCs expressed levels of CD80 and CD86 comparable to that of control cells, and slightly increased levels of I-A^b (n=2 mice per group). Similar results were found in a separate experiment where BMDCs were matured for 24 hours with IL-4. D. $2x10^5$ irradiated BMDCs from BMT or control mice were used as stimulators in an MLR using $1x10^5$ and $2x10^5$ Balb/c splenocytes as responders. BMT BMDCs were able to stimulate proliferation of responder cells at least as well as control cells; BMT BMDCs stimulated significantly more proliferation in the $2x10^5$ responder group (*p*=0.0003). Error bars represent differences between triplicate or quadruplicate wells.

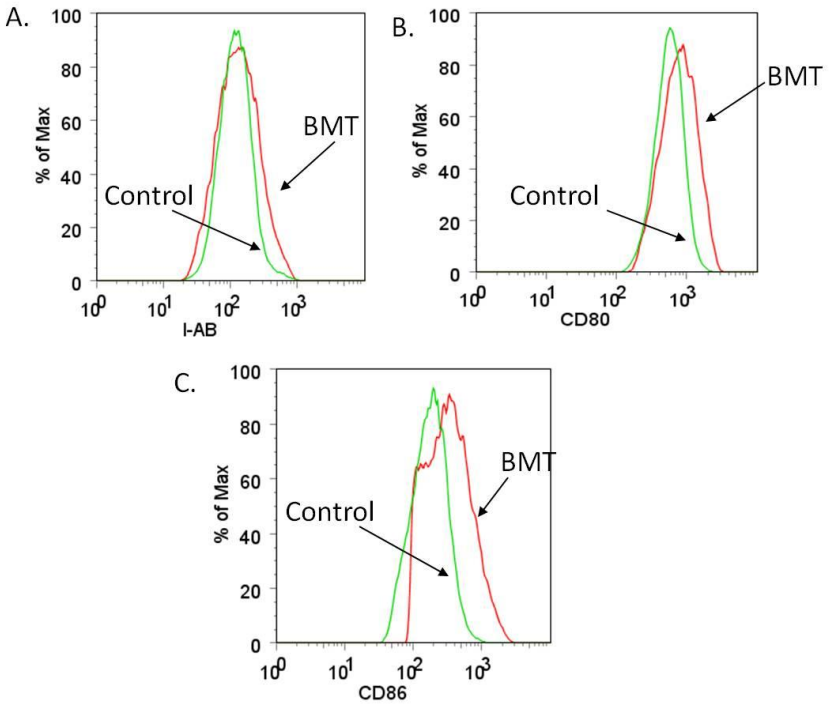

Figure 3.20 *Lung-derived CD11c+ I-A^B+ APCs from uninfected BMT mice express increased levels of MHC class II, CD80 and CD86 as compared to APCs from control mice.* Lungs from BMT and control mice were digested with collagenase and enriched for CD11c-expressing cells using magnetic separation. Cells were stained for expression of I-A^b (*A*), CD80 (*B*), and CD86 (*C*) and analyzed by flow cytometry. BMT APCs expressed increased levels of these three molecules when compared to control cells (*n*=5 mice per group).

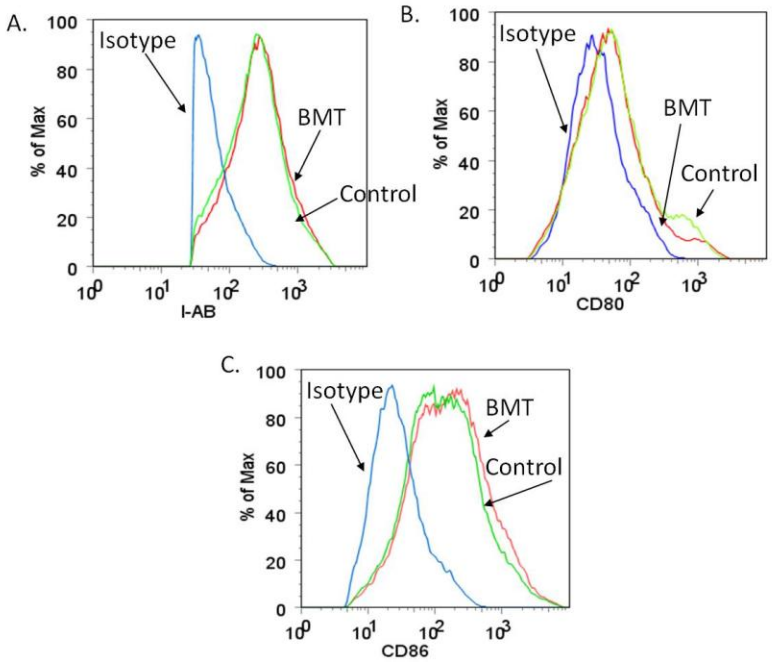

Figure 3.21 *Lung-derived CD11c+ I-A^B+ APCs from infected BMT mice express similar levels of MHC class II, CD80 and CD86 as APCs from control mice.* Lungs from BMT and control mice at d7 post-infection with γHV-68 were digested with collagenase and enriched for CD11c-expressing cells using magnetic separation. Cells were stained for expression of I-A^b (*A*), CD80 (*B*), and CD86 (*C*) and analyzed by flow cytometry. BMT APCs expressed equivalent levels of these three molecules when compared to control cells (*n*=5 mice per group).

To test the ability of the BMDCs from BMT mice to function as APCs, we set up MLRs using irradiated BMDCs from BMT or non-transplanted control mice as stimulators and Balb/c splenocytes as responders (Figure 3.19D). Our results demonstrated that BMDCs from BMT mice were capable of stimulating T cell proliferation equivalent to or even more effectively than stimulators from non-transplanted controls. Similar results were obtained when we tested unfractionated

splenocytes from control or BMT mice as APCs in an MLR (Figure 3.22). These data suggest that APCs derived from BMT mice have the ability to function *in vitro*.

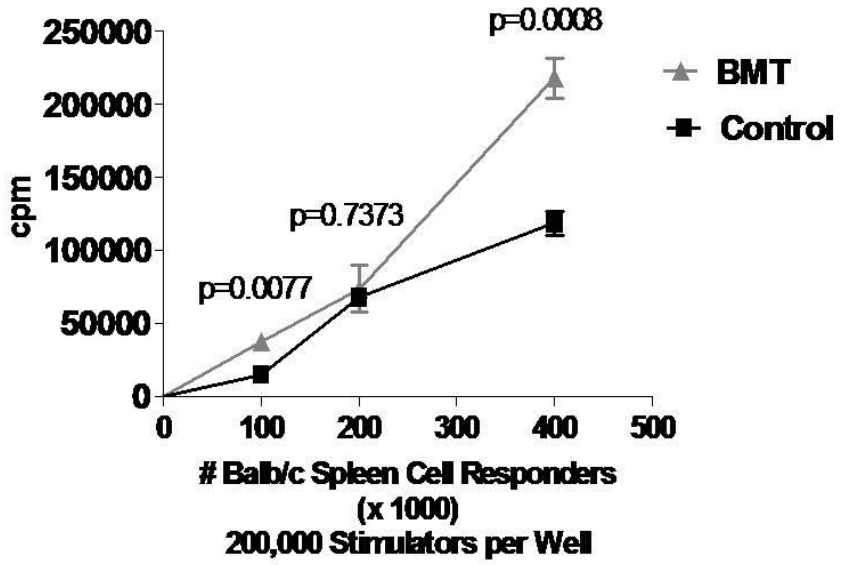

Figure 3.22 *BMT splenocytes are efficient stimulators in an MLR.* $2x10^5$ irradiated splenocytes from BMT or control mice were used as stimulators in a MLR using $1x10^5$, $2x10^5$, and $4x10^5$ Balb/c splenocytes as responders. BMT splenocytes were able to stimulate proliferation of responder cells at least as well as control cells. Error bars represent differences between triplicate or quadruplicate wells.

BMT T cells are impaired in an MLR response

We next explored the possibility that T cells from BMT mice had impaired function, a hypothesis supported by human HSCT patient data showing intrinsic T cell defects in *in vitro* assays (10-12). In order to assay T cell function, we set up MLRs using irradiated Balb/c splenocytes as stimulators and unfractionated BMT or control spleen cells as responders. The BMT responder splenocytes were impaired in their proliferative response (Figure 3.23A) despite the fact that there were no differences in the numbers of CD4 cells found in the spleens of control or BMT mice. To directly compare the

proliferative capacity of CD4 T cells from control and BMT mice, we next isolated splenic CD4 cells via magnetic purification and used these cells as responders against irradiated Balb/c splenocytes. Similar to the results seen with unfractionated splenocytes, purified CD4 T cells from BMT mice displayed impaired proliferative responses in this allo-MLR reaction (Figure 3.23B). These data suggest that BMT T cell responses are impaired *in vitro*.

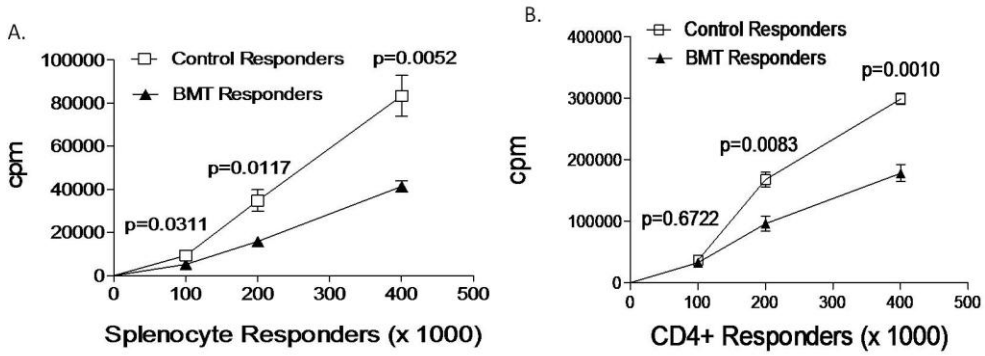

Figure 3.23 *BMT cells are poor responders in an MLR.* $2x10^5$ Balb/c irradiated splenocytes were used as stimulators in an MLR. In panel A, BMT whole spleen cell responders proliferated significantly less than control cells. In panel B, purified CD4 cells from BMT or control spleens were used as responders in a MLR. BMT CD4 cells responded significantly less than control cells when $2x10^5$ and $4x10^5$ responders were used. Error bars represent differences between triplicate or quadruplicate wells.

<u>BMT mice show increased levels of PGE_2 in the lung</u>

Our laboratory has previously shown that syngeneic BMT mice overexpress PGE_2 in the lungs at 5 weeks post-BMT, leading to defects in anti-bacterial macrophage and neutrophil function in these mice (60). Since PGE_2 has been linked to inhibition of T cell responses (171), we hypothesized that increased PGE_2 levels may also contribute to

impaired T cell responses and, therefore, impaired anti-viral immunity. We found that PGE_2 was significantly increased in the lungs of BMT mice at d7 post-infection with $5x10^4$ pfu γHV-68 (Figure 3.24A). However, treatment of mice with indomethacin (a cyclooxygenase inhibitor which blocks PGE_2 synthesis) during the infection did not improve control of viral replication, despite reductions in PGE_2 levels (Figure 3.24B,C). These data indicate that although PGE_2 is overproduced in the lungs of BMT mice, it does not limit anti-viral immunity to lytic γHV-68 infection. However, we did not evaluate the role of PGE_2 at other time points post-infection or on the development of fibrosis or pneumonitis.

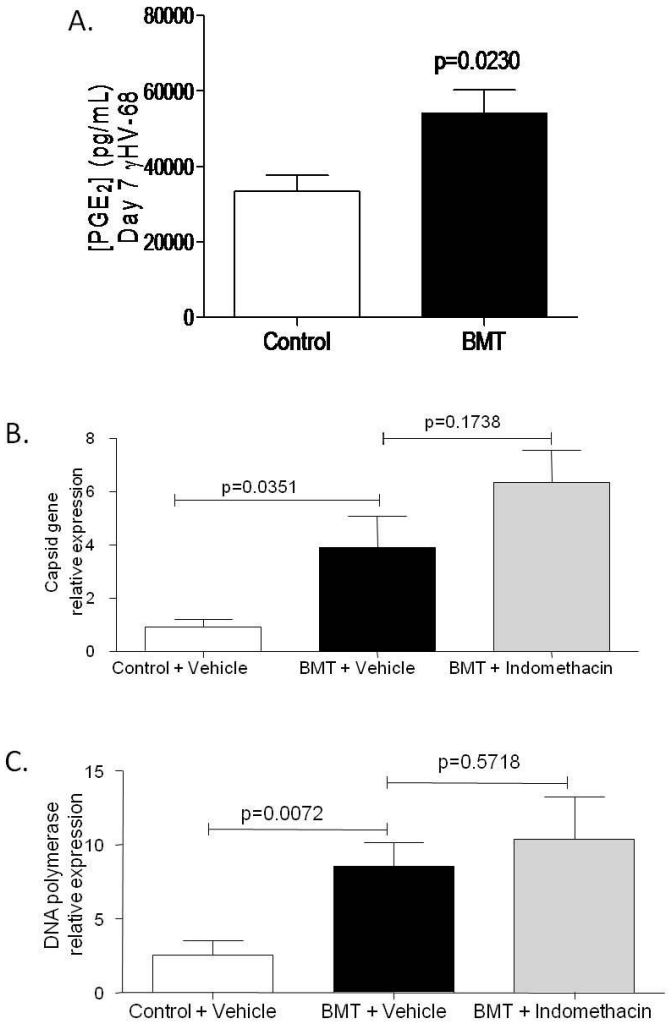

Figure 3.24 *Overproduction of PGE_2 in the lung post-BMT does not explain impaired anti-viral immunity.* BMT and control mice were infected i.n. with $5x10^4$ pfu γHV-68. *A.* Whole lungs were harvested at d7 post-infection and assayed for PGE_2 by ELISA. Lungs of BMT mice produced significantly more PGE_2 than non-transplanted controls (p=0.0230, n=5 mice per group, representative of 2 independent experiments). *B.* During each day of the infection, mice were given a i.p. injection containing indomethacin (1.2 mg/kg) or DMSO as a vehicle control. At d7 post-infection, left lungs were harvested for RNA and expression of lytic viral genes was determined using real time RT-PCR. Expression of the viral capsid gene (*B*) and the viral *DNA polymerase* (*C*) was significantly increased in both the indomethacin-treated and vehicle-treated BMT mice compared to non-transplanted controls. Indomethacin treatment effectively reduced PGE_2 levels in the BMT mice from 126.054 ng/mL to 7.779 ng/mL, as determined at day 7 post-infection by ELISA of right lungs (n=8-9 mice per group, representative of 2 independent experiments).

Altered T cell differentiation in BMT lungs

Proper cytokine production during lytic γHV-68 infection is required for efficient control of viral replication. Specifically, IFNγ production by CD4 cells is critical (77-79). Based on this knowledge, we hypothesized that T cell differentiation may be altered in the BMT setting in response to lytic γHV-68 infection in the lung. To test this hypothesis, lungs from BMT and control mice were harvested at d7 post-infection with γHV-68. Lungs were digested using collagenase, and expression of IFNγ, IL-17a, and Foxp3 was measured using intracellular staining and flow cytometry, as indicators of Th1, Th17, and Tregs in the lung. We find that at d7 post-infection, BMT mice have decreased numbers of Th1 cells, increased numbers of Th17 cells, and increased numbers of Foxp3+ Tregs when compared to control mice (Figure 3.25). Furthermore, numbers of Tregs were significantly increased in the lungs of BMT mice even prior to infection (Figure 3.25A).

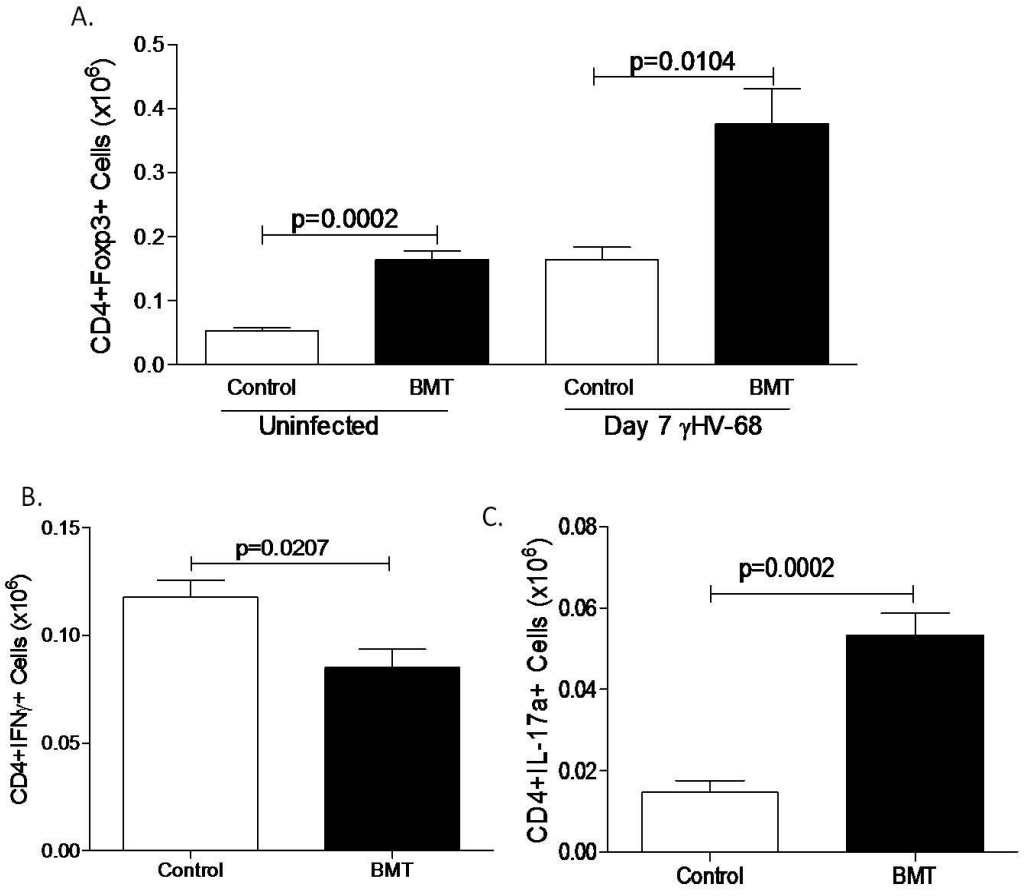

Figure 3.25 *Altered T cell differentiation in lungs of BMT mice in response to γHV-68.* Lungs from BMT and control mice, uninfected or infected ($5x10^4$ pfu γHV-68, i.n., d7), were digested with collagenase and analyzed by flow cytometry. *A.* Lungs from uninfected BMT mice had significantly more CD4+Foxp3+ cells than non-transplanted controls (p=0.0002, n=4 mice per group, representative of 2 independent experiments). At d7 post-infection, BMT lungs had significantly higher numbers of CD4+Foxp3+ cells than non-transplant controls (p=0.0104, n=4 mice per group, representative of at least 6 independent experiments) *B* and *C.* Lung cells were stimulated with PMA and ionomycin and analyzed by flow cytometry using antibodies against CD4, IFNγ and IL-17a. *B.* BMT mice showed a significant decrease in numbers of CD4+IFNγ+ cells compared to non-transplanted control mice (*p=0.0207*). *C.* BMT lungs had a significant increase (p=0.0002) in numbers of CD4+IL-17a+ cells compared to non-transplant controls (n=5 per group; data representative of 2 independent experiments).

Lungs from BMT mice overexpress TGFβ

TGFβ has been reported to promote Treg and Th17 differentiation, as well as limit Th1 differentiation. Thus, we hypothesized that TGFβ may be overexpressed in the lungs of BMT mice in our model. We found that lungs of uninfected BMT mice have significantly higher levels of TGFβ1 compared to non-transplanted control mice (Figure 3.26). We hypothesized that the increased levels of TGFβ1 may be attributed in part to epithelial cell damage as a result of the TBI conditioning regimen (33). To determine whether alveolar epithelial cells (AECs) were a significant source of TGFβ1 post-BMT, we purified AECs from non-transplanted control and BMT mice at week 5 post-transplant. AECs were then cultured and supernatants were analyzed for total TGFβ1 levels by ELISA. Figure 3.26B demonstrates that AECs from BMT mice are a source of TGFβ1 even 5 weeks post-transplant. In order to determine if radiation dose affected TGFβ1 levels in the lung, transplants were performed following increasing doses of irradiation. TGFβ1 levels were similarly elevated in all groups (Appendix Figure 2).

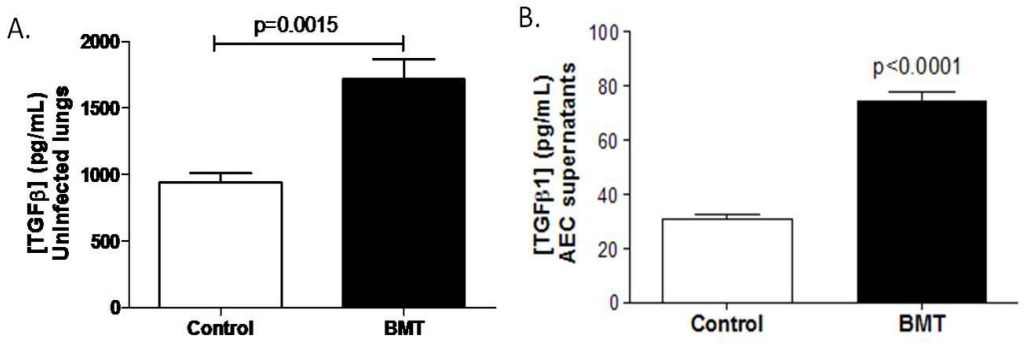

Figure 3.26 *BMT mice overexpress TGFβ1*. *A.* Lungs of uninfected BMT mice produced significantly more TGFβ1 than control, as determined by ELISA (p=0.0015, n=5 mice per group, representative of 2 independent experiments). *B.* Alveolar epithelial cells (AECs) were isolated from lungs of uninfected BMT and control mice and were assayed for production of TGFβ1 by ELISA following 24 hour culture in serum-free media. BMT AECs produced significantly more TGFβ1 than control AECs (p<0.0001, n=6 per group, representative of 2 independent experiments).

Depletion of Tregs from BMT mice does not restore anti-viral immunity

We hypothesized that the elevated number of Tregs in the lungs of BMT mice was suppressing anti-viral immunity. To test this hypothesis, BMT mice were treated with either anti-CD25 or isotype control at 4 weeks post-BMT. At 5 weeks post-BMT, (1 week following antibody treatment), mice were infected i.n. with $5x10^4$ pfu γHV-68. Left lungs were harvested for RNA, and expression of the lytic viral capsid gene *gB* and viral *DNA polymerase* was determined by real time RT-PCR. There was no difference in viral gene expression between BMT mice treated with isotype and those treated with anti-CD25. Both BMT groups showed a significant increase in viral gene expression compared to isotype-treated non-transplant controls (Figure 3.27). Flow cytometry for lung CD4+Foxp3+ cells showed that Treg numbers in anti-CD25-treated BMT mice (1

week following antibody treatment) were similar to those seen in isotype-treated, non-transplant control mice on the day of infection (Figure 3.28). Similar results were found at d7 post-infection, showing that Treg depletion persisted throughout the infection period (Figure 3.28).

These data indicate that increased numbers of Tregs in the BMT lung is not sufficient to limit antiviral immunity to γHV-68 replication. To test whether Tregs purified from the BMT setting were functional suppressor cells, Tregs were isolated from BMT and control spleens and used as suppressors in an *in vitro* T cell proliferation assay. BMT Tregs were capable of suppressing T cell proliferation as well as Tregs isolated from control mice (Figure 3.29).

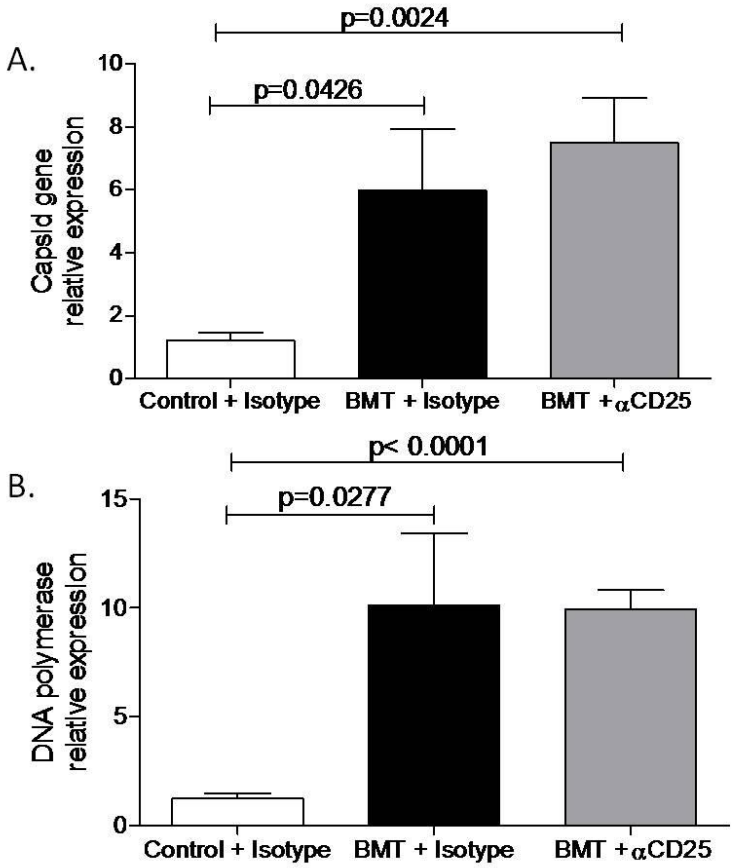

Figure 3.27 *Depletion of Tregs does not restore anti-viral immunity in BMT mice*. BMT mice were treated with a single dose of either anti-CD25 or isotype control antibody at 4 weeks post-BMT. At 5 weeks post-BMT (1 week following antibody treatment), mice were infected with $5x10^4$ pfu γHV-68. Left lungs were harvested for RNA at d7 post-infection, and expression of lytic viral genes was determined by real time RT-PCR. Expression of both the capsid gene *gB* and viral *DNA polymerase* was significantly increased in BMT mice treated with either isotype or anti-CD25 compared to isotype-control treated, non-transplanted animals (*n*=5 per group).

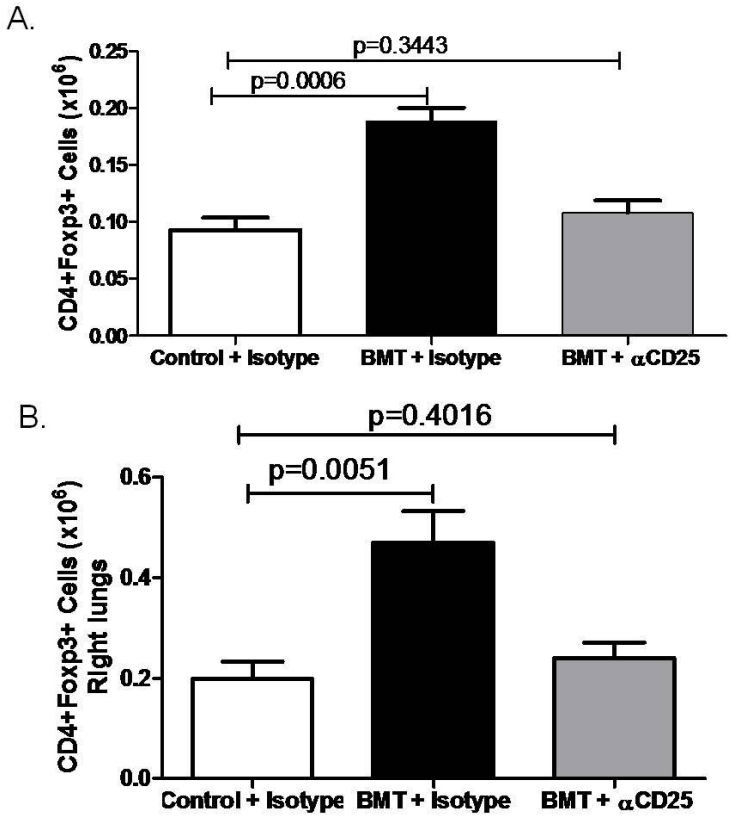

Figure 3.28 *Anti-CD25 treatment reduces BMT lung Treg numbers to control levels.* BMT mice were treated i.p. with a single dose of either anti-CD25 or isotype control antibody at 4 weeks post-BMT. At 5 weeks post-BMT (1 week following antibody treatment), lungs were harvested for flow cytometry or mice were infected with $5x10^4$ pfu γHV-68. *A.* Numbers of CD4+Foxp3+ cells in uninfected lungs were significantly increased in the isotype-treated BMT mice but were at control levels in anti-CD25-treated mice (*n*=4-5 per group). *B.* Numbers of CD4+Foxp3+ cells in right lungs remained decreased in anti-CD25 treated mice at d7 post-infection (*n*=5 per group).

Figure 3.29 *BMT Tregs are functional suppressors in vitro*. CD4+CD25+ Tregs and CD4+ responder cells were isolated from spleens using magnetic bead separation. $1x10^5$ CD4+ BMT responders were cultured for 3 days with anti-CD3 and syngeneic accessory cells (T depleted splenocytes) +/- $5x10^4$ BMT or control Tregs. After 3 days, ^3H was added to cultures and plates were harvested for scintillation counting 18 hours later (*n*=2-6 replicates per group).

IL-17a does not limit anti-viral immunity in the BMT setting

We reported increased numbers of IL-17a-expressing CD4 cells in the BMT mouse lung in response to γHV-68 infection (Figure 3.25). There are limited data regarding the role of IL-17a in viral infection; some reports indicate that IL-17a plays a protective role, while others indicate that IL-17a limits anti-viral responses, depending on the specific virus (172). There are no reports to date on the role of IL-17a in γHV-68 infection. To determine whether IL-17a limits immunity to γHV-68 and whether increased Th17 cells is the mechanism for impaired immunity to γHV-68, we set up infections using IL-17KO mice. We first compared lytic viral replication of γHV-68 infection in non-transplanted wild type and IL-17KO mice. We infected mice i.n. with $5x10^4$ pfu γHV-68 and harvested lungs for RNA at d7 post-infection. We found no difference by real time RT-PCR in expression of the lytic viral genes *gB* and *DNA polymerase* (Figure 3.30). We next set up transplants using wild type donors or IL-17KO

donors; the repopulated immune system in the IL-17KO BMT mice would be unable to produce IL-17a. Similar to the non-transplant setting, we found no difference in expression of lytic viral genes in the lung at d7 post-infection between wild type BMT and IL-17KO BMT mice. Taken together, these data suggest that overproduction of IL-17a post-transplant does not limit anti-viral immunity to lytic γHV-68 infection in the lung, at least at d7 post-infection.

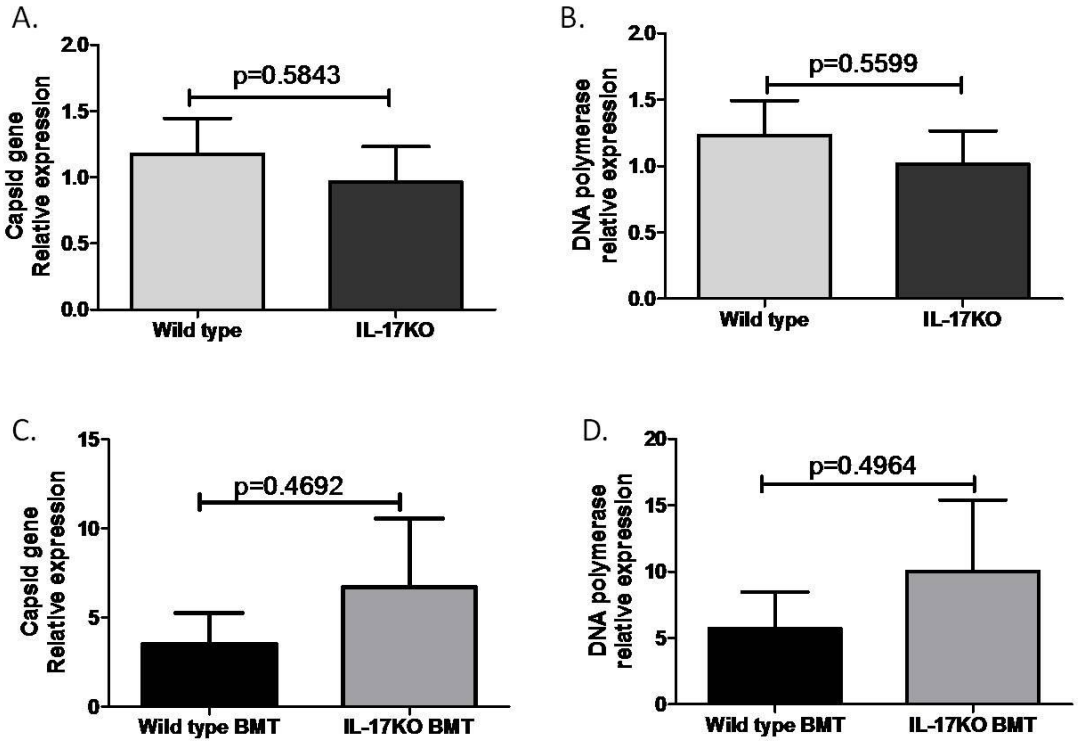

Figure 3.30 *IL-17a does not play a role in controlling lytic γHV-68 replication in the lung.* Wild type and IL-17KO non-transplanted mice (*A.* and *B.*) or wild type BMT and IL-17KO BMT mice (*C.* and *D.*) were infected with $5x10^4$ pfu γHV-68. At d7 post-infection, lungs were harvested for RNA, and expression of the viral capsid gene *gB* and the viral *DNA polymerase* was measured using real time RT-PCR. There was no significant difference in expression of either gene in non-transplant and transplant settings. (*A.* and *B. n*=9 wild type, 11 IL-17KO; data combined from 2 experiments). (*C.* and *D. n*=5 mice per group).

Reduced IL-12 production by BMT dendritic cells is not sufficient to alter Th1 differentiation *in vitro*

We next determined whether the diminished Th1 response in BMT lungs in response to γHV-68 infection (Figure 3.25B) was due to altered cytokine production by APCs. We first looked for IL-12 production by control and BMT APCs, as IL-12 is a critical cytokine for Th1 differentiation. We found that at baseline and upon TLR stimulation, BMDCs from BMT mice express significantly less IL-12p35 transcript compared to control (Figure 3.31A). This correlated with reduced IL-12p70 protein production upon TLR stimulation in BMT BMDCs (Figure 3.31B). Additionally, lung-derived CD11c cells from uninfected BMT mice express significantly less IL-12p35 compared to control (Figure 3.32A). However, lung CD11c cells derived from BMT lungs at d7 post-infection with γHV-68 express equivalent IL-12p35 as control mice (Figure 3.32B.)

To test whether reduced IL-12 production by BMT dendritic cells was sufficient to skew T cell responses away from Th1, we set up co-cultures with BMT and control BMDCs and T cells. Control or BMT BMDCs were incubated with OVA protein with or without LPS and then were cultured for 48h with OVA-specific OT-II splenic CD4 cells. ELISA on cell supernatants showed equivalent IFNγ production from T cells stimulated with BMT or control BMDCs (Figure 3.33). These data, in addition to the data showing that IL-12 production was not reduced in BMT mice at d7 post-infection (Figure 3.32B), suggest that reduced IL-12 production by BMT dendritic cells may not be sufficient to skew T cell responses away from Th1 in our OVA-specific *in vitro* assay.

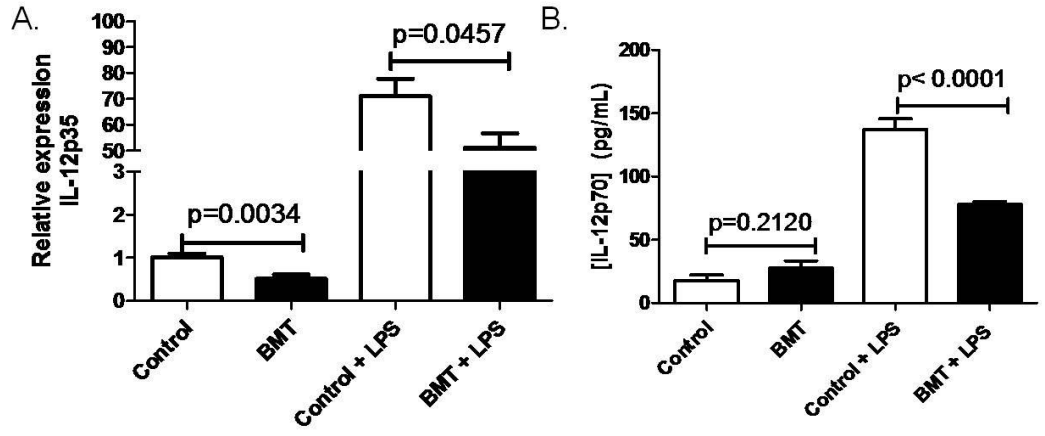

Figure 3.31 *Reduced IL-12 production by BMT BMDCs*. BMT and control BMDCs were cultured ($1x10^6$ cells/mL) with or without LPS (1 µg/mL) for 24h. Cells were harvested for RNA, and supernatants were harvested for ELISA. *A.* Expression of IL-12p35 in BMT cells was significantly decreased with and without LPS treatment, as determined by real time RT-PCR. *B.* ELISA on cell supernatants showed no difference in IL-12p70 production by unstimulated BMT and control cells; there was a significant decrease in IL-12p70 production in LPS-treated BMT cultures compared to control (*n*=6 per group, representative of 2 independent experiments).

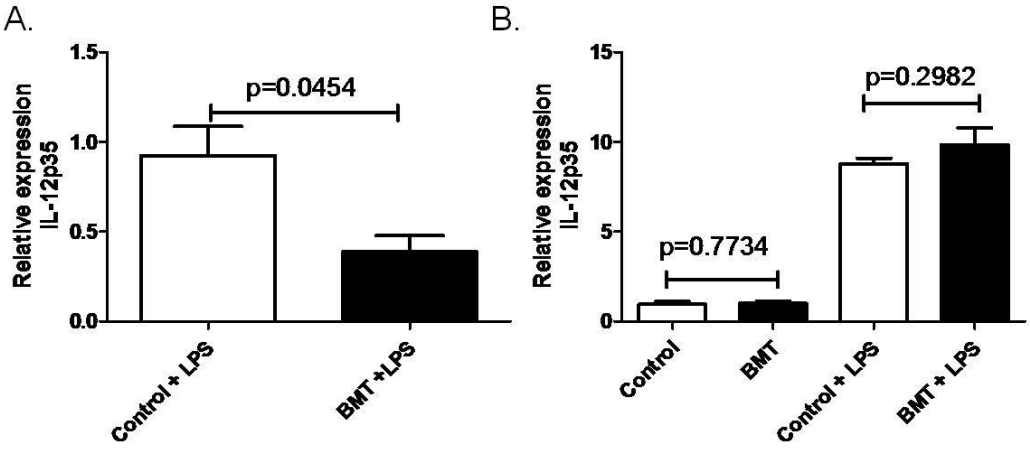

Figure 3.32 *Lung-derived CD11c+ cells have reduced IL-12p35 when harvested from uninfected, but not infected BMT mice*. CD11c+ cells were enriched by magnetic separation from BMT or control collagenase-digested lungs, either uninfected or at d7 post-infection with $5x10^4$ pfu γHV-68. $1x10^6$ cells/ mL were cultured for 24h with or without LPS at 1 µg/mL. Cells were then harvested for RNA, and expression of *IL-12p35* was determined using real time RT-PCR. *A.* Lung CD11c cells from uninfected BMT mice expressed decreased IL-12p35 compared to control when treated with LPS (*p=0.0454, n=3* per group). *B.* Lung CD11c cells from control and BMT mice at d7 post-infection expressed similar levels of IL-12p35 in the presence or absence of LPS (*n=6* per group).

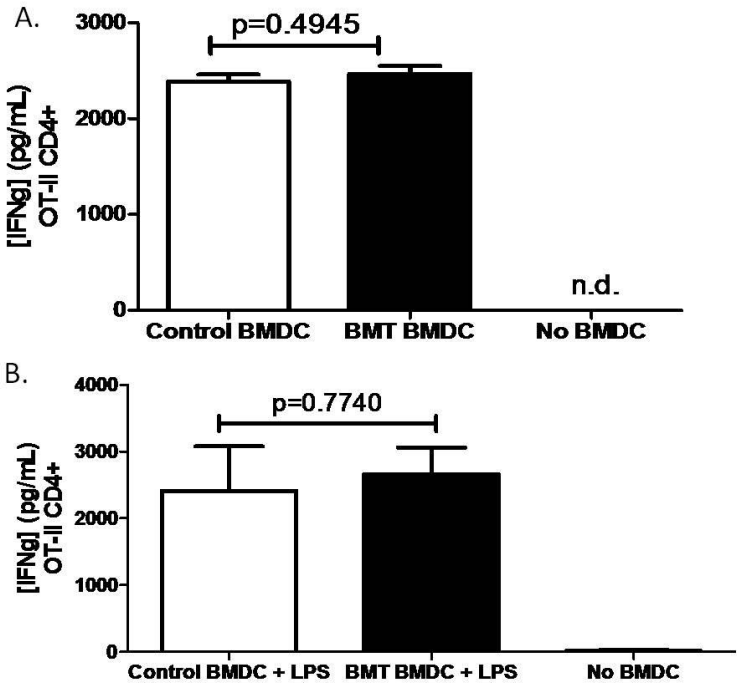

Figure 3.33 *BMT and Control BMDCs induce similar IFNγ production in vitro.* $8x10^4$ BMT or Control BMDCs were incubated with whole OVA protein (1 mg/mL used at 1:100 in culture) for 2h with (*B*) or without (*A*) LPS at 1 µg/mL. Media was removed and replaced with fresh media plus $8x10^5$ magnet-purified OVA-specific splenic OT-II CD4 cells from a naïve mouse. Supernatants were harvested 48h later and assayed for IFNγ by ELISA. (*A. n*=6 per group; representative of 2 independent experiments and *B. n*= 5 control, 4 BMT).

BMT T cells express reduced Tbet and increased TGFβ at baseline

Because the reduced IL-12 expression in BMT BMDCs was not sufficient to skew away from Th1 differentiation *in vitro*, we hypothesized that T cells from BMT mice had intrinsic alterations which may skew them away from Th1 differentiation. This hypothesis was supported by our data showing that BMT T cells had intrinsic defects in

proliferation *in vitro* (Figure 3.23). We found that T cells derived from BMT mice expressed decreased levels of the Th1 transcription factor *Tbet* at baseline, without any stimulation (Figure 3.34). Additionally, because TGFβ is known to limit Th1 differentiation by inhibiting *Tbet* (17), we hypothesized that T cells from BMT mice may overexpress TGFβ. Indeed, we find that both CD4 and CD8 cells from BMT mice produce increased TGFβ at baseline.

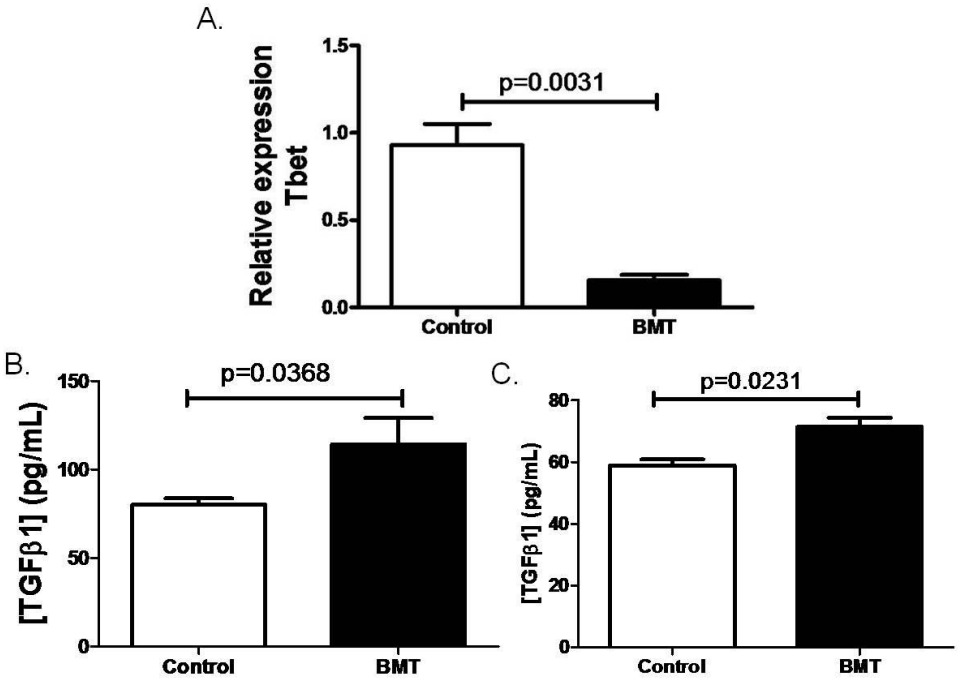

Figure 3.34 *BMT T cells express decreased Tbet and increased TGFβ at baseline. A. Tbet* expression in BMT splenic T cells was significantly reduced compared to control as determined by real time RT-PCR. *B.* Splenic CD4 cells from BMT mice produced increased TGFβ compared to control by ELISA (*n*=6 control, 5 BMT; representative of 2 independent experiments). *C.* Splenic CD8 cells from BMT mice produced increased TGFβ compared to control by ELISA (*n*=3 per group; representative of 2 independent experiments).

Mice transplanted with T cell-DN-TGFβRII bone marrow have restored immunity to lytic γHV-68

In order to determine whether the increased levels of TGFβ1 in the lung contributed to impaired anti-viral T cell responses in the BMT mice, we performed transplants using bone marrow from mice which express a dominant negative form of the TGFβ Receptor II under control of the CD4 promoter (T cell-DN-TGFβRII) (104). This particular promoter configuration is expressed in both CD4 and CD8 cells. This approach ensures that donor-derived T cells (CD4 and CD8) will be unresponsive to TGFβ1. Five weeks post-BMT, total cell numbers within the lung were not different in control, wild type syngeneic BMT and T cell-DN-TGFβRII BMT mice. At this time point, mice were infected i.n. with $5x10^4$ pfu γHV-68. At d7 post-infection, lungs from T cell-DN-TGFβRII BMT, wild type BMT and non-transplant control mice were analyzed for expression of lytic viral genes by real time RT-PCR. Our data demonstrate that T cell-DN-TGFβRII BMT mice (in which the donor-derived T cells are unresponsive to TGFβ1) have restored immunity to γHV-68, as expression of the viral capsid gene (Figure 3.35A) and viral DNA polymerase (Figure 3.35B) were not significantly different from expression in non-transplanted control mice.

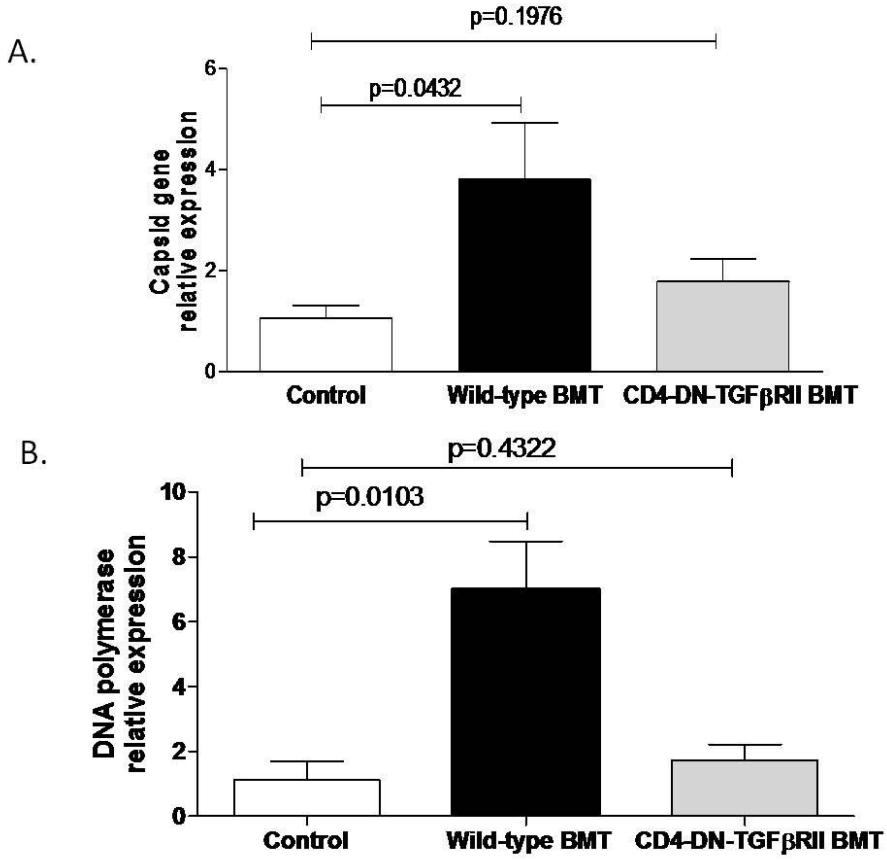

Figure 3.35 *Transplanting mice with T cell-DN-TGFβRII bone marrow restores immunity to γHV-68.* Control mice and mice transplanted with syngeneic wild type or T cell-DN-TGFβRII bone marrow were infected i.n. with $5x10^4$ pfu γHV-68 and analyzed at day 7 post-infection. *A.* Expression of the viral capsid gene *gB* was significantly increased in the lungs of wild type BMT mice compared to non-transplanted control mice; however, there was no significant difference between control and T cell-DN-TGFβRII BMT groups. *B.* Expression of viral *DNA polymerase* was significantly increased in wild type BMT lungs when compared to non-transplanted control mice. There was no significant difference between the control and T cell-DN-TGFβRII BMT mice (*n*=4-5 mice per group; data representative of 2 independent experiments).

We next determined whether T cell-DN-TGFβRII BMT mice would have restored numbers of Th1 cells in the lung in response to γHV-68. T cell-DN-TGFβRII BMT, wild type BMT, and non-transplant control mice were infected i.n. with $5x10^4$ pfu γHV-68. At d7 post-infection, lungs were digested in collagenase and analyzed by flow cytometry for expression of CD4 and IFNγ. Consistent with our earlier experiments (Figure 3.25), wild type BMT mice had significantly reduced numbers of CD4+IFNγ+ cells in the lung compared to non-transplant control. In contrast, T cell-DN-TGFβRII BMT mice had restored numbers of Th1 cells (Figure 3.36A). We next enriched T cells from the spleens of uninfected wild type BMT and T cell-DN-TGFβRII BMT mice and stimulated them with PMA and ionomycin *in vitro.* T cells from T cell-DN-TGFβRII BMT mice produced increased levels of IFNγ and lower levels of IL-17a suggesting that the T cell cytokine skewing was influenced by the ability of the T cells to respond to TGFβ1 (Figure 3.36B).

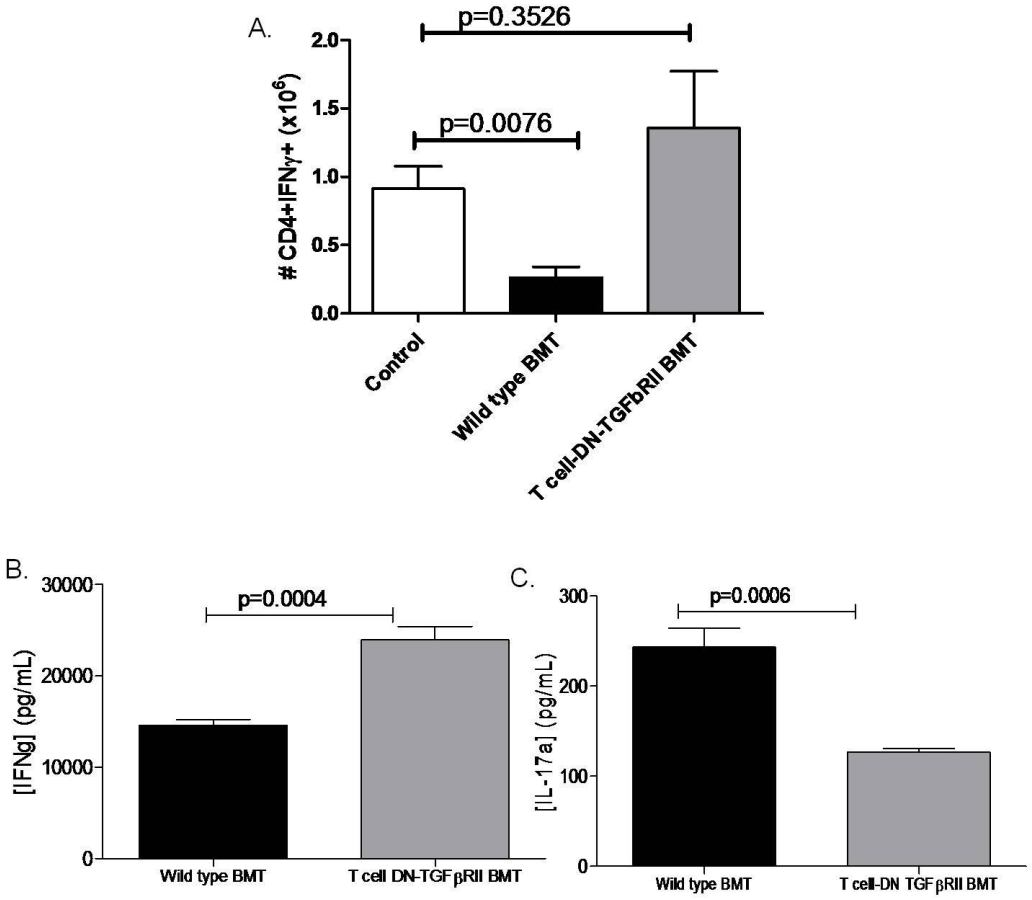

Figure 3.36 *T cells from T cell-DN-TGFβRII BMT mice express higher amounts of IFNγ and lesser amounts of IL-17a. A.* Right lungs from control, wild type BMT, and T cell-DN-TGFβRII BMT mice were harvested d7 post-infection with $5x10^4$ pfu γHV-68, digested in collagenase and analyzed using flow cytometry (*n*=5 per group). *B.* and *C.* Splenocytes from syngeneic BMT and T cell-DN-TGFβRII BMT mice were depleted of CD19-expressing cells via magnetic separation. Cells were then cultured with PMA and ionomycin for 24 hours. Supernatants were harvested and assayed for expression of IFNγ and IL-17a by ELISA. *B.* Wild type BMT cells expressed significantly less IFNγ than T cell-DN-TGFβRII BMT cells (*p=0.0004, n*=5 per group). C. Syngeneic BMT cells expressed significantly more IL-17a than T cell-DN-TGFβRII BMT cells (*p*=0.0006, *n*=5 per group).

We next analyzed lungs for the presence of Tregs in T cell-DN-TGFβRII BMT, wild type syngeneic BMT and non-transplanted control mice. Consistent with our previous observations (Figure 3.25), both groups of BMT mice showed elevated numbers of Tregs (Figure 3.37A). We also analyzed the lungs at d7 post-infection for Th17 cells. Consistent with the data shown in Figure 3.25, wild type BMT mice had increased numbers of Th17 cells compared to control. T cell-DN-TGFβRII BMT mice also had increased Th17 cells (Figure 3.37B). These data show that the T cell-DN-TGFβRII BMT mice are able to effectively control lytic viral replication despite the continued presence of increased numbers of Tregs and Th17 cells in the lungs post-BMT, further confirming the notion that Tregs and Th17 cells do not impair anti-viral immunity in the BMT setting (Figure 3.27, Figure 3.30).

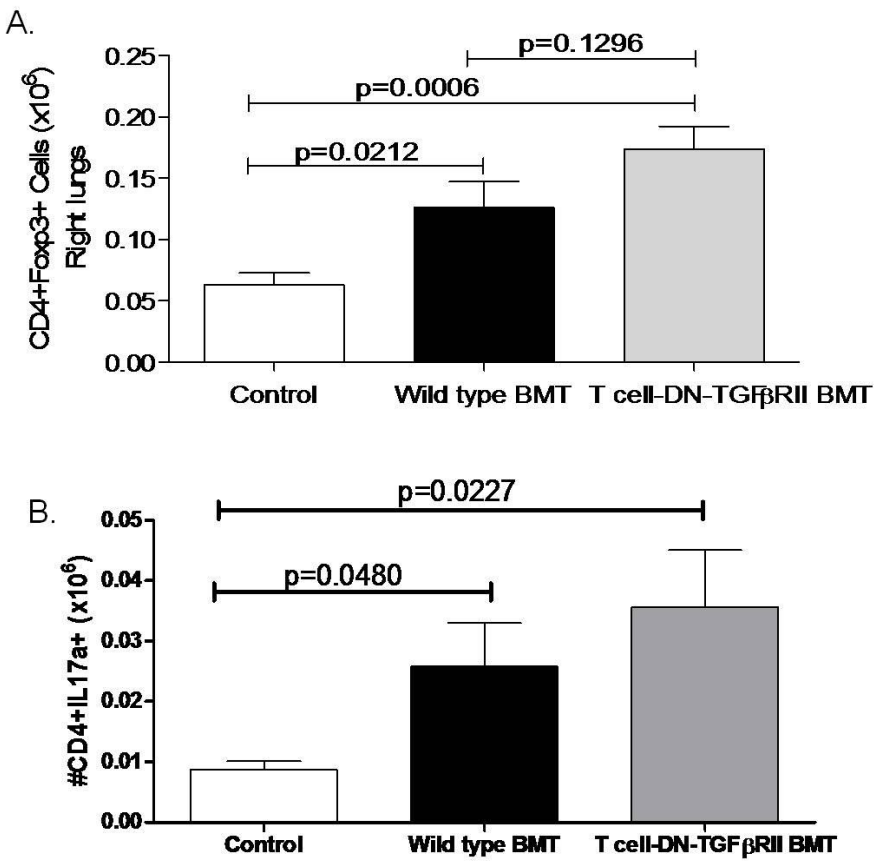

Figure 3.37 *T cell-DN-TGFβRII BMT mice have increased Tregs and Th17 cells at d7 post-infection with γHV-68.* Right lungs from non-transplant control, wild type BMT, and T cell-DN-TGFβRII BMT mice were harvested at d7 post-infection with $5x10^4$ pfu γHV-68, digested in collagenase and analyzed using flow cytometry. *A.* Both wild type and T cell-DN-TGFβRII BMT mice had significantly higher numbers of Tregs compared to non-transplanted controls (*n*=5 mice per group; data representative of 2 independent experiments). *B.* Both wild type and T cell-DN-TGFβRII BMT mice had significantly higher numbers of CD4+IL-17a+ cells compared to non-transplanted controls (*n*=5 per group).

Blocking TGFβ signaling in innate immune cells in the lung does not restore lytic viral load

Because TGFβ is a pleiotropic cytokine with immunosuppressive effects on multiple cell types (Table 1.1), we next determined whether overexpression of TGFβ post-transplant suppressed innate immune responses to lytic γHV-68 infection in the lung. We set up transplants using a CD11c-DN-TGFβRII donor mouse (114), expressing the DN-TGFβRII transgene under the CD11c promoter. In the lung, TGFβ signaling would be blocked in CD11c-expressing cells, including dendritic cells, natural killer cells, and likely lung macrophages. We infected non-transplant control, wild type BMT, and CD11c-DN-TGFβRII BMT mice with $5x10^4$ pfu γHV-68. At d7 post-infection, lungs were harvested for RNA and expression of lytic viral genes was determined using real time RT-PCR. We found that CD11c-DN-TGFβRII BMT mice express increased levels of lytic viral genes, similar to wild type BMT mice, suggesting that TGFβ signaling in CD11c-expressing cells does not contribute to the impaired acute anti-viral immune response in our model.

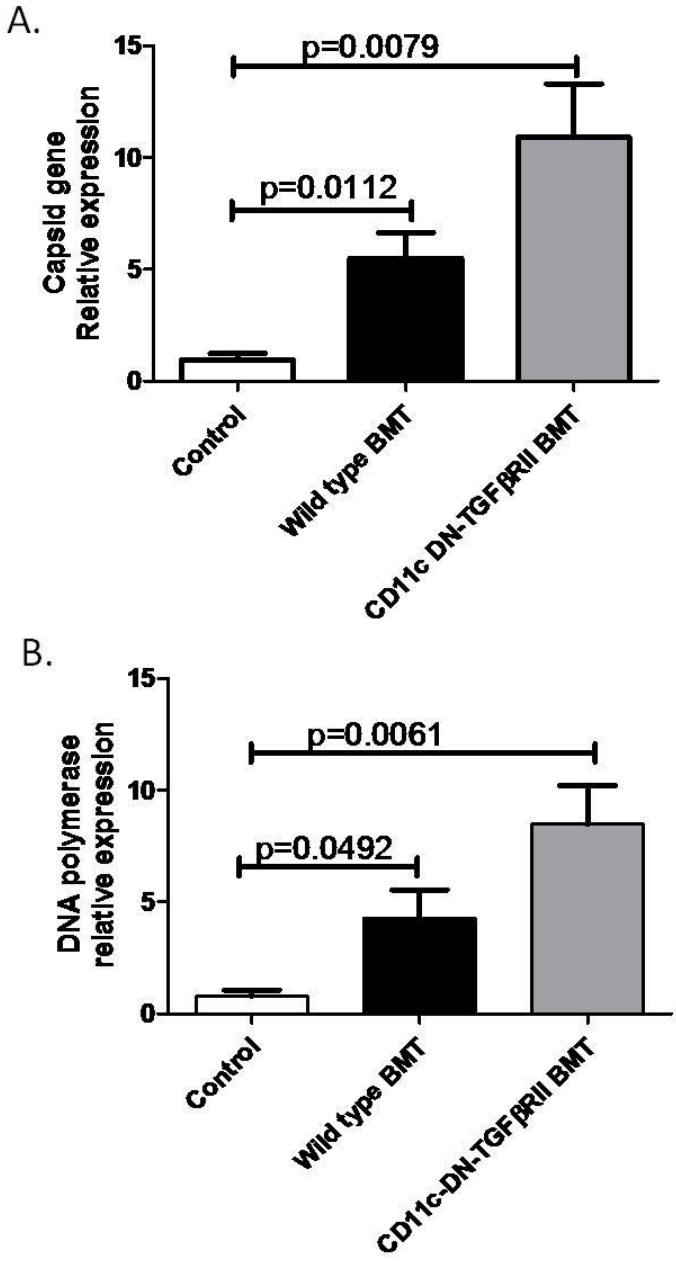

Figure 3.38 *CD11c-DN-TGFβRII BMT mice have increased lytic viral gene expression*. CD11c-DN-TGFβRII BMT mice showed a significant increase in viral capsid gene (*A*) and viral *DNA polymerase* (*B*) expression compared to non-transplant control mice. There was no significant difference between wild type BMT and CD11c-DN-TGFβRII BMT. (*n*=4 control, 5 wild type BMT, and 5 CD11c-DN-TGFβRII BMT). Expression of both genes is not significantly different between wild type BMT and CD11c-DN-TGFβRII BMT groups.

Blocking TGFβ signaling significantly improves pneumonitis and fibrosis in BMT mice

Because T cell-DN-TGFβRII BMT mice had restored control of lytic viral replication, we hypothesized that this would correlate with prevention of severe pneumonitis and fibrosis. We infected mice with $5x10^4$ pfu γHV-68 and harvested lungs for histology at d21 post-infection. We found a drastic reduction in pneumonitis, fibrosis, and overall histology score in BMT mice transplanted with T cell-DN-TGFβRII bone marrow (Figure 3.39). However, BMT mice transplanted with CD11c-DN-TGFβRII bone marrow had only a modest reduction in histology score (Figure 3.39). Taken together, these data suggest that TGFβ affects multiple cell types in promoting pneumonitis and fibrosis in response to γHV-68 in the BMT setting, but the most dramatic effects appear to be on T cells.

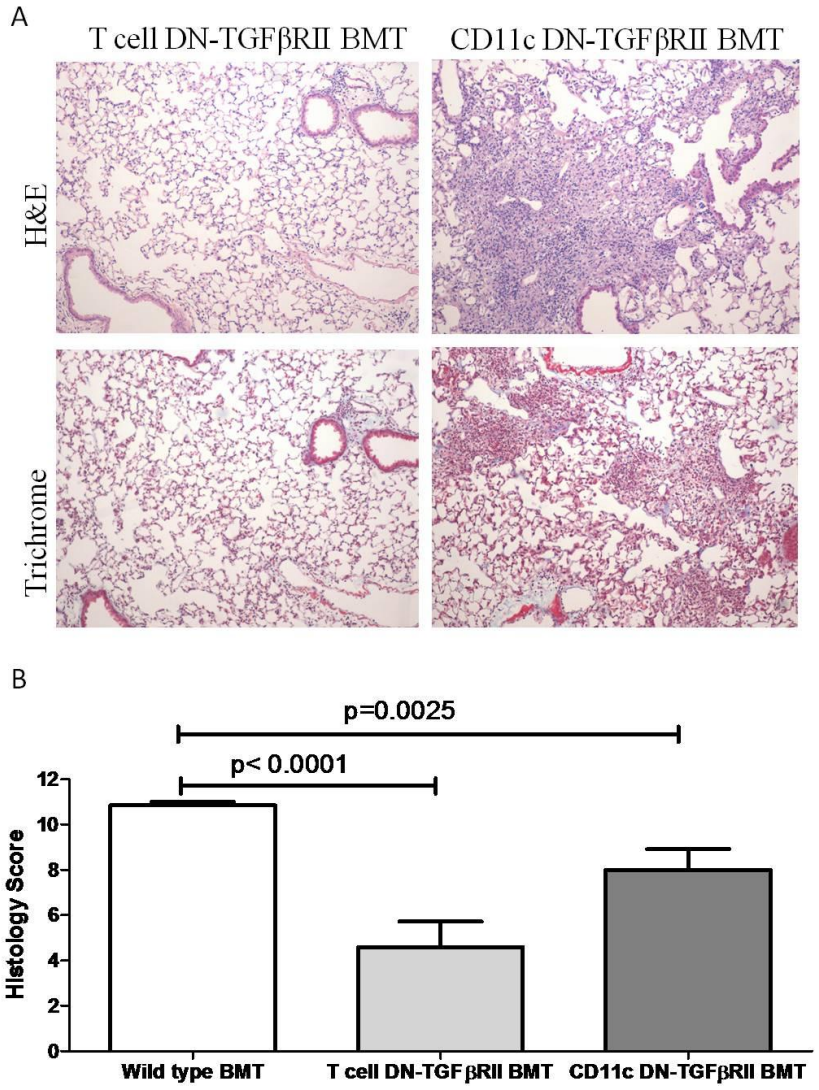

Figure 3.39 *Transplanting mice with T cell-DN-TGFβRII or CD11c-DN-TGFβRII bone marrow reduces presence of pneumonitis and fibrosis during latent γHV-68 infection.* BMT mice transplanted with T cell-DN-TGFβRII or CD11c-DN-TGFβRII bone marrow were infected with $5x10^4$ pfu γHV-68. Lungs were harvested at d21 post-infection for histology and stained for H&E and Masson's Trichrome. *A.* H&E and Trichrome stained lung sections (100x magnification). *B.* Lung sections were scored in a blinded fashion by a pathologist on the basis of presence and severity of pathological features (*n*=5 T cell-DN-TGFβRII and 4 CD11c-DN-TGFβRII BMT mice).

Severity of pneumonitis in BMT mice depends on initial viral dose

We next set up experiments to more directly test the hypothesis that uncontrolled lytic replication may contribute to the development of pneumonitis and fibrosis in the BMT setting during virus latency. We show in Figure 3.3 that BMT mice have an increasing inability to control lytic γHV-68 infection with higher viral challenge. Thus, we infected BMT mice with $1x10^3$, $5x10^4$ or $3x10^5$ pfu γHV-68 and harvested lungs for histology at d21 post-infection. We found that 4 out of the 5 BMT mice infected with $3x10^5$ pfu γHV-68 succumbed to infection around d14; however, we do not know whether this is due severely high lytic viral titers or due to pneumonitis. When lungs from BMT mice infected with $1x10^3$ and $5x10^4$ pfu were compared, we observed that pneumonitis was more severe, involving a greater area of the lung, in the BMT mice infected with higher viral inoculum (Figure 3.40). Thus, these data support a model wherein initial inability to control viral replication leads to later development of lung pathology.

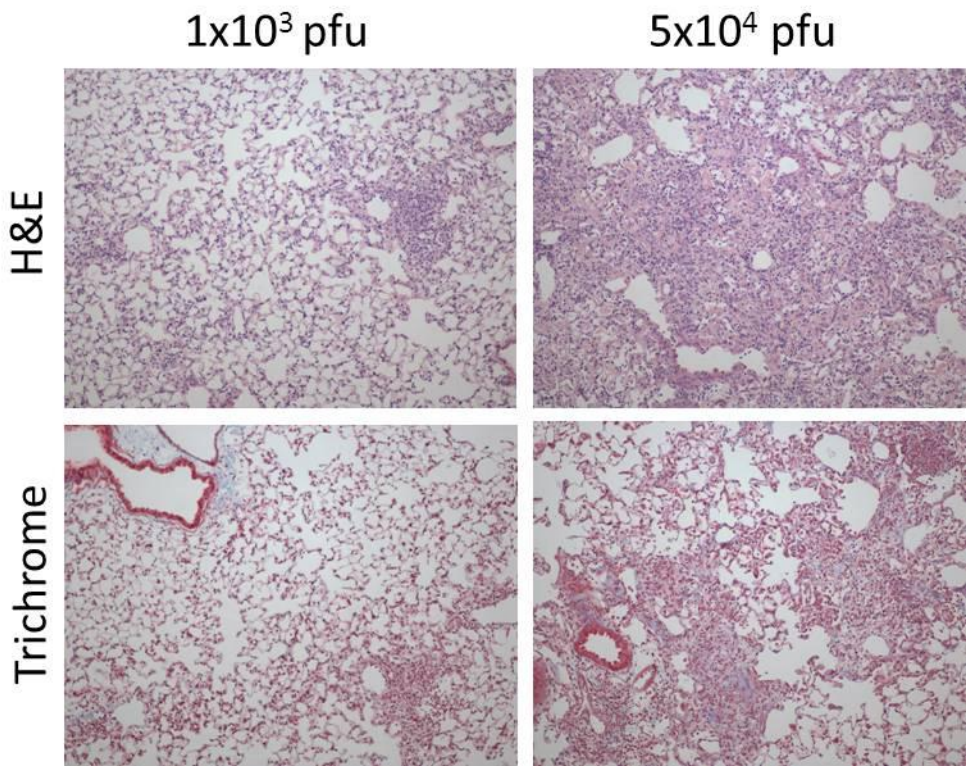

Figure 3.40 *BMT mice have more severe pneumonitis and fibrosis with higher viral challenge*. BMT mice were infected with $1x10^3$ or $5x10^4$ pfu γHV-68, and lungs were harvested for histology at d21. Lung sections were stained with H&E and Trichrome (100x magnification, representative of n=5 mice per group).

Chapter 4

Discussion

Summary of Results

In these studies we have established a murine syngeneic BMT model wherein transplanted mice have reduced ability to control lytic γHV-68 replication and subsequently develop pneumonitis and lung fibrosis during virus latency. In our model, BMT mice are challenged with γHV-68 at 5 weeks post-transplant, a time point when immune cell numbers in the lung are reconstituted. Following virus challenge, BMT mice have increased viral load at d7 post-infection with γHV-68, as determined by viral gene expression in the lungs, viral plaque assay, and viral immunohistochemistry. We find that increased viral gene expression in the lung persists at d14 post-infection.

By d21 post-infection, however, when γHV-68 is latent in the lungs, BMT and non-transplanted control mice have equivalent viral load. Histological analysis reveals that during virus latency, BMT mice develop severe pneumonitis characterized by foamy alveolar macrophages, increased levels of H_2O_2 and NO_2-, and increased infiltration of neutrophils and T cells in the alveolar space. Additionally, Trichrome staining and real time RT-PCR for collagen expression indicates development of lung fibrosis in BMT, but not control lungs, during virus latency. Correspondingly, BMT mice have reduced oxygen saturation at d21 post-infection with γHV-68 compared to control mice. The

phenotype observed during virus latency is virus-induced, as uninfected BMT mice do not develop pneumonitis, fibrosis, or reduced oxygen saturation.

We have also established that BMT mice are able to recruit inflammatory cells to the lung in response to lytic γHV-68 infection. Additionally, BMT APCs grown from bone marrow *in vitro* or isolated from the uninfected or infected lungs have expression of MHC Class II and costimulatory molecules equivalent to or greater than levels seen on control cells. Accordingly, BMT dendritic cells and splenocytes are efficient stimulators in an MLR. However, we find that BMT T cells are poor responders in an MLR.

Lungs from BMT mice overexpress TGFβ at baseline, and at d7 post-infection with γHV-68, there is a significant decrease in Th1 and increase in Th17 cells in the lungs of BMT mice compared to control. Treg numbers are increased in the BMT lung both prior to infection and at d7 post-infection. Treating mice during infection with a cyclooxygenase inhibitor which blocks PGE_2 synthesis does not restore anti-viral immunity. Additionally, depletion of Tregs or transplanting mice with IL-17KO bone marrow also does not alter the increased viral load in BMT mice.

Additionally, we have found that although BMT dendritic cells produce decreased levels of IL-12, we that this is not sufficient to skew away from a Th1 response *in vitro*. Rather, BMT T cells express decreased Tbet and increased TGFβ at baseline. We set up experiments using BMT mice transplanted with transgenic bone marrow expressing DN-TGFβRII in T cells or under the CD11c promoter, blocking TGFβ signaling in CD4 and CD8 cells or CD11c-expressing cells, respectively. T cell-DN-TGFβRII BMT mice have reduced lytic viral load and improved Th1 response; these mice are largely protected

from the pneumonitis phenotype. However, CD11c-DN-TGFβRII BMT mice show increased susceptibility to lytic infection, similar to wild type BMT, and are only moderately protected from pneumonitis. Furthermore, wild type BMT mice infected with lower amounts of virus have less severe pneumonitis. Taken together, our data support a model wherein overexpression of TGFβ post-BMT limits Th1 responses to acute γHV-68 infection, promoting higher initial viral titers and lung damage, leading to the development of pneumonitis and fibrosis in these mice.

Discussion: γHV-68 infection and pneumonitis in murine BMT

Studies in our model show that at 5 weeks post-transplant, syngeneic BMT mice are unable to control acute lytic replication as well as non-transplanted control mice (Figure 3.1). This corresponds with clinical reports showing opportunistic infections occurring late post-transplant in autologous HSCT recipients (6, 7). We find that the magnitude of the host defense defect is influenced both by the dose of irradiation used for conditioning and also by the dose of virus used for infection. Significant increases in viral load occurred in mice conditioned with 1350 rads of TBI (Figure 3.2). In our hands, conditioning with 1350 rads results in approximately 95% reconstitution within the spleen, 82% reconstitution of alveolar macrophages, and 93% lung lymphocytes (161). In contrast, 800 rads permitted approximately 88% reconstitution in the spleen, but only 36% reconstitution of donor-derived alveolar macrophages (170). Thus, increased susceptibility noted in the mice conditioned with 1350 rads may be related to increased myeloablation and enhanced donor cell reconstitution or increased radiation toxicity. The former seems more likely, as T cells from BMT mice have decreased expression of *Tbet* with increasing irradiation dose (Appendix Figure 3). BMT mice showed significant

elevations in viral replication (as noted by expression of a viral capsid protein) at all doses of virus tested, but the magnitude of the difference between control and BMT mice was increased with higher viral inoculums (Figure 3.3). This suggests that the immune response in BMT mice is overwhelmed by increasing pathogenic challenge.

We report that BMT and control mice have equivalent latent viral loads at d21 post-infection (Figure 3.5), despite increased lytic virus in BMT mice. Our results are consistent with previous studies showing that lytic virus titers do not correlate with latent levels of γHV-68 (70, 71). We hypothesize that much of the lytic replication at day 7 may be occurring in cell types that do not survive or remain resident in the lung by day 21. Despite having no difference in latent viral load, we find that BMT mice develop severe, persistent pneumonitis and fibrosis during latent γHV-68 infection (Figure 3.6). It is important to note that in our model, we find that the pneumonitis phenotype is virus-induced. Uninfected BMT mice show no signs of pneumonitis or fibrosis at 2 months post-transplant (Figure 3.11). Although irradiated C57BL/6 mice can develop irradiation-induced fibrosis, this does not occur until 20-30 weeks post-irradiation, long after the 8 week time point used in our studies (173). The development of pneumonitis in our model does not occur until lytic replication has largely subsided in the lung. In this respect, our model mimics results of a prospective study of pediatric allogeneic HSCT recipients showing that early respiratory virus infection post-transplant was correlated with later development of IPS and bronchiolitis obliterans. Importantly, patients had recovered from their initial respiratory symptoms prior to development of later respiratory symptoms associated with IPS or bronchiolitis obliterans, which are in part clinically defined by having no active infection (13). Our data support a model where an active

viral infection can lead to pneumonitis and lung injury at later time points, even after resolution of the initial lytic insult.

The concept that level of virus load does not correlate with lung pathology is in accordance with a study of HSV-1 pneumonitis where viral loads were decreased in allogeneic BMT mice with GVHD compared to non-GVHD allogeneic mice. In that study, lung pathology was more severe in mice that had developed GVHD, despite decreased viral loads (123). Similarly, another study found that viral titers were not predictive of interstitial pneumonitis development upon MCMV infection in GVHD mice versus controls (174). However, unlike our model, these studies both looked at viral titers early post-infection and involved the complication of GVHD.

In accordance with the severe inflammatory and fibrotic phenotype in BMT mice at d21 post-infection with γHV-68, our data show that these mice also have reduced oxygen saturation (Figure 3.15). It is important to highlight that this reduced oxygen saturation measures values at rest and might be even more substantial if mice were exercised. The reduced oxygen saturation in our BMT mice correlates with reports of abnormal pulmonary function tests which persist long-term in HSCT recipients (31). Our data suggest that unresolved inflammation from a previous infection may contribute to long-term reduced pulmonary function in HSCT recipients.

In our model, we find infiltration of inflammatory cells including neutrophils and lymphocytes in the alveolar space during latent γHV-68 infection in BMT mice (Figure 3.13). We find that the largest lymphocyte population present in the alveolar space in both BMT and control mice is CD8 cells, which are known to be an expanded population

during γHV-68 latency (175). We speculate that the infiltration of these cells into the alveolar space may be indicative of unresolved inflammation due to the initial virus infection, as a preliminary data indicate that a percentage of CD8 cells are specific for a viral epitope. The resident cell population in the alveolar space of uninfected BMT and control mice consists almost exclusively of monocytes/macrophages (data not shown). We also note the presence of large, foamy alveolar macrophages in BMT lungs (Figure 3.16) during latent γHV-68 infection. When the alveolar macrophage population was enriched from BMT mice at d21 post-infection, we found that these cells express the classical activation marker *iNOS*, an enzyme which catalyzes production of nitric oxide, as well as the alternative activation marker *Arginase 1*, an enzyme which promotes fibroblast proliferation and collagen production (Figure 3.16). Of note, the induction of *Arginase 1* is greater than the induction of *iNOS* on a population basis, but both are clearly induced. Classically activated macrophages are thought to promote inflammation while alternatively activated macrophages are associated with wound repair (134, 135). The dichotomy of function between these macrophage subsets correlates well with the inflammatory and fibrotic phenotypes in the BMT lung during γHV-68 latency. Future studies will determine whether these markers are expressed on the same macrophages, or whether there are two distinct populations present in the alveolar space.

Alternatively activated macrophages have been implicated in promoting pulmonary fibrosis during chronic γHV-68 infection in IFNγRKO mice. In these studies, the appearance of these macrophages was attributed to the Th2 environment and expression of IL-13 (136) in these Th2-biased mice. Interestingly, in our model, we find no evidence of upregulated IL-4 or IL-13 production by BAL cells, alveolar

macrophages, or in whole lung homogenates (Appendix Figure 1). However, we report a significant decrease in numbers of IFNγ-producing CD4 cells in the lungs of BMT mice during lytic γHV-68 infection at d7 post-infection (Figure 3.25), suggesting that the development of *Arginase 1*-expressing alveolar macrophages may occur in the absence of an overwhelming Th1 response, not simply to the presence of a Th2 response. It is also possible that increased TGFβ (Figure 3.26) or increased IL-10 noted at d21 post-infection (Appendix Figure 4) may contribute to the alternative activation phenotype (176). However, both CD11c-DN-TGFβRII BMT mice and transplants using IL-10KO donors still show evidence of foamy macrophages on lung histology as part of the composite score shown (Figure 3.39, Appendix Figure 4). Quantitative studies determining the relative expression of alternative activation markers in either the CD11c-DN-TGFβRII BMT or IL-10KO BMT mice have not been performed. It is also possible that in these transgenic BMT mice, the foamy alveolar macrophages are host-derived cells, as alveolar macrophages are only 82% donor-derived despite our high dose of conditioning (1350 rads) (170). Future studies may involve the use of congenic markers to determine whether these macrophages are donor or host-derived.

We also report increased oxidative stress in BMT mice at d21 post-infection with γHV-68, as shown by increased levels of H_2O_2 and NO_2- in BALF (Figure 3.17). These reactive intermediates can promote tissue damage and have been implicated in promoting pulmonary fibrosis (131). Reactive nitrogen intermediates have been shown in animal studies to stimulate production of TGFβ, a potent pro-fibrotic cytokine (130). Accordingly, we find a significant increase in levels of TGFβ in BALF from BMT mice at d21 post-infection (Figure 3.17). In turn, TGFβ has also been reported to increase

oxidative stress in pulmonary fibrosis (101). Whether these reactive intermediates upregulate TGFβ expression or are upregulated by TGFβ in this model has not been tested. Future studies using anti-oxidant compounds and examining oxidative stress in T cell-DN-TGFβRII BMT mice will differentiate between these possibilities and will determine a more direct role of oxidative stress in the development of pneumonitis and fibrosis in our model. Accordingly, the cellular source of the increased H_2O_2 and NO_2- has not been determined, though we hypothesize that the increased presence of neutrophils in the alveolar space of BMT mice (Figure 3.13) may contribute.

Discussion: Altered immune responses post-BMT

In Figure 3.18, we show that BMT mice are able to recruit inflammatory cells to the lung as well as control mice at d7 post-infection with γHV-68. These data correspond with previous studies from our laboratory showing that BMT and control mice were able to similarly recruit immune cells to the lung in response to *Pseudomonas aeruginosa* infection (59). Thus, we conclude that the inability to control lytic viral replication in BMT mice is not related to a defect in immune cell recruitment but rather a deficiency in immune cell function.

We initially hypothesized that the increased viral burden found in the lungs of BMT mice could be related to defective antigen presentation. DC are the principal APCs, linking innate to adaptive immunity and thus initiating the T cell response to pathogens (141). Our data indicate that BMT BMDCs are phenotypically similar to cells cultured from non-transplanted control mice in terms of expression of the costimulatory molecules CD80 and CD86 as well as MHC Class II (Figure 3.19). Additionally, lung APCs from

uninfected and infected BMT mice also showed equivalent or higher MHC class II and co-stimulatory molecule expression compared to controls (Figure 3.20, Figure 3.21). Using an MLR as a general measure of APC function, we found that BMT BMDCs were efficient stimulators of T cell proliferation, in some cases even more effective than control (Figure 3.19). To ensure that the potential inhibitory phenotype of the BMT APCs was not being lost during *in vitro* culture of BMDCs, we tested freshly isolated splenocytes as stimulators in an MLR. Similar results were found when irradiated BMT spleen cells were used as stimulators (Figure 3.22), suggesting that BMT-derived APCs are functional when freshly isolated as well. These results correlate with data from human patients undergoing autologous HSCT; it has been shown that DC generated from peripheral blood precursors post-transplant are effective stimulators in an MLR (10). Indeed, at six months post-transplant, these cells were even more potent APCs than DC generated prior to transplant (10). Thus, we conclude that APCs derived from BMT mice are capable of promoting T cell proliferation *in vitro,* and APC dysfunction is likely not a major contributor to the impaired anti-viral response in our BMT model.

Because of the central importance of CD4 T cells in controlling lytic γHV-68 infection (78), we hypothesized that T cell dysfunction may contribute to the impaired anti-viral response in BMT mice. Using an MLR as a general measure of T cell function, we observed that whole splenocytes and CD4 cells isolated from BMT spleen were impaired in their ability to respond in an MLR when compared with cells from non-transplanted control mice (Figure 3.23). Our findings are similar to clinical data showing that T cells from HSCT recipients have impaired responses in an MLR even one year post-transplant (10). It is likely that the impaired proliferative response of BMT T cells *in*

vitro is due to their overexpression of TGFβ post-transplant (Figure 3.34), as TGFβ is a potent inhibitor of naïve T cell proliferation (82). The fact that we see normal T cell accumulation in the lungs in response to γHV-68 at d7 post-infection (that is, no defect in proliferation *in vivo*), may be attributed to the fact that T cells, once activated, are refractory to the anti-proliferative effects of TGFβ, correlating with decreased TGFβRII expression (177). Additionally, the ability of TGFβ to impair T cell proliferation is also abrogated in the presence of strong costimulatory signals (82). It is also possible that the overproduction of PGE_2 post-BMT (Figure 3.24, (60)) contributes to impaired proliferation in the MLR, as PGE_2 is a known inhibitor of the MLR response (178). MLRs including cyclooxygenase inhibitors to block PGE_2 production could be used in future studies to test this.

Previous studies from our laboratory have found that overproduction of PGE_2 post-transplant severely limits alveolar macrophage function, therefore impairing immunity to *Pseudomonas aeruginosa* (60). In addition, PGE_2 has been reported to have suppressive effects on T cells (178). Thus, we first hypothesized that the impaired response to lytic γHV-68 in BMT mice could be attributed to PGE_2 overproduction. To test this hypothesis, BMT mice were treated with indomethacin, a cyclooxygenase inhibitor which blocks PGE_2 synthesis. We find that indomethacin treatment does not restore control of lytic γHV-68 replication, despite reductions in PGE_2 (Figure 3.24). Therefore, we conclude that, unlike our bacterial model, overproduction of PGE_2 in the lung post-transplant does not directly impair anti-viral responses. It is interesting to note that differential mechanisms appear to be responsible for impaired immunity to bacterial and viral infections. While we do not find a direct role of PGE_2 overproduction in

limiting immunity to viral infection, future studies should address the interplay between upregulated PGE_2 (Figure 3.24) and TGFβ (Figure 3.26) post-transplant in both our viral and bacterial models, as TGFβ has been reported to induce cyclooxgenase expression in other systems (179, 180).

In addition to the *in vitro* proliferation defects of BMT T cells, we have also found that CD4 T cell differentiation is altered in BMT mice in response to γHV-68 infection. At d7 post-infection, BMT mice have decreased numbers of Th1 cells and increased Th17 and Treg cells in the lung (Figure 3.25). It is likely that overexpression of TGFβ in the lungs post-transplant (Figure 3.26) contributes to the altered T cell phenotype in BMT mice. TGFβ has been reported to impair Th1 differentiation by decreasing expression of IL-12Rβ2, Tbet, and Stat4, molecules all important for IFNγ production by CD4 cells (82). Indeed, we have observed reduced expression of *Tbet* mRNA in T cells from BMT mice (Figure 3.34); BMT T cells also produce increased TGFβ post-transplant (Figure 3.34). These data correlate with previous studies showing that CD4 cells deficient in Tbet have increased TGFβ production (181). In conjunction with IL-6 signaling, TGFβ can induce differentiation of Th17 cells (105). The importance of T-cell produced TGFβ in promoting Th17 differentiation and inhibiting Th1 differentiation has been shown using transgenic mice with a T cell-specific deletion in TGFβ (103).

We found that numbers of CD4+Foxp3+ Tregs were increased in the lungs of BMT mice both prior to infection and at d7 post-infection (Figure 3.25). Tregs are a specific subset of CD4 cells which function to suppress effector T cells (149). In the setting of BMT, these cells have been best described by their ability to induce graft

tolerance and suppress GVHD (151). Interestingly, in our model, we have found using CD45 congenic transplants that 60% of the Tregs in the BMT lung are host-derived. This is striking, as we find that 93% of total lymphocytes in the lung at 5 weeks post-transplant are donor-derived. These data add to a previous study demonstrating that host-derived cells comprise the large majority of the Treg compartment in the spleen for a prolonged period following syngeneic BMT (155). We also demonstrate that Treg numbers increase in a radiation dose-dependent manner (Appendix Figure 2). Thus, our data show that Tregs may accumulate (perhaps by homeostatic proliferation of radio-resistant host Tregs (155)) in direct proportion to the size of the niche created by conditioning. However, experiments using congenic donors into CD4KO recipients show that in the absence of host-derived Tregs, donor-derived CD4+Foxp3+ cells will expand to the same extent as in wild type to wild type transplants (Appendix Figure 5), suggesting that there is preferential expansion of Tregs post-transplant regardless of source.

To determine the contribution of the Tregs to impaired anti-viral immunity post-BMT, we depleted Tregs using anti-CD25 and compared viral host defense in these mice or mice treated with an isotype control. Treatment with anti-CD25 effectively reduced the levels of CD4+Foxp3+ cells to the levels seen in non-transplanted control mice (Figure 3.28). However, despite the reduction in Tregs, the ability of the BMT mice to control lytic virus was still impaired (Figure 3.27). These data are consistent with recent studies demonstrating that adoptive transfer of Tregs into mice receiving an allogeneic BMT could limit GVHD, but did not impair the ability of the BMT mice to respond to lethal cytomegalovirus infection (156). Furthermore, we find that T cell-DN-TGFβRII BMT

mice have restored control of lytic γHV-68 despite the persistence of increased Tregs (Figure 3.37). In sum, we conclude that increased Tregs in the lung post-transplant do not impair anti-viral host defense to acute γHV-68 replication.

We next analyzed whether the increased numbers of Th17 cells in the lungs of BMT mice (Figure 3.25) could directly contribute to the impaired response to lytic γHV-68 infection. IL-17a is a cytokine known to be critical for immunity to many extracellular bacteria and fungus infections. The role of IL-17a and Th17 cells in anti-viral responses has been less well-studied. It appears that Th17 cells are protective in some viral infections, while detrimental in others (172). There are no data to date directly studying the role of IL-17a in immunity to γHV-68. Our experiments show that lytic viral load is equivalent in non-transplanted wild type and IL-17aKO mice infected with γHV-68. Accordingly, transplants performed with IL-17aKO donors showed no difference in lytic viral gene expression when compared to transplants performed with wild type donors (Figure 3.30). Additionally, we observe increased Th17 numbers in the lungs of T cell-DN-TGFβRII BMT mice, which have restored control of lytic γHV-68 (Figure 3.37). Taken together, we conclude that IL-17a does not play a critical role during the first 7 days post-infection with γHV-68 and that increased numbers of Th17 cells in the lung are not directly impairing control of lytic γHV-68 in our BMT model. We have not evaluated, however, whether IL-17a plays a role at later time points, such as in the clearance of lytic virus from the lungs or in the establishment of latency. Future studies may also define a role for IL-17a in regulating post-transplant cytokine alterations, as IL-17a has been shown to upregulate PGE_2, at least in synovial fibroblasts (182). It is also conceivable that IL-17 production contributes to the development of the pneumonitis and

fibrosis (183) phenotype at day 21 post-infection, and future studies will be needed to explore this further.

We next hypothesized that rather than increased Tregs or Th17 cells, it was the lack of protective Th1 cells in the lung which was impairing control of lytic viral replication in the BMT mice. Indeed, IFNγ expression by CD4 T cells is critical for control of γHV-68 replication (77-79). To determine the role of APC cytokine production in relation to the decreased Th1 cells in the lung, we isolated BMDCs and lung CD11c-expressing cells from uninfected BMT and control mice. Upon TLR stimulation, we found that BMT APCs had reduced expression of IL-12 compared to control (Figure 3.31, Figure 3.32). However, CD11c-expressing cells isolated from BMT and control lungs at d7 post-infection expressed similar levels of IL-12 (Figure 3.32). To test whether the impaired IL-12 production by BMT APCs could impair Th1 differentiation, we set up *in vitro* experiments using BMT or control BMDCs, OVA peptide, and OVA-specific OT-II CD4 T cells from a non-transplanted mouse. We found that BMT and control BMDCs were able to stimulate similar IFNγ production by CD4 cells in this assay (Figure 3.33). These data, in combination with the fact that IL-12 was not reduced in lung CD11c-expressing cells following γHV-68 infection, suggest that while IL-12 may be reduced at baseline in BMT BMDCs and lung CD11c-expressing cells, its reduction is not critical for impairing Th1 responses. Indeed, PBMCs from autologous HSCT patients have been reported to produce sufficient IL-12 and efficiently induce IFNγ production *in vitro* (184). We have not studied the mechanism by which IL-12 is reduced in BMT BMDCs and lung CD11c-expressing cells. However, we hypothesize that reduced IL-12

levels may be a result of increased PGE_2 post-transplant, a known inhibitor of IL-12p35 and p40 transcription (185).

Future studies may evaluate the role or function of antigen presentation by B cells post-transplant, as these cells express MHC class II and may be important contributors to the T cell response in our model. While we do find that unfractionated splenocytes are efficient stimulators of an MLR response (Figure 3.22), we have not carefully isolated B cells and characterized their response. B cells are important antigen-presenting cells, and their proliferation and phenotype are indeed known to be affected by the presence of TGFβ (82). These cells may also be sources of TGFβ and IL-10, mediators which are both upregulated in our model.

Discussion: Effects of blocking TGFβ signaling in murine BMT

To determine whether TGFβ was directly inhibiting Th1 differentiation (82) and therefore impairing control of γHV-68 replication in the BMT setting, we set up transplants using T cell-DN-TGFβRII as donors. Thus, we set up a model system where donor-derived T cells in the BMT setting would be non-responsive to TGFβ signaling (104). We report that blocking TGFβ signaling in T cells in the BMT setting is sufficient to control lytic γHV-68 replication and restore numbers of Th1 cells in the lung at d7 post-infection (Figure 3.35, Figure 3.36). In this regard, our results are similar to a study using T cell-DN-TGFβRII mice showing that TGF-β-mediated inhibition of Th1 differentiation led to increased susceptibility to *Leishmania major* in Balb/c mice (17). We conclude that TGFβ limits protective Th1 responses to γHV-68 lytic replication in murine BMT.

Furthermore, we find that blocking TGFβ signaling in T cells in the BMT setting leads to a dramatic reduction in inflammation, fibrosis and lung histology score (Figure 3.39). These data suggest direct or indirect involvement of T cells in the development of pneumonitis and fibrosis in this model. The observation that T cell TGFβ signaling is important for fibrosis development has been made previously in a study using T cell-DN-TGFβRII mice in a mouse model of chronic allograft rejection (183). Our data suggest that TGFβ limits Th1 responses to lytic γHV-68 infection in the BMT setting, thus causing an increase in lytic viral load. We hypothesize that subsequent pneumonitis and fibrosis during latent infection results from the enhanced lytic virus insult in wild type BMT mice (Figure 3.35), possibly causing increased epithelial cell destruction, the unresolved inflammatory response that accompanies the increased lytic viral load, or altered wound repair mechanisms to control tissue damage. The T cell-DN-TGFβRII BMT mice express decreased levels of TGFβ1 prior to infection compared to wild type BMT mice (Appendix Figure 6) and have restored numbers of Th1 cells in response to lytic γHV-68 infection (161). Thus, it is likely that the improved host response to the lytic infection in the T cell-DN-TGFβRII BMT mice may account for the improved pneumonitis phenotype noted in these mice at day 21 post-infection. It is interesting to note the persistence of increased Th17 cells in the lungs of the T cell-DN-TGFβRII BMT mice (Figure 3.37), as TGFβ has been considered an important factor in the development of T cells (105). This result is supported by a recent study showing that TGFβ is not directly necessary to promote Th17 differentiation (186).

We also note a modest, but significant reduction in lung histology score in BMT mice transplanted with donor cells expressing a DN-TGFβRII transgene under the CD11c

promoter (Figure 3.39). We find that CD11c-DN-TGFβRII BMT mice have high lytic viral loads at d7 post-infection which are similar to wild type BMT mice (Figure 3.38). These data indicate that TGFβ signaling plays little role in CD11c-expressing cells to control lytic infection. However, the fact that the CD11c-DN-TGFβRII BMT mice have a modestly improved pneumonitis phenotype suggests that some CD11c-expressing cell type may influence development of lung pathology at later time points despite a lytic infection level that is similar to wild type BMT mice. We have not analyzed whether the improved phenotype of the CD11c-DN-TGFβRII BMT is due to blockade of TGFβ signaling in lung macrophages, dendritic cells or natural killer cells; however, foamy alveolar macrophages were present in the CD11c-DN-TGFβRII BMT lungs. Whether there are quantitatively fewer alternatively activated macrophages in these mice remains a formal possibility and will require further study. We have not analyzed the T cell response in the CD11c-DN-TGFβRII BMT mice. While we do not find an improvement in lytic viral load, we do find a modest reduction in pneumonitis and fibrosis, which could be explained by the ability of the mice to prevent viral reactivation more efficiently than wild type BMT mice. It has been shown that non-transplanted CD11c-DN-TGFβRII mice have increased levels of innate IFNγ, derived from NK cells, which can affect T cell responses (114). Future studies may address these possibilities in our BMT model.

We find that the magnitude of the host defense defect in BMT mice in response to lytic γHV-68 is amplified with increasing viral challenge (Figure 3.3), suggesting that the immune response becomes overwhelmed with increased pathogen exposure. We hypothesize that this is due to the limiting effects of TGFβ on a protective Th1 response. Correspondingly, we find that BMT mice challenged with higher viral dose develop more

severe pneumonitis and fibrosis during virus latency (Figure 3.40), supporting the hypothesis that increased lytic replication is a major contributor to later development of lung pathology.

Taken together, our data support a model where increased TGFβ post-BMT, possibly due to conditioning-induced epithelial cell damage in the lung, limits a protective Th1 response, leading to a substantial increase in lytic γHV-68 replication. The enhanced viral replication leads to increased lung cell damage, causing unresolved inflammation, oxidative stress, and dysregulated wound repair mechanisms including increased TGFβ and alternatively activated macrophages even after lytic replication has subsided in the lung.

Implications and Contributions to Field

Data from these studies provide new insights into impaired anti-viral immune responses and pneumonitis development post-BMT. Specifically, the major contributions of our studies to the HSCT field include new insight into mechanisms of impaired anti-viral immunity post-HSCT, development of a novel model system of post-transplant pneumonitis, and defining a role of TGFβ in impairing immunity post-transplant.

Mechanisms of increased susceptibility to viral infections post-HSCT have largely been attributed to the presence of GVHD, immunosuppressive drug therapy, and lymphopenia post-transplant. Our studies now add an additional mechanism, providing direct evidence that development of transplanted cells in a conditioned host can result in significant alterations in immune response. Importantly, we observe impaired anti-viral responses in reconstituted BMT mice in the complete absence of GVHD and

immunosuppressive drug therapy. In our reconstituted syngeneic BMT model, we report reduced proliferative capacity of naïve T cells from BMT mice, as well as altered T cell differentiation in response to virus infection. These data add to previous studies from our laboratory showing that alveolar macrophage function is significantly impaired in murine syngeneic BMT (60). Thus, our studies provide further support that the susceptibility to pulmonary infection post-HSCT can be attributed to a number of factors, including the transplantation and conditioning procedure itself.

A major contribution of this work is the development of a novel model of post-transplant pneumonitis and fibrosis. Pneumonitis is a serious complication of HSCT, with reviews having estimated the incidence of IPS to be 7.6-10.6% of allogeneic patients and 5.7-5.8% of autologous patients (36, 187). Both IPS and bronchiolitis obliterans are considered to be non-infectious pulmonary complications of HSCT, based on the inability to find active infection in these patients. We find that while the pathology in our BMT model is virus-induced, it does not manifest until virus latency, when there is very little detectable active virus replication occurring (Figure 3.6, Figure 3.8). Thus, our model suggests the possibility that pneumonitis development in HSCT patients may result from unresolved inflammation and tissue damage induced by a previous active infection. Additionally, our model is unique in that we observe the development of severe lung pathology in the absence of alloreactive cells. Murine models of IPS have been studied almost exclusively in the allogeneic setting, associating GVHD development with the appearance of lung pathology that resembles IPS. In these models, syngeneic BMT mice used as controls have normal lung histology several weeks post-transplant, reflecting what we observe in our uninfected syngeneic BMT mice (188). Our model provides

direct evidence that lung damage from a previous active infection may promote later development of pneumonitis and fibrosis, especially in the autologous setting, where alloreactive T cells are absent.

Studies have indicated that HSCT patients may have reduced pulmonary function post-transplant, with abnormalities persisting long-term (31, 32). Specifically, one study found that pediatric HSCT patients had reduced pulmonary function 3-6 months post-transplant, and despite partial recovery, patients had not returned to their pre-transplant values even 12-24 months post-transplant (21). Our data indicates that reduced pulmonary function post-HSCT may be related to unresolved inflammation and/ or lung damage induced by a previous pulmonary infection, as BMT mice in our model had reduced oxygen saturation at d21 post-infection with γHV-68 (Figure 3.15) and pathology which persisted even at 7 weeks post-infection (Figure 3.12).

Additionally, our studies have uniquely described a role of TGFβ in limiting anti-viral immune responses and promoting pneumonitis post-BMT. Previous work in a murine allogeneic GVHD model showed that induction of HSV-1 pneumonitis at late time points post-transplant was also mediated by effects of TGFβ (123). While our model also implicates TGFβ in promoting pneumonitis, there are several important differences between the models. First, pneumonitis in the HSV-1 model developed at days 5-7 post-infection and involved periluminal, but not parenchymal inflammation and no indication of fibrosis. Additionally, the authors concluded that pneumonitis in the HSV-1 model resulted from GVHD, as non-GVHD allogeneic BMT mice did not develop lung pathology (123). However, because of the difference in timing, it is interesting to

speculate that fibrosis and lung pathology in the non-GVHD allogeneic mice would manifest at later time points following HSV-1 infection as well.

Our studies also have significant implications for interpretation of experiments using bone marrow chimeras. Our laboratory has shown numerous alterations which occur simply as a result of TBI and transfer of cells. Thus, it is critical that bone marrow chimera experiments are tightly controlled. Experiments should first compare wild type into wild type and non-transplanted wild type mice as controls to understand how the phenotype being studied may be affected by TBI and transplant. In our model, we find significant changes in the immune response occur even at 5 weeks post-transplant, the time point when our studies were performed.

Limitations of Model System

Despite the advantages of controlled study, there are several important limitations of using a murine model to understand immune responses post-HSCT. Conditioning in murine models has traditionally been via the administration of TBI (58), partially due to the limitations of chemotherapy in promoting donor cell reconstitution post-HSCT (170) and due to chemotherapy-related morbidity in mice. While the administration of TBI in combination with cyclophosphamide has been considered the "gold standard" among conditioning regimens, non-TBI conditioning regimens are now common in human HSCT recipients (24). While chemotherapeutic agents and TBI have both been implicated in promoting lung damage in humans (33-35), it is unclear whether the mechanisms by which TBI affects lung cells in our murine model reflects the mechanisms of chemotherapeutic-induced lung damage in HSCT patients. Accordingly,

shielding may be used to protect organs from TBI-related damage in human patients, while we have not used shielding in our mouse model. Our model also does not allow us to discriminate the effects of cell transfer and reconstitution versus the direct effects of the conditioning regimen, limiting more careful mechanistic study. Future studies may include transfer of cells into SCID mice to determine whether the effects are due to transfer, conditioning, or both. Because we do not achieve 100% donor cell reconstitution in our model (170), transplants using congenic markers might be used to study the differences in donor versus host T cells to give an idea of whether conditioning or transfer of cells causes changes.

Additionally, we use naïve mice in our studies as both bone marrow donors and recipients. HSCT patients receive transplants as a curative option for many disorders, particularly malignancies and, as such, are not healthy when transplanted. The effects of previous chemotherapy, disease, and infections which may be present in humans (and contribute to susceptibility to infection) are not reflected in our model. Transplant donors, also, will be antigen-experienced and may have a wider repertoire of memory cells, especially if transplanted cells are harvested from the peripheral blood. Accordingly, our studies use γHV-68 infection as a model to understand how anti-viral immunity is altered post-transplant. However, in human patients, disease associated with herpesvirus infections generally occurs as a result of viral reactivation, either from donor cells or preexisting infection in the recipient. Future studies should address immunity to reactivation of virus infection, since reactivation, not primary infection, is the principal cause of herpesvirus-related disease in transplant recipients.

The study of T cell responses post-transplant in a murine model is somewhat limited, as we do not see the inverted CD4/CD8 ratio in our model that is observed in the peripheral blood of HSCT patients post-transplant (54-56). This fact may be due to intrinsic differences in reconstitution between humans and mice or could be that lung tissue cells differ in number compared to peripheral counts.

Long-term studies in T cell-DN-TGFβRII BMT mice in our model are limited, as the donor mice develop spontaneous autoimmune disease, characterized by inflammatory bowel disease and lung infiltration at 3-4 months of age (104). We think that this autoimmune response may be quickened in our infected T cell-DN-TGFβRII BMT mice, as some mice developed wasting disease even prior to d21 post-infection.

Finally, while the syngeneic model provides a system to understand how conditioning and subsequent transfer of cells leads to alterations in anti-viral immune responses, it is unclear whether the mechanisms observed in our model are translatable to the allogeneic setting. Many infectious and non-infectious pulmonary complications which occur post-transplant are more common in the allogeneic setting (3, 36, 38), so it will be important to determine whether general mechanisms observed in our studies are applicable to both autologous and allogeneic transplants. Preliminary data discussed in the Future Directions section of this dissertation will address these issues.

Future Directions

Our studies establish a murine BMT model wherein transplanted mice have a reduced ability to control lytic viral replication, following immune cell reconstitution, and subsequently develop virus-induced pneumonitis and fibrosis. Our data indicate that

BMT mice overexpress TGFβ and that blocking TGFβ signaling in T cells in the BMT setting is sufficient to restore Th1 responses, control lytic viral replication, and prevent severe pneumonitis. For future studies, it will be important to develop a more complete understanding of the underlying mechanisms contributing to the increased lytic viral load and development of pneumonitis in our BMT model. There are three main lines of investigation, supported by preliminary data that we have developed, that will be important to study in order to achieve this goal, including developing a more mechanistic understanding of the effects of TGFβ on BMT T cells, teasing out which post-BMT alterations specifically contribute to pneumonitis development, and understanding how these effects translate to allogeneic BMT models.

Future Directions: BMT T cells and TGFβ

Data from these studies support a model in which transplant-induced TGFβ overexpression skews the phenotype of CD4 T cells away from a Th1 response by inhibiting Tbet. For future studies, it will be important to more carefully define the mechanisms by which BMT T cells are skewed away from a protective Th1 response *in vivo* and determine how TGFβ mediates its effects. TGFβ is potent regulator of both CD4 and CD8 T cell differentiation, proliferation, and function (82), and it will be pertinent to determine the specific mechanism(s) by which TGFβ limits T cell responses in the BMT model.

Our *in vitro* assays showed that although BMT BMDCs and lung CD11c-expressing cells produce decreased IL-12, BMT BMDCs are able to induce efficient IFNγ production by antigen-specific CD4 T cells (Figure 3.33), suggesting that the

decreased *Tbet* (Figure 3.34) and diminished Th1 response to γHV-68 (Figure 3.25) are independent of the BMT dendritic cell phenotype. However, an important experiment to validate the claim that the deficiency is T cell intrinsic and not dendritic cell-related would be to set up analogous assays using either BMT or control CD4 cells as responders stimulated with BMT or control dendritic cells. We would expect, based on our model, that BMT T cells would have reduced IFNγ production, regardless of whether they were stimulated with dendritic cells from a BMT or control mouse. Accordingly, it is important to confirm that the T cell phenotype observed in BMT splenic T cells is analogous with T cells derived from BMT lungs, as these cells would be exposed to different structural cells which may be differentially affected by the conditioning regimen. While we do see that reduced Th1 responses in the lung correspond with reduced *Tbet* expression in splenic T cells, there may be location-specific differences. Indeed, data from our laboratory indicate that alveolar, but not peritoneal, macrophages from BMT mice have functional deficits post-transplant (unpublished observations).

Next, it will be pertinent to determine how TGFβ may be mediating its effects on the T cell phenotype in the BMT setting. TGFβ is known to have several roles in the regulation of T cells. In Figure 3.35, we demonstrate that T cell-DN-TGFβRII BMT mice have restored control of lytic viral replication compared to wild type BMT mice. This correlates with a restoration in numbers of Th1 cells in the lung at d7 post-infection (Figure 3.36), a cell type required for efficient control of lytic viral replication (77-79). A preliminary experiment shows that lungs from T cell-DN-TGFβRII BMT mice produce decreased levels of TGFβ compared to wild type BMT mice (Appendix Figure 6), indicating that TGFβ signaling in T cells in the wild type BMT setting promotes

overproduction of TGFβ. This suggests a model wherein TGFβ produced post-transplant in the lung, either from structural cells or another cell type, signals T cells to either produce increased TGFβ themselves or promote other cell types to produce TGFβ, by a positive feedback mechanism (Figure 4.1). Indeed, TGFβ is known to promote its own expression (93, 172, 189). In support of this model, we find that splenic CD4 and CD8 T cells from BMT mice overproduce TGFβ (Figure 3.34). However, future studies will determine whether lung-derived T cells from BMT mice also overproduce TGFβ. It will be important to test whether T cell-produced TGFβ is sufficient to impair anti-viral immunity. This can be analyzed by setting up transplants using bone marrow from mice which have a T cell-specific deletion of the *Tgfβ1* gene (103). Reconstituted, donor-derived T cells in these transplanted mice would not be able to produce TGFβ1. Analyzing lytic viral loads and T cell differentiation in these mice in the BMT setting will provide insight into the role of T cell-produced TGFβ in our model. Additionally, determining production of TGFβ by resident lung cells in these mice would provide a better understanding of mechanism of TGFβ upregulation. Long-term studies may be somewhat limited, similar to the T cell-DN-TGFβRII BMT mice, as the donor strain (lacking T cell *Tgfb1*) develops multiorgan autoimmunity with spontaneously differentiated Th1 and Th2 cells at 4 months of age (103).

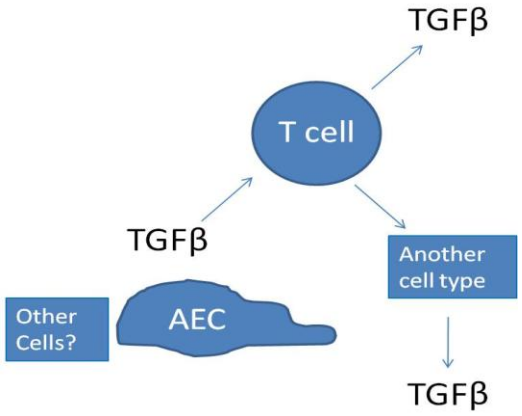

Figure 4.1 *Potential mechanism for overproduction of TGFβ in the lung post-BMT*. Preliminary data support a model where TGFβ produced by epithelial or other cell types in the lung affects T cell production of TGFβ and/or T cell induction of TGFβ production by other cell types in the lung. Future studies should discriminate between these possibilities.

Because of the importance of Th1 cells in lytic γHV-68 infection, our studies have largely focused on CD4 cells post-transplant. However, TGFβ has important effects on CD8 cells as well, including inhibiting expression of perforin and FasL (82). TGFβ can also reduce IFNγ production by CD8 cells via inhibition of Tbet (190). CD8 cells are an important, expanded population during γHV-68 latency. Thus, future studies should address the effector function of CD8 cells isolated from BMT mice. We do find that CD8 cells from BMT mice produce increased levels of TGFβ post-transplant (Figure 3.34). Future studies may include *in vitro* analysis of CD8 cytotoxic function. If effector function of BMT CD8 cells is reduced, we might hypothesize that inclusion of a neutralizing TGFβ antibody in these assays would restore function. *In vivo* studies should include a kinetic analysis of perforin, IFNγ, and FasL expression by CD8 cells in BMT and control mouse lungs following γHV-68 infection. This would give some insight into

whether a TGFβ-induced phenotype is present in BMT CD8 cells. Additionally, future studies should evaluate the contribution of CD8 cells in the restoration of lytic anti-viral immune responses in T cell-DN-TGFβRII BMT mice, as TGFβ signaling is blocked in both CD4 and CD8 T cells in these mice. Studies involving adoptive transfer of CD8 cells from γHV-68-infected BMT or control mice into naïve mice and challenging with γHV-68 may provide insight into the function of these cells.

Our studies look at total TGFβ production in the lungs post-BMT by ELISA (Figure 3.26). This shows that BMT mice have more total TGFβ available for activation and potential roles in immune responses. However, we did not directly measure the active protein present in the lungs. We find that despite increasing susceptibility to γHV-68 with increasing irradiation dose (Figure 3.2), total TGFβ levels in the lung are similarly increased between mice conditioned with 650, 900 or 1350 rads (Appendix Figure 2); we do not yet know whether *active* TGFβ levels increase in parallel with radiation dose. We hypothesize that there may be more active TGFβ present post-transplant, perhaps through dysregulation of integrins as a result of conditioning. It is also possible that T cell responsiveness to TGFβ post-transplant may be altered and that this may also be radiation dose-dependent. This can be analyzed by determining levels of TGFβ receptor expression and SMAD phosphorylation as a result of TGFβ treatment of T cells from control mice and BMT mice conditioned with 650, 900, or 1350 rads. We would hypothesize that sensitivity to TGFβ may increase with increasing conditioning. Preliminary studies examined the expression of the TGFβ1 receptors I and II on splenic T cells from control and BMT mice and found no differences; interestingly, however, treatment of splenic T cells from control and syngeneic BMT mice with 5 ng/ml TGFβ1 for 24 h resulted in

approximately 3 fold greater induction in COX-2, a known TGFβ1-responsive gene (191) over unstimulated levels in the BMT T cells when compared to control T cells. Thus, there may be increased senstitivity to TGFβ signaling in T cells post-BMT due to alterations in intracellular signaling pathways.

Finally, future studies may address the possibility that there is a limited T cell receptor repertoire post-transplant, which may contribute to impaired response to γHV-68. While we find that there is no decrease in numbers of virus-specific CD8 cells in BMT mouse lungs at d14 post-infection (Appendix Figure 7), this does not rule out the possibility that a limited CD4 repertoire is contributing to impaired responses. Indeed, homeostatic proliferation post-transplant has been described to limit the T cell repertoire in HSCT patients even 3 years post-transplant (56). This can be studied using PCR to analyze variability in CDR3 lengths in T cells post-transplant compared to non-transplant control cells (56).

Future Directions: Mechanisms of Pneumonitis Development

Our data describe severe pneumonitis and fibrosis which occur during virus latency, characterized by inflammation, presence of foamy alveolar macrophages, oxidative stress, and altered cytokine profile. While we find that pneumonitis development can be largely inhibited by blocking TGFβ signaling in T cells in the BMT setting, we have not explored the specific mechanisms that contribute to the development of lung pathology. Future studies should determine the relative contribution of these factors in determining lung pathology.

We have found that alveolar macrophages from BMT mice at d21 post-infection with γHV-68 as a population express increased levels of both the alternative activation marker *Arginase 1* as well as increased *iNOS* (Figure 3.16). Immunohistochemistry and/or flow cytometry studies should discriminate whether individual macrophages are expressing both markers or whether there are 2 distinct populations of macrophages. Additionally, the relative contribution of these macrophages to the lung pathology phenotype can be determined by performing similar studies on macrophages from T cell-DN-TGFβRII BMT mice. While we do find the presence of foamy alveolar macrophages in these mice, we have not analyzed whether they express markers of alternative activation. More direct experiments to test the role of these macrophages in promoting fibrosis should involve adoptive transfer of alveolar macrophages from BMT mice into non-transplanted control mice infected with γHV-68. We would hypothesize that if foamy alveolar macrophages are the main contributor to pneumonitis and fibrosis development, adoptive transfer of these cells would induce lung pathology in the infected, non-transplanted mice.

We have found increased levels of both H_2O_2 and NO_2- in the alveolar space of BMT mice at d21 post-infection with γHV-68 (Figure 3.17). To determine whether oxidative stress may be contributing to lung pathology in our model, BMT mice infected with γHV-68 should be treated with anti-oxidants such as n-acetylcysteine (192). We hypothesize that anti-oxidant therapy would minimize lung damage, resulting in less severe pathology in our latently-infected BMT mice. The presence of H_2O_2 and NO_2- in T cell-DN-TGFβRII BMT mice should also be determined, as these mice have significantly reduced lung pathology.

Future studies should also determine whether the altered cytokine expression noted in BMT mice contributes to γHV-68-induced pathology. We note increased levels of IL-10 production by BMT lung cells at d21 post-infection (Appendix Figure 4). We initially hypothesized that IL-10 may be contributing to pathology via induction of alternatively activated macrophages (176); however, a preliminary experiment shows that mice transplanted with IL-10KO bone marrow still develop pneumonitis, with a pathology score of approximately 8 out of 11 (Appendix Figure 4). Wild type BMT mice were not included as controls in this preliminary study, so it is unclear whether there is some protection in these mice. The overproduction of IL-10 in BMT mouse lungs during virus latency may be secondary to enhanced TGFβ production by T cells (193).

Although we do not see any reduction in lytic viral load in BMT mice transplanted with IL-17aKO bone marrow compared to wild type BMT mice (Figure 3.30), we have not ruled out the possibility IL-17a could play a role in promoting pneumonitis and fibrosis. Indeed, IL-17a has been implicated in promoting fibrosis in several model systems, including a chronic allograft model (183), a model of hypersensitivity pneumonitis and lung fibrosis (194), and bronchiolitis obliterans development in lung transplant patients (195). However, we think the overall contribution of IL-17a to fibrosis development in our model may be limited, as T cell-DN-TGFβRII BMT mice have increased numbers of Th17 cells similar to wild type BMT, yet have a significant reduction in fibrosis development (Figure 3.37, Figure 3.39). Future studies using IL-17aKO mice as transplant donors should determine whether IL-17a promotes pneumonitis and fibrosis in our model.

While we find that blocking TGFβ signaling in T cells is sufficient to significantly reduce development of pneumonitis and fibrosis (Figure 3.39), it is important to more carefully assess the timing of the effects of TGFβ in our model system. It is possible that increased TGFβ may have effects on our lung pathology phenotype during immune cell reconstitution, lytic infection, or latent infection. These experiments may be performed using a neutralizing TGFβ antibody given at various time points prior to and post-infection. Using anti-TGFβ will also be advantageous in that its administration can be titered to reduce, but not completely abrogate, TGFβ levels in our BMT mice. This may avoid and/ or delay the effects of autoimmunity which develop in our T cell-DN-TGFβRII BMT mice. It would also more closely mimic a potential therapeutic regimen that could be useful in humans.

It is interesting to note that the virus-induced pathology observed in our BMT mice does not appear during the lytic phase, but rather manifests later, during virus latency. It is plausible that the lung pathology observed may be due to increased viral reactivation. To test this idea, we will infect BMT and control mice with wild type γHV-68 or a mutant γHV-68, lacking ORF72, a viral cyclin-D homolog that is required for reactivation from latency (ΔORF72). The ΔORF72 mutant replicates normally in the lung *in vivo* during acute infection and establishes normal latent viral load, but it does not efficiently reactivate from latency (196). If virus-induced lung pathology in BMT mice occurs due to increased viral reactivation, then we would expect a significant reduction in histology score in BMT mice infected with ΔORF72. Increased viral reactivation could possibly be due to decreased effector function of CD8 T cells in the BMT setting. It may be possible that there is a diminished IFNγ response during latency. IFNγ is known to

prevent virus reactivation from latency; studies have shown that depleting IFNγ following the establishment of latency leads to enhanced reactivation(172). It is possible that the increased CD8 T cells in the alveolar space of BMT mice during virus latency (Figure 3.14) are either protective, preventing virus reactivation, or are immunopathological, causing damage to the lung. If they are functionally suppressing virus reactivation, it is curious why there would be increased numbers of CD8 cells in the BMT lungs, as the latent viral load between BMT and control lungs is similar (Figure 3.5). However, it may be that effector function of these CD8 cells is limited by the increased levels of TGFβ (82) in the alveolar space at d21 post-infection (Figure 3.17), thus having increased numbers in an attempt to maintain viral latency.

In addition, future studies should carefully characterize whether it is the delay of lytic clearance or the absolute lytic viral titers that determine the development of pneumonitis and fibrosis. Mutant viruses that have an inability to establish latency or the ability to establish latency without development of lytic replication may be useful in making these determinations (69, 197).

Our studies have not evaluated the role of B cells in the development of pneumonitis and fibrosis during virus latency. B cells are the main reservoir for latent γHV-68 *in vivo*, and these cells are important for prevention of disease during persistent infection (69). The antibody response to γHV-68 infection is largely non-specific for viral antigens, and it is unclear what role these antibodies play in protection from disease. It has been postulated that the importance of B cells during chronic infection may involve their antigen-presenting function (69). Future studies may include assessment of the ability of B cells from BMT mice to proliferate and produce isotype-switched antibody *in*

vitro, followed by analysis of the antibody response by BMT mice to γHV-68 infection. Indeed, it has been shown that B cells from HSCT patients are impaired in their ability to produce isotype-switched antibody for years post-transplant (9). However, it may be more relevant to functionally characterize the ability of B cells from BMT mice to act as antigen-presenting cells, using *in vitro* assays such as MLR. Additionally, flow cytometry may be used to analyze the phenotype and expression of costimulatory and MHC molecules on B cells in BMT mice during virus latency.

We are also interested in understanding whether the severe pneumonitis and fibrosis phenotype that we observe in our BMT model can be induced by pathogens or inflammatory stimuli other than γHV68. Unlike γHV-68, a preliminary experiment from our laboratory shows that BMT and control mice have similar control of lytic murine CMV (MCMV) infection, a member of the β-herpesvirus family (Appendix Figure 8). This may be related to the importance of NK cells in controlling lytic replication of MCMV. We have not evaluated the functionality of NK cells in our murine model; however, human studies have indicated that NK cell function is not diminished post-transplant (8). Looking at whether pneumonitis and fibrosis develop during latent MCMV infection in BMT mice would provide insight into whether uncontrolled viral replication is the main factor contributing to pneumonitis. We would anticipate that if uncontrolled lytic replication was, in fact, the mechanism, then BMT mice in our model would not develop pneumonitis in response to MCMV latency.

Additionally, we have not identified the role of chemokines in the recruitment or persistence of inflammatory cells to the BMT mouse lung in response to γHV-68 infection. A murine allogeneic IPS model found that overexpression of MCP-1

contributed to pathology development, as transplants using CCR2KO donors had a significant reduction in lung pathology. MCP-1 was also found to be increased in BALF from allogeneic HSCT patients with IPS (189). Additionally, increased MCP-1 levels were observed in a model of lung injury after high dose chemotherapy and syngeneic BMT in mice (198). A preliminary experiment in our model looking at chemokine expression in collagenase-digested lungs from BMT and control mice at d21 post-infection indicates no increase in chemokine levels in BMT lungs, with a significant *decrease* in MCP-1 (Appendix Figure 9). However, the majority of cells in this cell suspension are leukocytes, and future studies should evaluate chemokine and receptor expression on structural cells as well. Additionally, it would be pertinent to investigate the expression of chemokines throughout the post-transplant and post-infection time periods in our model to understand how chemokine expression may be altered in BMT lungs. We might expect chemokine levels to be increased during the initial increased accumulation of inflammatory cells in the lung, which occurs between d7 and d14 post-infection (Figure 3.6).

Future studies may also determine whether the pneumonitis and fibrosis phenotype persist when BMT mice are conditioned with chemotherapeutic agents, rather than TBI, prior to transplant.

Future Directions: Allogeneic Models

We are also interested in understanding whether the results from our studies are translatable to allogeneic BMT models. Performing experiments in allogeneic models will allow us to understand the similarities and differences of anti-viral immunity and

pneumonitis development between syngeneic BMT and BMT complicated with the presence of alloreactive T cells. Clinically, both infectious and non-infectious pulmonary complications are more frequent in the allogeneic setting (3); this is likely related both to alloimmunity as well as immunosuppressive drug regimens to mitigate GVHD.

We have performed some preliminary studies looking at γHV-68 infection in a fully allogeneic murine BMT model. Our results show that allogeneic BMT mice have an increase in lytic viral replication, similar to syngeneic BMT mice as shown by increased expression of the lytic viral genes *gB* and *DNA polymerase* in the lung at d7 post-infection (Appendix Figure 10). Allogeneic BMT mice also have similar increases in TGFβ and Tregs in the lung (Appendix Figure 11). Interesting, these mice do not show signs of GVHD during the post-transplant time period, as there is no substantial weight loss compared to syngeneic BMT mice (Appendix Figure 10). Thus, we hypothesize that the decreased control of lytic viral replication at d7 post-infection in the allogeneic BMT mice may be due to mechanisms similar to what we observe in our syngeneic model. Future studies in the allogeneic model should include an analysis of Th1 cells in the lung in response to lytic γHV-68.

However, our preliminary studies do show significant differences between syngeneic BMT and allogeneic BMT mice during virus latency. We have found that γHV-68 latency is lethal in allogeneic BMT mice by d20 post-infection, with severe weight loss during the course of infection (Appendix Figure 12). This is in contrast with control and syngeneic BMT mice which survive infection with $5x10^4$ pfu γHV-68. Future studies should differentiate between whether the allogeneic BMT mice succumb because viral infection promotes GVHD pathogenesis or whether this is related to uncontrolled

lytic replication. Histology studies at d14 post-infection in these allogeneic BMT mice do indicate the development of pneumonitis and fibrosis not observed in uninfected allogeneic BMT mice (Appendix Figure 13). We hypothesize that stimulation of the immune response to γHV-68 leads to activation of alloreactive T cells in our model. Indeed, TLR9 activation has been noted to promote GVHD in murine models (199), and as a DNA virus, we would expect that TLR9 would be activated during γHV-68 infection.

Future studies should monitor these mice post-infection and look at histology of gut as well as lungs to determine whether they succumb to pulmonary-related pathology or gut-related pathology which is a major GVHD target. In these allogeneic BMT mice, we have not determined whether there is increased TGFβ or indication of oxidative stress as we see in the syngeneic BMT model. Experiments looking at the role of TGFβ in promoting pneumonitis and susceptibility to γHV-68 infection in allogeneic BMT models is complicated, as TGFβ is important in suppressing acute GVHD effects (117, 120). Thus, preliminary experiments in our laboratory using T cell-DN-TGFβRII donors on C57BL/6 background into Balb/c recipients ended in lethality. It may be important to challenge these allogeneic BMT mice with a lower dose of virus or perform experiments across a minor MHC mismatch. These modifications may allow survival of the allogeneic BMT mice post-infection and will allow analysis of immune mechanisms.

Recent studies have shown some success in using etanercept, blocking TNF, in IPS treatment in allogeneic patients (38, 93). Because of this, we were curious to know whether TNFα levels may be increased in our pneumonitis model at d21 post-infection. However, preliminary studies indicate that TNFα is *decreased* in our syngeneic BMT

setting, both in whole lung homogenates and in alveolar macrophages (Appendix Figure 14). Future studies should address whether TNFα expression is altered during pneumonitis development in allogeneic BMT mice latently infected with γHV-68. If TNFα is increased in allogeneic BMT mice in our model, this will provide important insight into the possible differences between pneumonitis pathogenesis in autologous and allogeneic HSCT recipients.

Concluding Remarks

In sum, our studies have established a murine BMT model that has allowed us to analyze alterations in immune responses to viral infection and pneumonitis development which occur post-transplant, in the absence of GVHD or immunosuppressive therapy. We find that cells transplanted into a conditioned host have significant phenotypic changes compared to cells isolated from a non-transplanted host, leading to impaired control of lytic viral infection and later development of pneumonitis and fibrosis during virus latency. Our model may provide important insight into the mechanisms of pneumonitis development in HSCT patients, as we show that factors other than alloresponses can contribute to lung pathology post-transplant.

Appendix

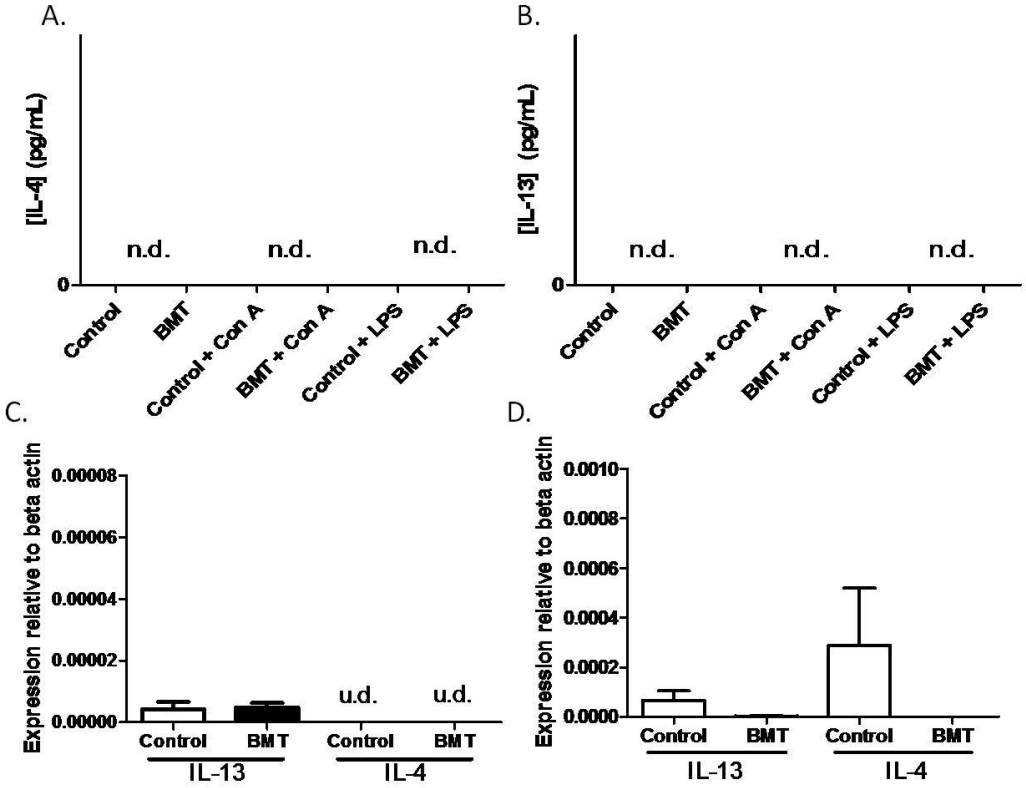

Appendix Figure 1. *Very little IL-4 and IL-13 expression in the lung at d21 post-infection.* BMT and control mice were infected with $5x10^4$ pfu γHV-68 and lungs were harvested at d21 post-infection. *A.* and *B.* Collagenase-digested cells from BMT and control mice were cultured at $5x10^6$ cells per mL for 24h, either untreated, plus ConA or LPS (*n*=5 per group) and analyzed by ELISA for IL-4 or IL-13 (*n*=5 per group; n.d. = not detectable). *C.* $5x10^6$ BAL cells were cultured overnight, harvested for RNA and analyzed for IL-13 and IL-14 by real time RT-PCR (u.d. = undetermined, *n*=4 per group). *D.* Alveolar macrophages were enriched by plastic adherence in serum-free media for 1h. Cells were then harvested for RNA and analyzed for IL-13 and IL-4 by real time RT-PCR. (*n*=4 per group).

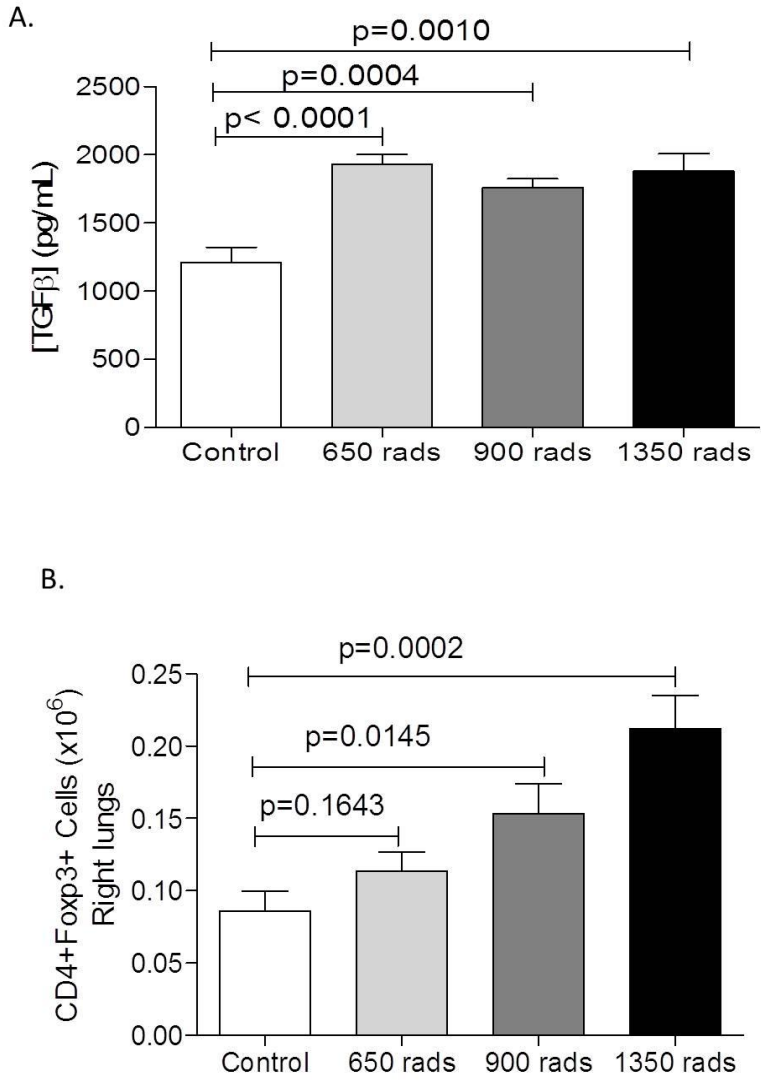

Appendix Figure 2. *Treg numbers in the lungs of syngeneic BMT mice are dependent on radiation dose, while levels of TGFβ1 are not.* Syngeneic transplants were performed in mice receiving 650, 900, or 1350 rads. *A.* Levels of total TGFβ1 were analyzed in the lungs of BMT mice by ELISA; TGFβ1 was significantly increased in all conditioning regimens (data combined from 2 experiments; *n*= at least 9 per group). *B.* At d7 post-infection with γHV-68, right lungs were digested in collagenase and analyzed for expression of CD4 and Foxp3 by flow cytometry. There were significantly elevated numbers of Tregs in mice conditioned with 900 and 1350 rads compared to non-transplant controls (data combined from 2 independent experiments, *n*=10 per group).

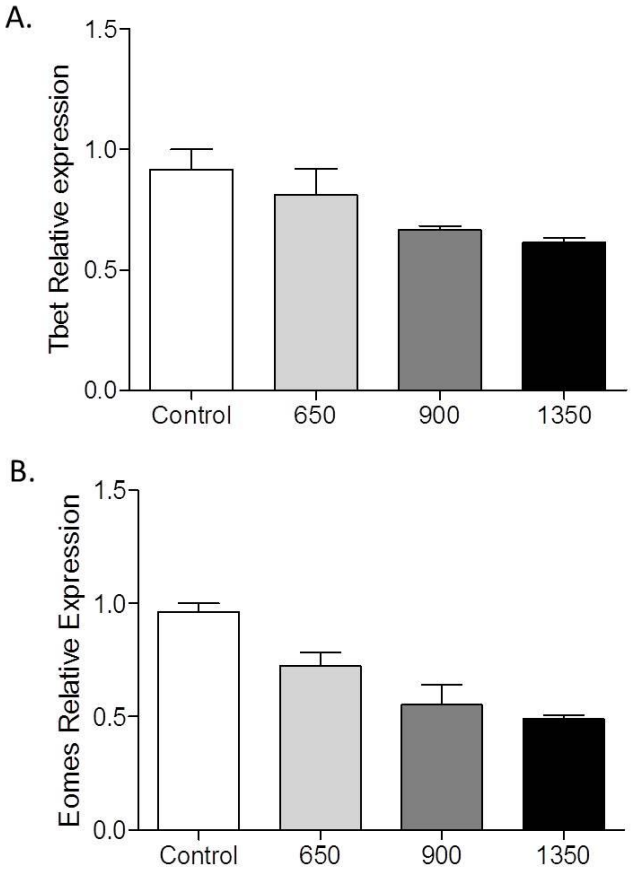

Appendix Figure 3. *Tbet and eomesodermin expression in BMT T cells decreases with increasing radiation dose*. Transplants were performed in mice receiving 650, 900, or 1350 rads. T cells were enriched from the spleen by CD19 depletion, and cells were cultured overnight. Expression of *Tbet* and *Eomesodermin* was determined using real time RT-PCR (n=2-3 per group).

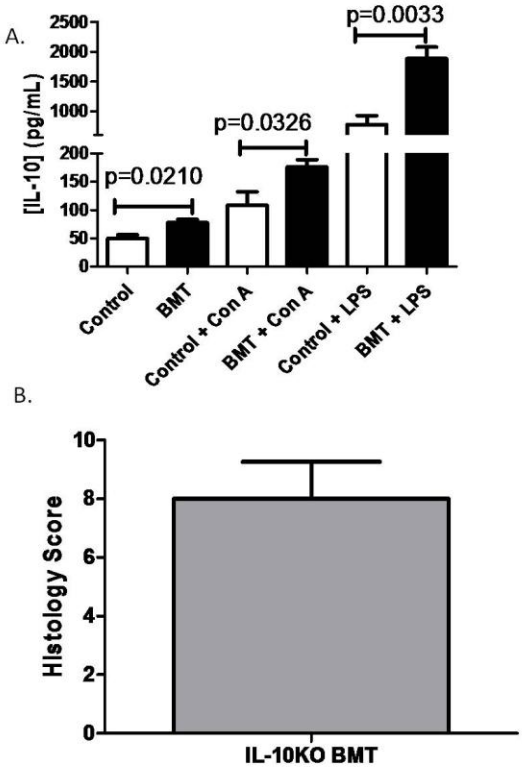

Appendix Figure 4. *BMT mice overexpress IL-10 in the lungs at d21 post-infection*. *A.* Lungs from BMT and control mice at d21 post-infection with $5x10^4$ pfu γHV-68 were digested in collagenase. $5x10^6$ cells were cultured for 24h without treatment or with ConA or LPS. Cell supernatants were analyzed for IL-10 by ELISA. *B.* Mice transplanted with bone marrow from an IL-10KO donor were infected with $5x10^4$ pfu γHV-68. At d21 post-infection, lungs were harvested for histology and scored (n=5). Wild type BMT mice were not infected in parallel for this preliminary experiment, but scored 10-11 in previous experiments (Figure 3.10).

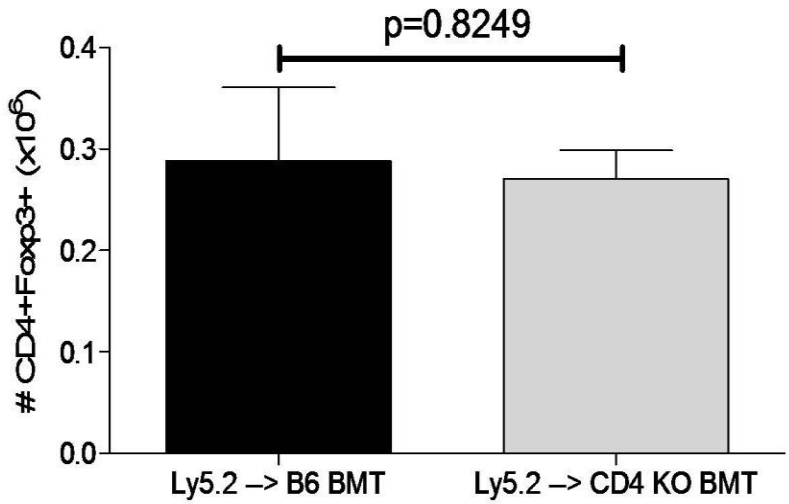

Appendix Figure 5. *Lung Tregs expand post-BMT even in absence of host-derived CD4 cells*. CD45.2 recipients (either wild type C57BL/6 or CD4KO) were conditioned with 1350 rads and were transplanted with whole bone marrow from CD45.1+ (Ly5.2) donors. Mice were infected with $5x10^4$ pfu γHV-68. At d7 post-infection, right lungs were digested with collagenase and analyzed for expression of CD4 and Foxp3 by flow cytometry (*n*=5 per group; representative of 2 independent experiments).

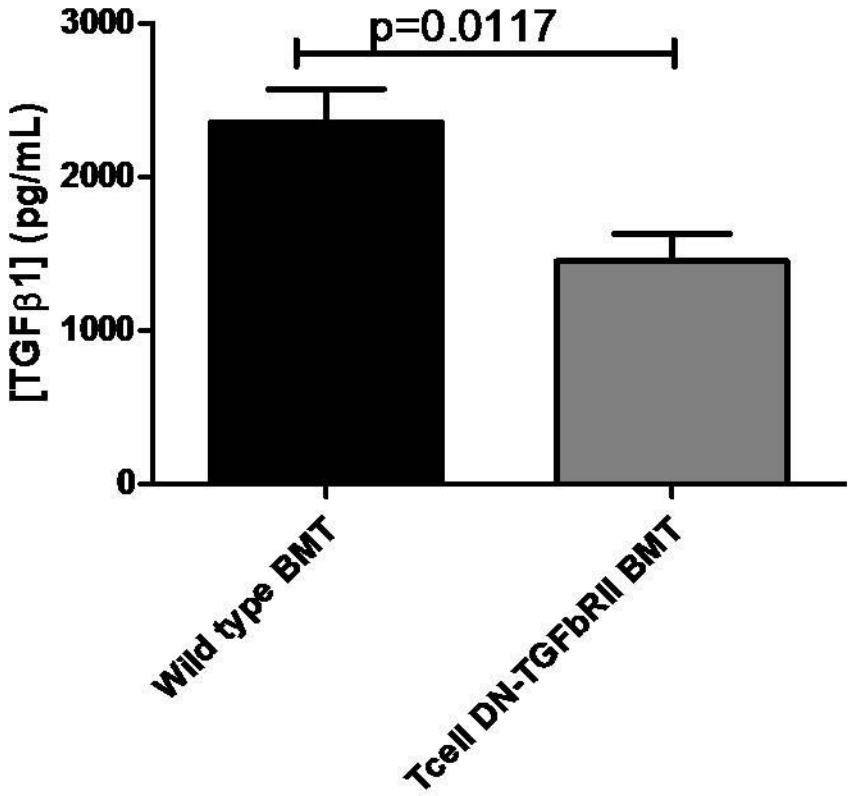

Appendix Figure 6. *T cell-DN-TGFβRII BMT mice have reduced lung TGFβ compared to wild type BMT mice*. Lung homogenates from uninfected wild type BMT or T cell-DN-TGFβRII BMT mice were analyzed for total TGFβ1 by ELISA (*n*=5 mice per group)

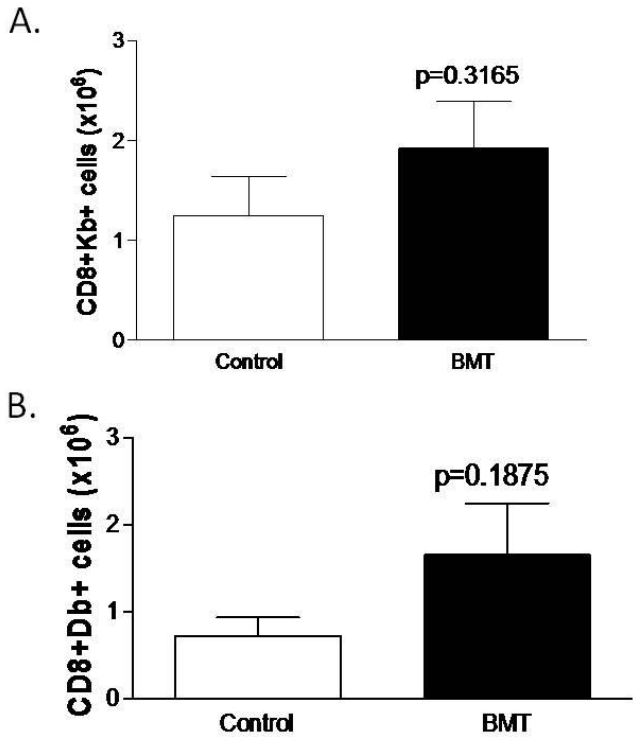

Appendix Figure 7. *BMT and control lungs have similar numbers of tetramer-positive CD8 cells on d14 post-infection.* Lungs were harvested from BMT and control mice at d14 post-infection with $5x10^4$ pfu γHV-68 and digested in collagenase. Cells were then stained for flow cytometry using CD8 antibody and tetramers loaded with H-2K(b)- and H-2D(b)-restricted viral peptides (*n*=4 per group).

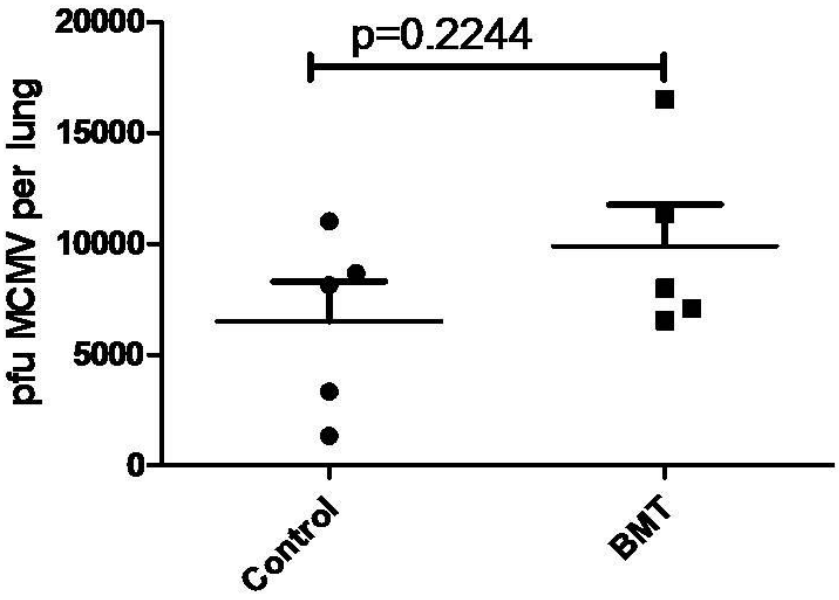

Appendix Figure 8. *BMT and control mice have similar control of MCMV infection*. Control and BMT mice were infected i.n. with $5x10^4$ pfu MCMV. At d7 post-infection, lungs were homogenized and analyzed by plaque assay on 3T12 monolayers (*n*=5 per group).

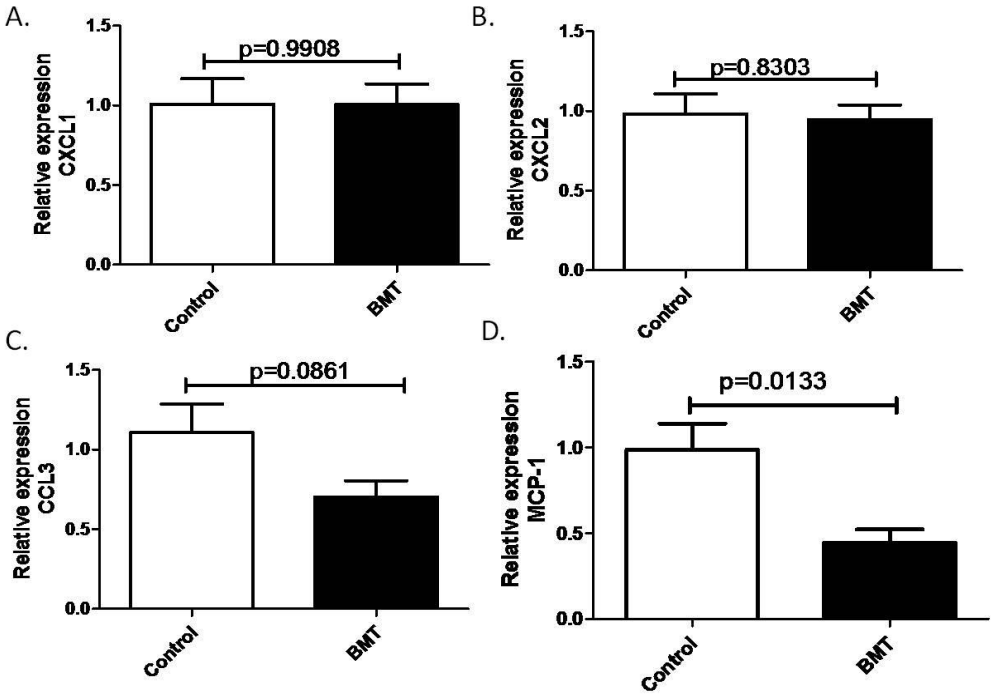

Appendix Figure 9. *BMT collagenase-digested cells do not have increased chemokine expression at d21 post-infection.* Collagenase-digested lungs from BMT and control mice at d21 post-infection with $5x10^4$ pfu γHV-68 were harvested for RNA. Expression of chemokines was determined using real time RT-PCR (*n*=5 per group).

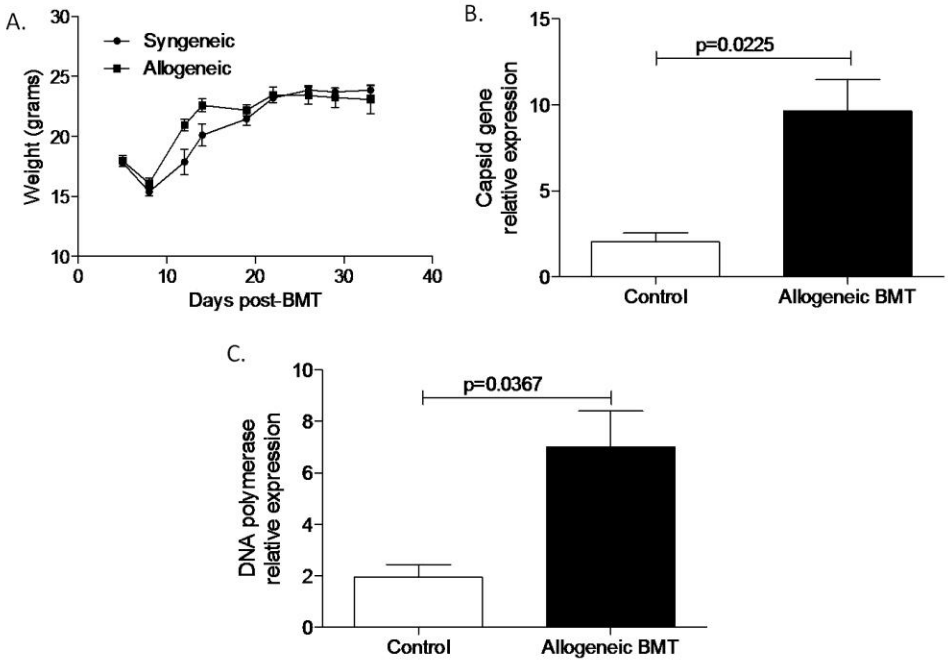

Appendix Figure 10. *Allogeneic BMT mice show increased susceptibility to γHV-68 in absence of GVHD. A.* Mice receiving syngeneic or allogeneic (Balb/c → C57BL/6) BMT were weighed twice a week as a measure of GVHD for 5 weeks post-BMT (*n*=5 syngeneic, 10 allogeneic per time point; data representative of 2 independent experiments). *B.* and *C.* Left lungs were harvested from control and allogeneic BMT mice at d7 post-infection with γHV-68, processed for RNA, and analyzed for expression of lytic viral genes. Viral gene expression was significantly increased in allogeneic BMT mice when compared to non-transplanted control mice (*p*=0.0225 for viral capsid gene, *p*=0.0367 for viral *DNA polymerase*; *n*= 3 control, 5 allogeneic BMT, data representative of 2 independent experiments).

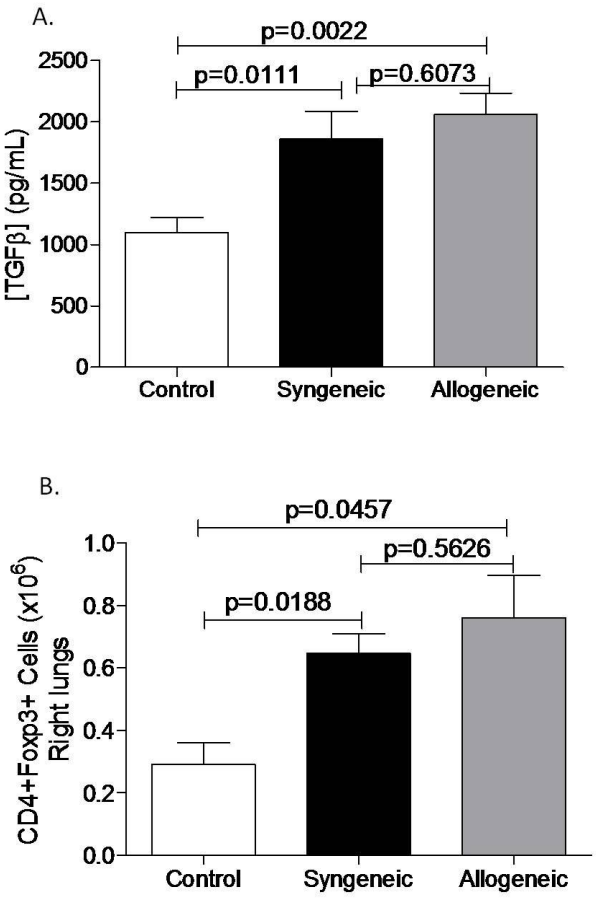

Appendix Figure 11. *Allogeneic BMT mice have increased TGFβ1 and increased Treg numbers in the lungs. A.* TGFβ1 levels in the lungs of syngeneic and allogeneic BMT mice were determined by ELISA. Both BMT groups expressed similar increases in TGFβ1 levels (*n*= 3 control, 3 syngeneic, and 5 allogeneic). *B.* Control, syngeneic, and allogeneic BMT mice were infected with $5x10^4$ pfu γHV-68. At d7 post-infection, right lungs were digested in collagenase and analyzed by flow cytometry for expression of CD4 and Foxp3. CD4+Foxp3+ cells were significantly increased in both syngeneic and allogeneic BMT mice compared to non-transplanted controls (*n*= 7 control, 7 syngeneic, 3 allogeneic).

A.

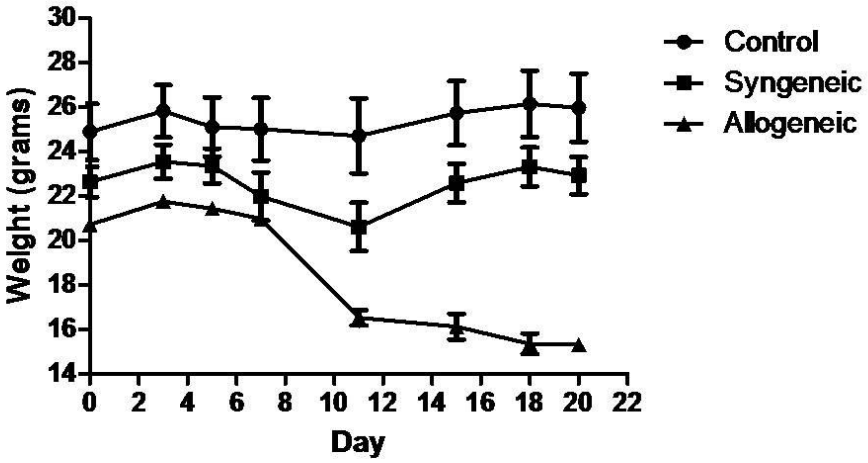

B.

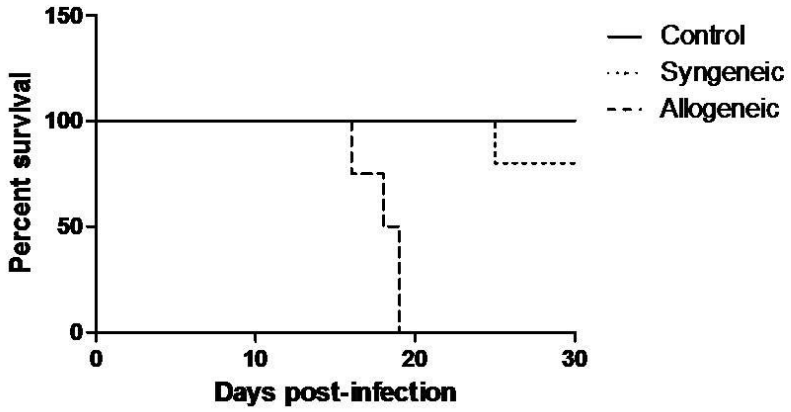

Appendix Figure 12. *Allogeneic BMT mice succumb to γHV-68 infection.* Control, syngeneic, or allogeneic BMT mice were infected with $5x10^4$ pfu γHV-68, and weights and survival were monitored for 20 and 30 days post-infection, respectively (*n*=4-5 per group).

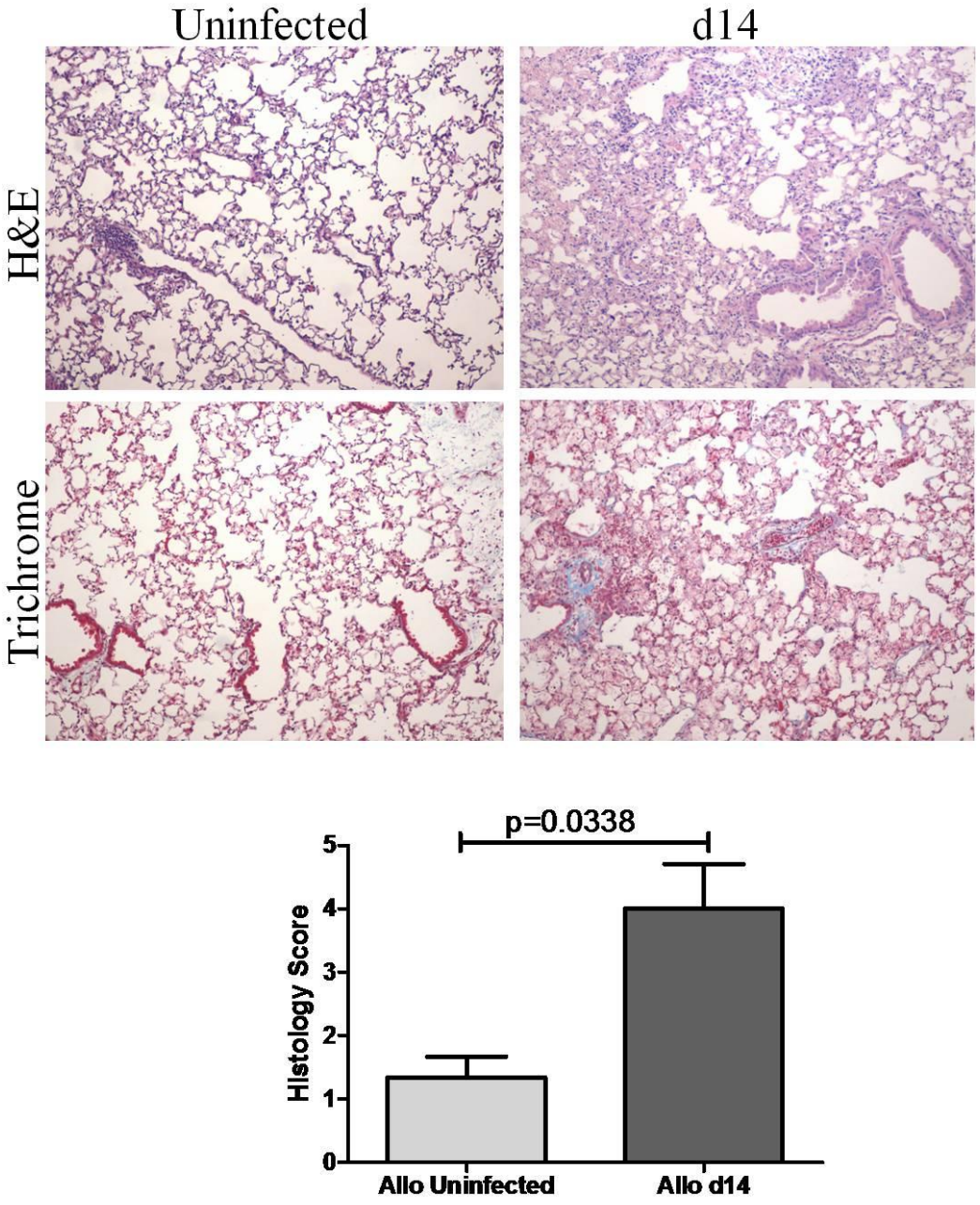

Appendix Figure 13. *Allogeneic BMT mice display virus-induced pathology at d14 post-infection*. Lungs were harvested for histology from uninfected allogeneic BMT mice (8 weeks post-BMT) or at d21 post-infection with $5x10^4$ pfu γHV-68. Lung sections were stained with H&E or Trichrome. Slides were scored in a blinded fashion by a pulmonary pathologist (*n*=3 uninfected, 5 infected).

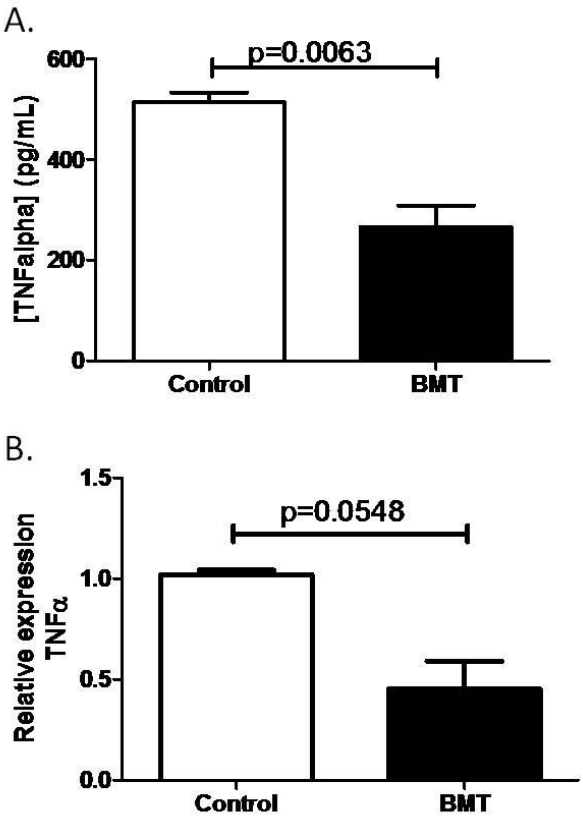

Appendix Figure 14. *BMT lungs and alveolar macrophages express decreased TNFα at d21 post-infection*. Control and syngeneic BMT mice were infected with $5x10^4$ pfu γHV-68 and analyzed at d21. *A.* Lung homogenates were analyzed for TNFα by ELISA (*n*=3 control, 3 BMT). *B.* Alveolar macrophages were harvested by BAL and enriched by plastic adherence. TNFα expression was determined using real time RT-PCR (*n*=2 control, 2 BMT).

References

1. Staal FJ, Luis TC. 2010. Wnt signaling in hematopoiesis: crucial factors for self-renewal, proliferation, and cell fate decisions. *J Cell Biochem* 109: 844-9
2. Ramirez J, Lukin K, Hagman J. 2010. From hematopoietic progenitors to B cells: mechanisms of lineage restriction and commitment. *Curr Opin Immunol* 22: 177-84
3. Afessa B, Peters SG. 2006. Major complications following hematopoietic stem cell transplantation. *Semin Respir Crit Care Med* 27: 297-309
4. Coomes SM, Hubbard LL, Moore BB. Impaired pulmonary immunity post-bone marrow transplant. *Immunol Res*
5. Coomes SM, Moore BB. 2010. Pleiotropic effects of transforming growth factor-beta in hematopoietic stem-cell transplantation. *Transplantation* 90: 1139-44
6. Burns LJ. 2009. Late effects after autologous hematopoietic cell transplantation. *Biol Blood Marrow Transplant* 15: 21-4
7. Jantunen E, Itala M, Siitonen T, Koivunen E, Leppa S, Juvonen E, Kuittinen O, Lehtinen T, Koistinen P, Nyman H, Nousiainen T, Volin L, Remes K. 2006. Late non-relapse mortality among adult autologous stem cell transplant recipients: a nation-wide analysis of 1,482 patients transplanted in 1990-2003. *Eur J Haematol* 77: 114-9
8. Storek J, Geddes M, Khan F, Huard B, Helg C, Chalandon Y, Passweg J, Roosnek E. 2008. Reconstitution of the immune system after hematopoietic stem cell transplantation in humans. *Semin Immunopathol* 30: 425-37
9. Small TN, Keever CA, Weiner-Fedus S, Heller G, O'Reilly RJ, Flomenberg N. 1990. B-cell differentiation following autologous, conventional, or T-cell depleted bone marrow transplantation: a recapitulation of normal B-cell ontogeny. *Blood* 76: 1647-56
10. Avigan D, Wu Z, Joyce R, Elias A, Richardson P, McDermott D, Levine J, Kennedy L, Giallombardo N, Hurley D, Gong J, Kufe D. 2000. Immune reconstitution following high-dose chemotherapy with stem cell rescue in patients with advanced breast cancer. *Bone Marrow Transplant* 26: 169-76
11. Soiffer RJ, Bosserman L, Murray C, Cochran K, Daley J, Ritz J. 1990. Reconstitution of T-cell function after CD6-depleted allogeneic bone marrow transplantation. *Blood* 75: 2076-84
12. Sugita K, Nojima Y, Tachibana K, Soiffer RJ, Murray C, Schlossman SF, Ritz J, Morimoto C. 1994. Prolonged impairment of very late activating antigen-mediated T cell proliferation via the CD3 pathway after T cell-depleted allogeneic bone marrow transplantation. *J Clin Invest* 94: 481-8
13. Versluys AB, Rossen JW, van Ewijk B, Schuurman R, Bierings MB, Boelens JJ. 2010. Strong association between respiratory viral infection early after hematopoietic stem cell transplantation and the development of life-threatening acute and chronic alloimmune lung syndromes. *Biol Blood Marrow Transplant* 16: 782-91
14. Thomas ED, Lochte HL, Jr., Cannon JH, Sahler OD, Ferrebee JW. 1959. Supralethal whole body irradiation and isologous marrow transplantation in man. *J Clin Invest* 38: 1709-16

15. Thomas ED, Lochte HL, Jr., Lu WC, Ferrebee JW. 1957. Intravenous infusion of bone marrow in patients receiving radiation and chemotherapy. *N Engl J Med* 257: 491-6
16. Copelan EA. 2006. Hematopoietic stem-cell transplantation. *N Engl J Med* 354: 1813-26
17. Sullivan KM, Muraro P, Tyndall A. 2010. Hematopoietic cell transplantation for autoimmune disease: updates from Europe and the United States. *Biol Blood Marrow Transplant* 16: S48-56
18. Zhong XY, Zhang B, Asadollahi R, Low SH, Holzgreve W. Umbilical cord blood stem cells: what to expect. *Ann N Y Acad Sci* 1205: 17-22
19. Bensinger WI, Weaver CH, Appelbaum FR, Rowley S, Demirer T, Sanders J, Storb R, Buckner CD. 1995. Transplantation of allogeneic peripheral blood stem cells mobilized by recombinant human granulocyte colony-stimulating factor. *Blood* 85: 1655-8
20. Horowitz MM, Loberiza FR, Bredeson CN, Rizzo JD, Nugent ML. 2001. Transplant registries: guiding clinical decisions and improving outcomes. *Oncology (Williston Park)* 15: 649-59; discussion 63-4, 66
21. Kaya Z, Weiner DJ, Yilmaz D, Rowan J, Goyal RK. 2009. Lung function, pulmonary complications, and mortality after allogeneic blood and marrow transplantation in children. *Biol Blood Marrow Transplant* 15: 817-26
22. Osawa M, Hanada K, Hamada H, Nakauchi H. 1996. Long-term lymphohematopoietic reconstitution by a single CD34-low/negative hematopoietic stem cell. *Science* 273: 242-5
23. Lapidot T, Dar A, Kollet O. 2005. How do stem cells find their way home? *Blood* 106: 1901-10
24. Aschan J. 2007. Risk assessment in haematopoietic stem cell transplantation: conditioning. *Best Pract Res Clin Haematol* 20: 295-310
25. Milanetti F, Abinun M, Voltarelli JC, Burt RK. Autologous hematopoietic stem cell transplantation for childhood autoimmune disease. *Pediatr Clin North Am* 57: 239-71
26. Flomenberg N, Devine SM, Dipersio JF, Liesveld JL, McCarty JM, Rowley SD, Vesole DH, Badel K, Calandra G. 2005. The use of AMD3100 plus G-CSF for autologous hematopoietic progenitor cell mobilization is superior to G-CSF alone. *Blood* 106: 1867-74
27. Fry TJ, Willasch A, Bader P. The graft-versus-tumor effect in pediatric malignancy. *Pediatr Clin North Am* 57: 67-81
28. Baker KS, Bresters D, Sande JE. 2010. The burden of cure: long-term side effects following hematopoietic stem cell transplantation (HSCT) in children. *Pediatr Clin North Am* 57: 323-42
29. Soubani AO, Miller KB, Hassoun PM. 1996. Pulmonary complications of bone marrow transplantation. *Chest* 109: 1066-77
30. Sharma S, Nadrous HF, Peters SG, Tefferi A, Litzow MR, Aubry MC, Afessa B. 2005. Pulmonary complications in adult blood and marrow transplant recipients: autopsy findings. *Chest* 128: 1385-92

31. Gower WA, Collaco JM, Mogayzel PJ, Jr. 2010. Lung function and late pulmonary complications among survivors of hematopoietic stem cell transplantation during childhood. *Paediatr Respir Rev* 11: 115-22
32. Marras TK, Szalai JP, Chan CK, Lipton JH, Messner HA, Laupacis A. 2002. Pulmonary function abnormalities after allogeneic marrow transplantation: a systematic review and assessment of an existing predictive instrument. *Bone Marrow Transplant* 30: 599-607
33. Martin M, Lefaix J, Delanian S. 2000. TGF-beta1 and radiation fibrosis: a master switch and a specific therapeutic target? *Int J Radiat Oncol Biol Phys* 47: 277-90
34. Anscher MS, Kong FM, Jirtle RL. 1998. The relevance of transforming growth factor beta 1 in pulmonary injury after radiation therapy. *Lung Cancer* 19: 109-20
35. Limper AH. 2004. Chemotherapy-induced lung disease. *Clin Chest Med* 25: 53-64
36. Afessa B, Litzow MR, Tefferi A. 2001. Bronchiolitis obliterans and other late onset non-infectious pulmonary complications in hematopoietic stem cell transplantation. *Bone Marrow Transplant* 28: 425-34
37. Ferrara JL, Levine JE, Reddy P, Holler E. 2009. Graft-versus-host disease. *Lancet* 373: 1550-61
38. Afessa B, Peters SG. 2008. Noninfectious pneumonitis after blood and marrow transplant. *Curr Opin Oncol* 20: 227-33
39. Shankar G, Cohen DA. 2001. Idiopathic pneumonia syndrome after bone marrow transplantation: the role of pre-transplant radiation conditioning and local cytokine dysregulation in promoting lung inflammation and fibrosis. *Int J Exp Pathol* 82: 101-13
40. Wong R, Rondon G, Saliba RM, Shannon VR, Giralt SA, Champlin RE, Ueno NT. 2003. Idiopathic pneumonia syndrome after high-dose chemotherapy and autologous hematopoietic stem cell transplantation for high-risk breast cancer. *Bone Marrow Transplant* 31: 1157-63
41. Bilgrami SF, Metersky ML, McNally D, Naqvi BH, Kapur D, Raible D, Bona RD, Edwards RL, Feingold JM, Clive JM, Tutschka PJ. 2001. Idiopathic pneumonia syndrome following myeloablative chemotherapy and autologous transplantation. *Ann Pharmacother* 35: 196-201
42. Martin-Pena A, Aguilar-Guisado M, Espigado I, Parody R, Miguel Cisneros J. Prospective study of infectious complications in allogeneic hematopoietic stem cell transplant recipients. *Clin Transplant*
43. Gil L, Styczynski J, Komarnicki M. 2007. Infectious complication in 314 patients after high-dose therapy and autologous hematopoietic stem cell transplantation: risk factors analysis and outcome. *Infection* 35: 421-7
44. Auner HW, Sill H, Mulabecirovic A, Linkesch W, Krause R. 2002. Infectious complications after autologous hematopoietic stem cell transplantation: comparison of patients with acute myeloid leukemia, malignant lymphoma, and multiple myeloma. *Ann Hematol* 81: 374-7
45. Collaco JM, Gower WA, Mogayzel PJ, Jr. 2007. Pulmonary dysfunction in pediatric hematopoietic stem cell transplant patients: overview, diagnostic considerations, and infectious complications. *Pediatr Blood Cancer* 49: 117-26

46. Dvorak CC, Steinbach WJ, Brown JM, Agarwal R. 2005. Risks and outcomes of invasive fungal infections in pediatric patients undergoing allogeneic hematopoietic cell transplantation. *Bone Marrow Transplant* 36: 621-9
47. Ozyilmaz E, Aydogdu M, Sucak G, Aki SZ, Ozkurt ZN, Yegin ZA, Kokturk N. 2010. Risk factors for fungal pulmonary infections in hematopoietic stem cell transplantation recipients: the role of iron overload. *Bone Marrow Transplant* 45: 1528-33
48. Gasink LB, Blumberg EA. 2005. Bacterial and mycobacterial pneumonia in transplant recipients. *Clin Chest Med* 26: 647-59, vii
49. Kanne JP, Godwin JD, Franquet T, Escuissato DL, Muller NL. 2007. Viral pneumonia after hematopoietic stem cell transplantation: high-resolution CT findings. *J Thorac Imaging* 22: 292-9
50. Kotloff RM, Ahya VN, Crawford SW. 2004. Pulmonary complications of solid organ and hematopoietic stem cell transplantation. *Am J Respir Crit Care Med* 170: 22-48
51. Boeckh M, Nichols WG, Papanicolaou G, Rubin R, Wingard JR, Zaia J. 2003. Cytomegalovirus in hematopoietic stem cell transplant recipients: Current status, known challenges, and future strategies. *Biol Blood Marrow Transplant* 9: 543-58
52. Wingard JR, Hsu J, Hiemenz JW. 2010. Hematopoietic stem cell transplantation: an overview of infection risks and epidemiology. *Infect Dis Clin North Am* 24: 257-72
53. Williams KM, Gress RE. 2008. Immune reconstitution and implications for immunotherapy following haematopoietic stem cell transplantation. *Best Pract Res Clin Haematol* 21: 579-96
54. Leino L, Lilius EM, Nikoskelainen J, Pelliniemi TT, Rajamaki A. 1991. The reappearance of 10 differentiation antigens on peripheral blood lymphocytes after allogeneic bone marrow transplantation. *Bone Marrow Transplant* 8: 339-44
55. Gratama JW, Naipal A, Oljans P, Zwaan FE, Verdonck LF, de Witte T, Vossen JM, Bolhuis RL, de Gast GC, Jansen J. 1984. T lymphocyte repopulation and differentiation after bone marrow transplantation. Early shifts in the ratio between T4+ and T8+ T lymphocytes correlate with the occurrence of acute graft-versus-host disease. *Blood* 63: 1416-23
56. Wu CJ, Chillemi A, Alyea EP, Orsini E, Neuberg D, Soiffer RJ, Ritz J. 2000. Reconstitution of T-cell receptor repertoire diversity following T-cell depleted allogeneic bone marrow transplantation is related to hematopoietic chimerism. *Blood* 95: 352-9
57. Miller RA, Daley J, Ghalie R, Kaizer H. 1991. Clonal analysis of T-cell deficiencies in autotransplant recipients. *Blood* 77: 1845-50
58. Reddy P, Negrin R, Hill GR. 2008. Mouse models of bone marrow transplantation. *Biol Blood Marrow Transplant* 14: 129-35
59. Ojielo CI, Cooke K, Mancuso P, Standiford TJ, Olkiewicz KM, Clouthier S, Corrion L, Ballinger MN, Toews GB, Paine R, 3rd, Moore BB. 2003. Defective phagocytosis and clearance of Pseudomonas aeruginosa in the lung following bone marrow transplantation. *J Immunol* 171: 4416-24
60. Ballinger MN, Aronoff DM, McMillan TR, Cooke KR, Olkiewicz K, Toews GB, Peters-Golden M, Moore BB. 2006. Critical role of prostaglandin E2

overproduction in impaired pulmonary host response following bone marrow transplantation. *J Immunol* 177: 5499-508
61. Hubbard LL, Ballinger MN, Thomas PE, Wilke CA, Standiford TJ, Kobayashi KS, Flavell RA, Moore BB. 2010. A role for IL-1 Receptor-associated kinase-M in Prostaglandin E(2)-induced immunosuppression post-bone marrow transplantation. *J Immunol* 184: 6299-308
62. Virgin HWt, Latreille P, Wamsley P, Hallsworth K, Weck KE, Dal Canto AJ, Speck SH. 1997. Complete sequence and genomic analysis of murine gammaherpesvirus 68. *J Virol* 71: 5894-904
63. Blaskovic D, Stancekova M, Svobodova J, Mistrikova J. 1980. Isolation of five strains of herpesviruses from two species of free living small rodents. *Acta Virol* 24: 468
64. Nash AA, Dutia BM, Stewart JP, Davison AJ. 2001. Natural history of murine gamma-herpesvirus infection. *Philos Trans R Soc Lond B Biol Sci* 356: 569-79
65. Stevenson PG, Simas JP, Efstathiou S. 2009. Immune control of mammalian gamma-herpesviruses: lessons from murid herpesvirus-4. *J Gen Virol* 90: 2317-30
66. Olivadoti M, Toth LA, Weinberg J, Opp MR. 2007. Murine gammaherpesvirus 68: a model for the study of Epstein-Barr virus infections and related diseases. *Comp Med* 57: 44-50
67. Stoolman JS, Vannella KM, Coomes SM, Wilke CA, Sisson TH, Toews GB, Moore BB. 2010. Latent Infection by Gammaherpesvirus Stimulates Pro-fibrotic Mediator Release from Multiple Cell Types. *Am J Physiol Lung Cell Mol Physiol*
68. Nash AA, Sunil-Chandra NP. 1994. Interactions of the murine gammaherpesvirus with the immune system. *Curr Opin Immunol* 6: 560-3
69. Barton E, Mandal P, Speck SH. 2011. Pathogenesis and host control of gammaherpesviruses: lessons from the mouse. *Annu Rev Immunol* 29: 351-97
70. Stevenson PG, Belz GT, Castrucci MR, Altman JD, Doherty PC. 1999. A gamma-herpesvirus sneaks through a CD8(+) T cell response primed to a lytic-phase epitope. *Proc Natl Acad Sci U S A* 96: 9281-6
71. Clambey ET, Virgin HWt, Speck SH. 2000. Disruption of the murine gammaherpesvirus 68 M1 open reading frame leads to enhanced reactivation from latency. *J Virol* 74: 1973-84
72. Tibbetts SA, Loh J, Van Berkel V, McClellan JS, Jacoby MA, Kapadia SB, Speck SH, Virgin HWt. 2003. Establishment and maintenance of gammaherpesvirus latency are independent of infective dose and route of infection. *J Virol* 77: 7696-701
73. Rochford R, Lutzke ML, Alfinito RS, Clavo A, Cardin RD. 2001. Kinetics of murine gammaherpesvirus 68 gene expression following infection of murine cells in culture and in mice. *J Virol* 75: 4955-63
74. Cardin RD, Brooks JW, Sarawar SR, Doherty PC. 1996. Progressive loss of CD8+ T cell-mediated control of a gamma-herpesvirus in the absence of CD4+ T cells. *J Exp Med* 184: 863-71
75. Christensen JP, Cardin RD, Branum KC, Doherty PC. 1999. CD4(+) T cell-mediated control of a gamma-herpesvirus in B cell-deficient mice is mediated by IFN-gamma. *Proc Natl Acad Sci U S A* 96: 5135-40

76. Stevenson PG, Cardin RD, Christensen JP, Doherty PC. 1999. Immunological control of a murine gammaherpesvirus independent of CD8+ T cells. *J Gen Virol* 80 (Pt 2): 477-83
77. Sparks-Thissen RL, Braaten DC, Hildner K, Murphy TL, Murphy KM, Virgin HWt. 2005. CD4 T cell control of acute and latent murine gammaherpesvirus infection requires IFNgamma. *Virology* 338: 201-8
78. Sparks-Thissen RL, Braaten DC, Kreher S, Speck SH, Virgin HWt. 2004. An optimized CD4 T-cell response can control productive and latent gammaherpesvirus infection. *J Virol* 78: 6827-35
79. Steed A, Buch T, Waisman A, Virgin HWt. 2007. Gamma interferon blocks gammaherpesvirus reactivation from latency in a cell type-specific manner. *J Virol* 81: 6134-40
80. Thomson RC, Petrik J, Nash AA, Dutia BM. 2008. Expansion and activation of NK cell populations in a gammaherpesvirus infection. *Scand J Immunol* 67: 489-95
81. Usherwood EJ, Meadows SK, Crist SG, Bellfy SC, Sentman CL. 2005. Control of murine gammaherpesvirus infection is independent of NK cells. *Eur J Immunol* 35: 2956-61
82. Li MO, Wan YY, Sanjabi S, Robertson AK, Flavell RA. 2006. Transforming growth factor-beta regulation of immune responses. *Annu Rev Immunol* 24: 99-146
83. Kisseleva T, Brenner DA. 2008. Mechanisms of fibrogenesis. *Exp Biol Med (Maywood)* 233: 109-22
84. Govinden R, Bhoola KD. 2003. Genealogy, expression, and cellular function of transforming growth factor-beta. *Pharmacol Ther* 98: 257-65
85. Annes JP, Munger JS, Rifkin DB. 2003. Making sense of latent TGFbeta activation. *J Cell Sci* 116: 217-24
86. Gentry LE, Nash BW. 1990. The pro domain of pre-pro-transforming growth factor beta 1 when independently expressed is a functional binding protein for the mature growth factor. *Biochemistry* 29: 6851-7
87. Yu Q, Stamenkovic I. 2000. Cell surface-localized matrix metalloproteinase-9 proteolytically activates TGF-beta and promotes tumor invasion and angiogenesis. *Genes Dev* 14: 163-76
88. Munger JS, Huang X, Kawakatsu H, Griffiths MJ, Dalton SL, Wu J, Pittet JF, Kaminski N, Garat C, Matthay MA, Rifkin DB, Sheppard D. 1999. The integrin alpha v beta 6 binds and activates latent TGF beta 1: a mechanism for regulating pulmonary inflammation and fibrosis. *Cell* 96: 319-28
89. Lyons RM, Keski-Oja J, Moses HL. 1988. Proteolytic activation of latent transforming growth factor-beta from fibroblast-conditioned medium. *J Cell Biol* 106: 1659-65
90. Massague J. 1998. TGF-beta signal transduction. *Annu Rev Biochem* 67: 753-91
91. Derynck R, Zhang YE. 2003. Smad-dependent and Smad-independent pathways in TGF-beta family signalling. *Nature* 425: 577-84
92. Kruisbeek AM, Shevach E, Thornton AM. 2004. Proliferative assays for T cell function. In *Current Protocols in Immunology*: John Wiley & Sons, Inc.

93. Yanik GA, Ho VT, Levine JE, White ES, Braun T, Antin JH, Whitfield J, Custer J, Jones D, Ferrara JL, Cooke KR. 2008. The impact of soluble tumor necrosis factor receptor etanercept on the treatment of idiopathic pneumonia syndrome after allogeneic hematopoietic stem cell transplantation. *Blood* 112: 3073-81
94. Wahl SM. 2007. Transforming growth factor-beta: innately bipolar. *Curr Opin Immunol* 19: 55-62
95. Shull MM, Ormsby I, Kier AB, Pawlowski S, Diebold RJ, Yin M, Allen R, Sidman C, Proetzel G, Calvin D, et al. 1992. Targeted disruption of the mouse transforming growth factor-beta 1 gene results in multifocal inflammatory disease. *Nature* 359: 693-9
96. Kulkarni AB, Huh CG, Becker D, Geiser A, Lyght M, Flanders KC, Roberts AB, Sporn MB, Ward JM, Karlsson S. 1993. Transforming growth factor beta 1 null mutation in mice causes excessive inflammatory response and early death. *Proc Natl Acad Sci U S A* 90: 770-4
97. Adams DH, Hathaway M, Shaw J, Burnett D, Elias E, Strain AJ. 1991. Transforming growth factor-beta induces human T lymphocyte migration in vitro. *J Immunol.* 147: 609-12.
98. Kehrl JH, Wakefield LM, Roberts AB, Jakowlew S, Alvarez-Mon M, Derynck R, Sporn MB, Fauci AS. 1986. Production of transforming growth factor beta by human T lymphocytes and its potential role in the regulation of T cell growth. *J Exp Med* 163: 1037-50
99. Ludviksson BR, Seegers D, Resnick AS, Strober W. 2000. The effect of TGF-beta1 on immune responses of naive versus memory CD4+ Th1/Th2 T cells. *Eur J Immunol* 30: 2101-11
100. Gorelik L, Fields PE, Flavell RA. 2000. Cutting edge: TGF-beta inhibits Th type 2 development through inhibition of GATA-3 expression. *J Immunol* 165: 4773-7
101. Brabletz T, Pfeuffer I, Schorr E, Siebelt F, Wirth T, Serfling E. 1993. Transforming growth factor beta and cyclosporin A inhibit the inducible activity of the interleukin-2 gene in T cells through a noncanonical octamer-binding site. *Mol Cell Biol* 13: 1155-62
102. Gorelik L, Constant S, Flavell RA. 2002. Mechanism of transforming growth factor beta-induced inhibition of T helper type 1 differentiation. *J Exp Med* 195: 1499-505
103. Li MO, Wan YY, Flavell RA. 2007. T cell-produced transforming growth factor-beta1 controls T cell tolerance and regulates Th1- and Th17-cell differentiation. *Immunity* 26: 579-91
104. Gorelik L, Flavell RA. 2000. Abrogation of TGFbeta signaling in T cells leads to spontaneous T cell differentiation and autoimmune disease. *Immunity* 12: 171-81
105. Veldhoen M, Hocking RJ, Atkins CJ, Locksley RM, Stockinger B. 2006. TGFbeta in the context of an inflammatory cytokine milieu supports de novo differentiation of IL-17-producing T cells. *Immunity* 24: 179-89
106. Chen W, Jin W, Hardegen N, Lei KJ, Li L, Marinos N, McGrady G, Wahl SM. 2003. Conversion of peripheral CD4+CD25- naive T cells to CD4+CD25+ regulatory T cells by TGF-beta induction of transcription factor Foxp3. *J Exp Med* 198: 1875-86

107. Peng Y, Laouar Y, Li MO, Green EA, Flavell RA. 2004. TGF-beta regulates in vivo expansion of Foxp3-expressing CD4+CD25+ regulatory T cells responsible for protection against diabetes. *Proc Natl Acad Sci U S A* 101: 4572-7
108. Cazac BB, Roes J. 2000. TGF-beta receptor controls B cell responsiveness and induction of IgA in vivo. *Immunity* 13: 443-51
109. Borsutzky S, Cazac BB, Roes J, Guzman CA. 2004. TGF-beta receptor signaling is critical for mucosal IgA responses. *J Immunol* 173: 3305-9
110. Brandes ME, Mai UE, Ohura K, Wahl SM. 1991. Type I transforming growth factor-beta receptors on neutrophils mediate chemotaxis to transforming growth factor-beta. *J Immunol.* 147: 1600-6.
111. Wahl SM, Hunt DA, Wakefield LM, McCartney-Francis N, Wahl LM, Roberts AB, Sporn MB. 1987. Transforming growth factor type beta induces monocyte chemotaxis and growth factor production. *Proc Natl Acad Sci U S A* 84: 5788-92
112. Tsunawaki S, Sporn M, Ding A, Nathan C. 1988. Deactivation of macrophages by transforming growth factor-beta. *Nature* 334: 260-2
113. Rook AH, Kehrl JH, Wakefield LM, Roberts AB, Sporn MB, Burlington DB, Lane HC, Fauci AS. 1986. Effects of transforming growth factor beta on the functions of natural killer cells: depressed cytolytic activity and blunting of interferon responsiveness. *J Immunol* 136: 3916-20
114. Laouar Y, Sutterwala FS, Gorelik L, Flavell RA. 2005. Transforming growth factor-beta controls T helper type 1 cell development through regulation of natural killer cell interferon-gamma. *Nat Immunol* 6: 600-7
115. Gruber BL, Marchese MJ, Kew RR. 1994. Transforming growth factor-beta 1 mediates mast cell chemotaxis. *J Immunol.* 152: 5860-7.
116. Liem LM, Fibbe WE, van Houwelingen HC, Goulmy E. 1999. Serum transforming growth factor-beta1 levels in bone marrow transplant recipients correlate with blood cell counts and chronic graft-versus-host disease. *Transplantation* 67: 59-65
117. Malone FR, Leisenring WM, Storer BE, Lawler R, Stern JM, Aker SN, Bouvier ME, Martin PJ, Batchelder AL, Schoch HG, McDonald GB. 2007. Prolonged anorexia and elevated plasma cytokine levels following myeloablative allogeneic hematopoietic cell transplant. *Bone Marrow Transplant* 40: 765-72
118. Panoskaltsis-Mortari A, Taylor PA, Yaeger TM, Wangensteen OD, Bitterman PB, Ingbar DH, Vallera DA, Blazar BR. 1997. The critical early proinflammatory events associated with idiopathic pneumonia syndrome in irradiated murine allogeneic recipients are due to donor T cell infusion and potentiated by cyclophosphamide. *J Clin Invest* 100: 1015-27
119. Wu JM, Thoburn CJ, Wisell J, Farmer ER, Hess AD. CD20, AIF-1, and TGF-beta in graft-versus-host disease: a study of mRNA expression in histologically matched skin biopsies. *Mod Pathol* 2010: 26
120. Banovic T, MacDonald KP, Morris ES, Rowe V, Kuns R, Don A, Kelly J, Ledbetter S, Clouston AD, Hill GR. 2005. TGF-beta in allogeneic stem cell transplantation: friend or foe? *Blood* 106: 2206-14
121. Border WA, Noble NA. 1994. Transforming growth factor beta in tissue fibrosis. *N Engl J Med* 331: 1286-92

122. Barao I, Hanash AM, Hallett W, Welniak LA, Sun K, Redelman D, Blazar BR, Levy RB, Murphy WJ. 2006. Suppression of natural killer cell-mediated bone marrow cell rejection by CD4+CD25+ regulatory T cells. *Proc Natl Acad Sci U S A* 103: 5460-5
123. Adler H, Beland JL, Kozlow W, Del-Pan NC, Kobzik L, Rimm IJ. 1998. A role for transforming growth factor-beta1 in the increased pneumonitis in murine allogeneic bone marrow transplant recipients with graft-versus-host disease after pulmonary herpes simplex virus type 1 infection. *Blood* 92: 2581-9
124. Coomes SM, Wilke CA, Moore TA, Moore BB. 2010. Induction of transforming growth factor beta-1, not regulatory T cells, impairs anti-viral immunity in the lung following bone marrow transplant. *J Immunol*: In press
125. Hinz B, Celetta G, Tomasek JJ, Gabbiani G, Chaponnier C. 2001. Alpha-smooth muscle actin expression upregulates fibroblast contractile activity. *Mol Biol Cell.* 12: 2730-41.
126. Anscher MS, Peters WP, Reisenbichler H, Petros WP, Jirtle RL. 1993. Transforming growth factor beta as a predictor of liver and lung fibrosis after autologous bone marrow transplantation for advanced breast cancer. *N Engl J Med* 328: 1592-8
127. Marks LB, Yu X, Vujaskovic Z, Small W, Jr., Folz R, Anscher MS. 2003. Radiation-induced lung injury. *Semin Radiat Oncol* 13: 333-45
128. Psathakis K, Mermigkis D, Papatheodorou G, Loukides S, Panagou P, Polychronopoulos V, Siafakas NM, Bouros D. 2006. Exhaled markers of oxidative stress in idiopathic pulmonary fibrosis. *Eur J Clin Invest* 36: 362-7
129. Carpenter M, Epperly MW, Agarwal A, Nie S, Hricisak L, Niu Y, Greenberger JS. 2005. Inhalation delivery of manganese superoxide dismutase-plasmid/liposomes protects the murine lung from irradiation damage. *Gene Ther* 12: 685-93
130. Hsu YC, Wang LF, Chien YW. 2007. Nitric oxide in the pathogenesis of diffuse pulmonary fibrosis. *Free Radic Biol Med* 42: 599-607
131. Kliment CR, Oury TD. 2010. Oxidative stress, extracellular matrix targets, and idiopathic pulmonary fibrosis. *Free Radic Biol Med* 49: 707-17
132. Murrell GA, Francis MJ, Bromley L. 1990. Modulation of fibroblast proliferation by oxygen free radicals. *Biochem J* 265: 659-65
133. Scotton CJ, Krupiczojc MA, Konigshoff M, Mercer PF, Lee YC, Kaminski N, Morser J, Post JM, Maher TM, Nicholson AG, Moffatt JD, Laurent GJ, Derian CK, Eickelberg O, Chambers RC. 2009. Increased local expression of coagulation factor X contributes to the fibrotic response in human and murine lung injury. *J Clin Invest* 119: 2550-63
134. Martinez FO, Helming L, Gordon S. 2009. Alternative activation of macrophages: an immunologic functional perspective. *Annu Rev Immunol* 27: 451-83
135. Gordon S, Martinez FO. 2010. Alternative activation of macrophages: mechanism and functions. *Immunity* 32: 593-604
136. Mora AL, Torres-Gonzalez E, Rojas M, Corredor C, Ritzenthaler J, Xu J, Roman J, Brigham K, Stecenko A. 2006. Activation of alveolar macrophages via the alternative pathway in herpesvirus-induced lung fibrosis. *Am J Respir Cell Mol Biol* 35: 466-73

137. Ebrahimi B, Dutia BM, Brownstein DG, Nash AA. 2001. Murine gammaherpesvirus-68 infection causes multi-organ fibrosis and alters leukocyte trafficking in interferon-gamma receptor knockout mice. *Am J Pathol* 158: 2117-25
138. Gangadharan B, Hoeve MA, Allen JE, Ebrahimi B, Rhind SM, Dutia BM, Nash AA. 2008. Murine gammaherpesvirus-induced fibrosis is associated with the development of alternatively activated macrophages. *J Leukoc Biol* 84: 50-8
139. McMillan TR, Moore BB, Weinberg JB, Vannella KM, Fields WB, Christensen PJ, van Dyk LF, Toews GB. 2008. Exacerbation of established pulmonary fibrosis in a murine model by gammaherpesvirus. *Am J Respir Crit Care Med* 177: 771-80
140. Vannella KM, Luckhardt TR, Wilke CA, van Dyk LF, Toews GB, Moore BB. 2010. Latent herpesvirus infection augments experimental pulmonary fibrosis. *Am J Respir Crit Care Med* 181: 465-77
141. Schuurhuis DH, Fu N, Ossendorp F, Melief CJ. 2006. Ins and outs of dendritic cells. *Int Arch Allergy Immunol* 140: 53-72
142. Nachbaur D, Kircher B. 2005. Dendritic cells in allogeneic hematopoietic stem cell transplantation. *Leuk Lymphoma* 46: 1387-96
143. Nachbaur D, Kircher B, Eisendle K, Latzer K, Haun M, Gastl G. 2003. Phenotype, function and chimaerism of monocyte-derived blood dendritic cells after allogeneic haematopoietic stem cell transplantation. *Br J Haematol* 123: 119-26
144. Bluestone JA, Mackay CR, O'Shea JJ, Stockinger B. 2009. The functional plasticity of T cell subsets. *Nat Rev Immunol* 9: 811-6
145. Wang YH, Voo KS, Liu B, Chen CY, Uygungil B, Spoede W, Bernstein JA, Huston DP, Liu YJ. 2010. A novel subset of CD4(+) T(H)2 memory/effector cells that produce inflammatory IL-17 cytokine and promote the exacerbation of chronic allergic asthma. *J Exp Med* 207: 2479-91
146. Kaiko GE, Horvat JC, Beagley KW, Hansbro PM. 2008. Immunological decision-making: how does the immune system decide to mount a helper T-cell response? *Immunology* 123: 326-38
147. Murphy KM, Stockinger B. 2010. Effector T cell plasticity: flexibility in the face of changing circumstances. *Nat Immunol* 11: 674-80
148. Guillaume T, Sekhavat M, Rubinstein DB, Hamdan O, Leblanc P, Symann ML. 1994. Defective cytokine production following autologous stem cell transplantation for solid tumors and hematologic malignancies regardless of bone marrow or peripheral origin and lack of evidence for a role for interleukin-10 in delayed immune reconstitution. *Cancer Res* 54: 3800-7
149. Wan YY, Flavell RA. 2007. Regulatory T cells, transforming growth factor-beta, and immune suppression. *Proc Am Thorac Soc* 4: 271-6
150. Wan YY, Flavell RA. 2007. 'Yin-Yang' functions of transforming growth factor-beta and T regulatory cells in immune regulation. *Immunol Rev* 220: 199-213
151. Le NT, Chao N. 2007. Regulating regulatory T cells. *Bone Marrow Transplant* 39: 1-9
152. Atanackovic D, Cao Y, Luetkens T, Panse J, Faltz C, Arfsten J, Bartels K, Wolschke C, Eiermann T, Zander AR, Fehse B, Bokemeyer C, Kroger N. 2008. CD4+CD25+FOXP3+ T regulatory cells reconstitute and accumulate in the bone

marrow of patients with multiple myeloma following allogeneic stem cell transplantation. *Haematologica* 93: 423-30

153. Mielke S, Rezvani K, Savani BN, Nunes R, Yong AS, Schindler J, Kurlander R, Ghetie V, Read EJ, Solomon SR, Vitetta ES, Barrett AJ. 2007. Reconstitution of FOXP3+ regulatory T cells (Tregs) after CD25-depleted allotransplantation in elderly patients and association with acute graft-versus-host disease. *Blood* 110: 1689-97
154. Nadal E, Garin M, Kaeda J, Apperley J, Lechler R, Dazzi F. 2007. Increased frequencies of CD4(+)CD25(high) T(regs) correlate with disease relapse after allogeneic stem cell transplantation for chronic myeloid leukemia. *Leukemia* 21: 472-9
155. Bayer AL, Jones M, Chirinos J, de Armas L, Schreiber TH, Malek TR, Levy RB. 2009. Host CD4+CD25+ T cells can expand and comprise a major component of the Treg compartment after experimental HCT. *Blood* 113: 733-43
156. Nguyen VH, Shashidhar S, Chang DS, Ho L, Kambham N, Bachmann M, Brown JM, Negrin RS. 2008. The impact of regulatory T cells on T-cell immunity following hematopoietic cell transplantation. *Blood* 111: 945-53
157. Kontoyiannis DP, Lewis RE, Marr K. 2009. The burden of bacterial and viral infections in hematopoietic stem cell transplant. *Biol Blood Marrow Transplant* 15: 128-33
158. Gohring K, Feuchtinger T, Mikeler E, Lang P, Jahn G, Handgretinger R, Hamprecht K. 2009. Dynamics of the Emergence of a Human Cytomegalovirus UL97 Mutant Strain Conferring Ganciclovir Resistance in a Pediatric Stem-Cell Transplant Recipient. *J Mol Diagn*
159. Konoplev S, Champlin RE, Giralt S, Ueno NT, Khouri I, Raad I, Rolston K, Jacobson K, Tarrand J, Luna M, Nguyen Q, Whimbey E. 2001. Cytomegalovirus pneumonia in adult autologous blood and marrow transplant recipients. *Bone Marrow Transplant* 27: 877-81
160. Ljungman P. 2002. Prevention and treatment of viral infections in stem cell transplant recipients. *Br J Haematol* 118: 44-57
161. Coomes SM, Wilke CA, Moore TA, Moore BB. 2010. Induction of TGF-beta 1, not regulatory T cells, impairs antiviral immunity in the lung following bone marrow transplant. *J Immunol* 184: 5130-40
162. Livak KJ, Schmittgen TD. 2001. Analysis of relative gene expression data using real-time quantitative PCR and the 2(-Delta Delta C(T)) Method. *Methods* 25: 402-8
163. Kolodsick JE, Toews GB, Jakubzick C, Hogaboam C, Moore TA, McKenzie A, Wilke CA, Chrisman CJ, Moore BB. 2004. Protection from fluorescein isothiocyanate-induced fibrosis in IL-13-deficient, but not IL-4-deficient, mice results from impaired collagen synthesis by fibroblasts. *J Immunol* 172: 4068-76
164. Huffnagle GB, Strieter RM, Standiford TJ, McDonald RA, Burdick MD, Kunkel SL, Toews GB. 1995. The role of monocyte chemotactic protein-1 (MCP-1) in the recruitment of monocytes and CD4+ T cells during a pulmonary Cryptococcus neoformans infection. *J Immunol* 155: 4790-7

165. Lutz MB, Kukutsch N, Ogilvie AL, Rossner S, Koch F, Romani N, Schuler G. 1999. An advanced culture method for generating large quantities of highly pure dendritic cells from mouse bone marrow. *J Immunol Methods* 223: 77-92
166. Charbeneau RP, Christensen PJ, Chrisman CJ, Paine R, 3rd, Toews GB, Peters-Golden M, Moore BB. 2003. Impaired synthesis of prostaglandin E2 by lung fibroblasts and alveolar epithelial cells from GM-CSF-/- mice: implications for fibroproliferation. *Am J Physiol Lung Cell Mol Physiol* 284: L1103-11. Epub 2003 Feb 21.
167. Corti M, Brody AR, Harrison JH. 1996. Isolation and primary culture of murine alveolar type II cells. *Am J Respir Cell Mol Biol* 14: 309-15
168. Nguyen Y, McGuffie BA, Anderson VE, Weinberg JB. 2008. Gammaherpesvirus modulation of mouse adenovirus type 1 pathogenesis. *Virology* 380: 182-90
169. Weck KE, Dal Canto AJ, Gould JD, O'Guin AK, Roth KA, Saffitz JE, Speck SH, Virgin HW. 1997. Murine gamma-herpesvirus 68 causes severe large-vessel arteritis in mice lacking interferon-gamma responsiveness: a new model for virus-induced vascular disease. *Nat Med.* 3: 1346-53.
170. Hubbard LL, Ballinger MN, Wilke CA, Moore BB. 2008. Comparison of conditioning regimens for alveolar macrophage reconstitution and innate immune function post bone marrow transplant. *Exp Lung Res* 34: 263-75
171. Shapiro AC, Wu D, Meydani SN. 1993. Eicosanoids derived from arachidonic and eicosapentaenoic acids inhibit T cell proliferative response. *Prostaglandins* 45: 229-40
172. Steed AL, Barton ES, Tibbetts SA, Popkin DL, Lutzke ML, Rochford R, Virgin HWt. 2006. Gamma interferon blocks gammaherpesvirus reactivation from latency. *J Virol* 80: 192-200
173. Moore BB, Hogaboam CM. 2008. Murine models of pulmonary fibrosis. *Am J Physiol Lung Cell Mol Physiol* 294: L152-60
174. Grundy JE, Shanley JD, Shearer GM. 1985. Augmentation of graft-versus-host reaction by cytomegalovirus infection resulting in interstitial pneumonitis. *Transplantation* 39: 548-53
175. Doherty PC, Christensen JP, Belz GT, Stevenson PG, Sangster MY. 2001. Dissecting the host response to a gamma-herpesvirus. *Philos Trans R Soc Lond B Biol Sci* 356: 581-93
176. Schreiber T, Ehlers S, Heitmann L, Rausch A, Mages J, Murray PJ, Lang R, Holscher C. 2009. Autocrine IL-10 induces hallmarks of alternative activation in macrophages and suppresses antituberculosis effector mechanisms without compromising T cell immunity. *J Immunol* 183: 1301-12
177. Cottrez F, Groux H. 2001. Regulation of TGF-beta response during T cell activation is modulated by IL-10. *J Immunol* 167: 773-8
178. Nataraj C, Thomas DW, Tilley SL, Nguyen MT, Mannon R, Koller BH, Coffman TM. 2001. Receptors for prostaglandin E(2) that regulate cellular immune responses in the mouse. *J Clin Invest* 108: 1229-35
179. Shao J, Sheng H, Aramandla R, Pereira MA, Lubet RA, Hawk E, Grogan L, Kirsch IR, Washington MK, Beauchamp RD, DuBois RN. 1999. Coordinate regulation of cyclooxygenase-2 and TGF-beta1 in replication error-positive colon cancer and azoxymethane-induced rat colonic tumors. *Carcinogenesis* 20: 185-91

180. Ding Q, Bai YF, Wang YQ, An RH. 2010. TGF-beta1 reverses inhibition of COX-2 with NS398 and increases invasion in prostate cancer cells. *Am J Med Sci* 339: 425-32
181. Neurath MF, Weigmann B, Finotto S, Glickman J, Nieuwenhuis E, Iijima H, Mizoguchi A, Mizoguchi E, Mudter J, Galle PR, Bhan A, Autschbach F, Sullivan BM, Szabo SJ, Glimcher LH, Blumberg RS. 2002. The transcription factor T-bet regulates mucosal T cell activation in experimental colitis and Crohn's disease. *J Exp Med* 195: 1129-43
182. Fossiez F, Djossou O, Chomarat P, Flores-Romo L, Ait-Yahia S, Maat C, Pin JJ, Garrone P, Garcia E, Saeland S, Blanchard D, Gaillard C, Das Mahapatra B, Rouvier E, Golstein P, Banchereau J, Lebecque S. 1996. T cell interleukin-17 induces stromal cells to produce proinflammatory and hematopoietic cytokines. *J Exp Med* 183: 2593-603
183. Faust SM, Lu G, Marini BL, Zou W, Gordon D, Iwakura Y, Laouar Y, Bishop DK. 2009. Role of T cell TGFbeta signaling and IL-17 in allograft acceptance and fibrosis associated with chronic rejection. *J Immunol* 183: 7297-306
184. Guillaume T, Kubin M, Sekhavat M, Rubinstein DB, Trinchieri G, Symann M. 1996. Peripheral blood mononuclear cells from autologous hematopoietic stem cell transplantation recipients produce and respond to IL-12. *Bone Marrow Transplant* 18: 733-9
185. Mitsuhashi M, Liu J, Cao S, Shi X, Ma X. 2004. Regulation of interleukin-12 gene expression and its anti-tumor activities by prostaglandin E2 derived from mammary carcinomas. *J Leukoc Biol* 76: 322-32
186. Das J, Ren G, Zhang L, Roberts AI, Zhao X, Bothwell AL, Van Kaer L, Shi Y, Das G. 2009. Transforming growth factor beta is dispensable for the molecular orchestration of Th17 cell differentiation. *J Exp Med* 206: 2407-16
187. Kantrow SP, Hackman RC, Boeckh M, Myerson D, Crawford SW. 1997. Idiopathic pneumonia syndrome: changing spectrum of lung injury after marrow transplantation. *Transplantation* 63: 1079-86
188. Cooke KR, Yanik G. 2004. Acute lung injury after allogeneic stem cell transplantation: is the lung a target of acute graft-versus-host disease? *Bone Marrow Transplant* 34: 753-65
189. Hildebrandt GC, Duffner UA, Olkiewicz KM, Corrion LA, Willmarth NE, Williams DL, Clouthier SG, Hogaboam CM, Reddy PR, Moore BB, Kuziel WA, Liu C, Yanik G, Cooke KR. 2004. A critical role for CCR2/MCP-1 interactions in the development of idiopathic pneumonia syndrome after allogeneic bone marrow transplantation. *Blood* 103: 2417-26
190. Ahmadzadeh M, Rosenberg SA. 2005. TGF-beta 1 attenuates the acquisition and expression of effector function by tumor antigen-specific human memory CD8 T cells. *J Immunol* 174: 5215-23
191. Sheng H, Shao J, Hooton EB, Tsujii M, DuBois RN, Beauchamp RD. 1997. Cyclooxygenase-2 induction and transforming growth factor beta growth inhibition in rat intestinal epithelial cells. *Cell Growth Differ* 8: 463-70
192. Hagiwara SI, Ishii Y, Kitamura S. 2000. Aerosolized administration of N-acetylcysteine attenuates lung fibrosis induced by bleomycin in mice. *Am J Respir Crit Care Med* 162: 225-31

193. Kitani A, Fuss I, Nakamura K, Kumaki F, Usui T, Strober W. 2003. Transforming growth factor (TGF)-beta1-producing regulatory T cells induce Smad-mediated interleukin 10 secretion that facilitates coordinated immunoregulatory activity and amelioration of TGF-beta1-mediated fibrosis. *J Exp Med* 198: 1179-88
194. Simonian PL, Roark CL, Wehrmann F, Lanham AK, Diaz del Valle F, Born WK, O'Brien RL, Fontenot AP. 2009. Th17-polarized immune response in a murine model of hypersensitivity pneumonitis and lung fibrosis. *J Immunol* 182: 657-65
195. Burlingham WJ, Love RB, Jankowska-Gan E, Haynes LD, Xu Q, Bobadilla JL, Meyer KC, Hayney MS, Braun RK, Greenspan DS, Gopalakrishnan B, Cai J, Brand DD, Yoshida S, Cummings OW, Wilkes DS. 2007. IL-17-dependent cellular immunity to collagen type V predisposes to obliterative bronchiolitis in human lung transplants. *J Clin Invest* 117: 3498-506
196. van Dyk LF, Virgin HWt, Speck SH. 2000. The murine gammaherpesvirus 68 v-cyclin is a critical regulator of reactivation from latency. *J Virol* 74: 7451-61
197. Kayhan B, Yager EJ, Lanzer K, Cookenham T, Jia Q, Wu TT, Woodland DL, Sun R, Blackman MA. 2007. A replication-deficient murine gamma-herpesvirus blocked in late viral gene expression can establish latency and elicit protective cellular immunity. *J Immunol* 179: 8392-402
198. Bhalla KS, Folz RJ. 2002. Idiopathic pneumonia syndrome after syngeneic bone marrow transplant in mice. *Am J Respir Crit Care Med* 166: 1579-89
199. Taylor PA, Ehrhardt MJ, Lees CJ, Panoskaltsis-Mortari A, Krieg AM, Sharpe AH, Murphy WJ, Serody JS, Hemmi H, Akira S, Levy RB, Blazar BR. 2008. TLR agonists regulate alloresponses and uncover a critical role for donor APCs in allogeneic bone marrow rejection. *Blood* 112: 3508-16